

# **MODELING AND SIMULATION OF ZINC BASED BATTERIES**

**A Thesis Submitted to  
The Graduate School of Engineering and Sciences of  
Izmir Institute of Technology  
In Partial Fulfillment of the Requirements for the Degree of**

**MASTER OF SCIENCE**

**in Energy Engineering**

**by  
Evren TOPTOP**

**January 2016  
İZMİR**

We approve the thesis of **Evren TOPTOP**

**Examining Committee Members:**

---

**Assist. Prof. Dr. Özgenç EBİL**

Department of Chemical Engineering, Izmir Institute of Technology

---

**Assist. Prof. Dr. Ayben TOP**

Department of Chemical Engineering, Izmir Institute of Technology

---

**Assist. Prof. Dr. Güler NARİN**

Department of Chemical Engineering, Usak University

**11 January 2016**

---

**Assist. Prof. Dr. Özgenç EBİL**

Supervisor, Department of Chemical Engineering, Izmir Institute of Technology

---

**Assist. Prof. Dr. Aşlı YÜKSEL ÖZŞEN**

Co-Supervisor, Chemical Engineering, Izmir Institute of Technology

---

**Prof. Dr. Gülden GÖKÇEN AKKURT**

Head of the Department of Energy Engineering

---

**Prof. Dr. Bilge KARAÇALI**

Dean of the Graduate School of Engineering and Sciences

## **ACKNOWLEDGEMENTS**

First of all I am heartily thankful to my supervisor and my mentor, Assist. Prof. Dr. Özgeç EBİL. His knowledge has broadened my mind during my studies. His encouragements were motivating, and his sincerity made everything easy. His support became the reason of my willing to learn and study more in the pursuit of excellence during this Master's thesis study. I am also grateful to the research assistants Gizem PAYER and Selcan ATEŞ. They have shared their knowledge and their experience whenever I needed, and with their help I did put some good effort into my studies.

Also, I would like to express my gratitude to Dr. Ogan OCALI and Prof. Dr. Mustafa DEMİRCİOĞLU for sharing their deep knowledge and the positive influence contributing on my ambition.

I am grateful to my dear friends Çağatay İPBÜKER and Özben KAYMAZ. I appreciate all their selfless helps in the most crucial times.

At last I want to express my gratitude to the most important people in my life, to my parents Ethem and Mine TOPTOP and my brother Koral TOPTOP. Their unlimited patience with me and their supports about anything that I have decided, especially coming in Izmir to make a graduate study, made everything so easy for me to focus on my studies.

# **ABSTRACT**

## **MODELING AND SIMULATION OF ZINC BASED BATTERIES**

Energy is the determining factor of productivity and quality of living. Electric energy is the most used energy form and lack of reserve for it hinders widespread use of renewable energy technologies. Advancements in renewable energy technologies, electric vehicles and consumer electronics are highly dependent on developments of new battery technologies. High energy density, long service life, using benign and abundant materials are few of the key requirements for next generation batteries. A model, a mathematical description of the system, is an effective tool to predict the behavior of batteries under specific conditions, thus reducing cost and time for the development.

A mathematical model using finite element method was designed to simulate the discharge behavior of an experimental nickel-zinc battery that includes composite zinc and commercial nickel electrodes. The model employs thermodynamic and kinetic expressions for porous electrodes considering the concentration dependency of battery characteristics.

The effects of initial zinc and nickel concentrations, anodic transfer coefficients of zinc and nickel electrode reactions on the electrochemical performance of the battery have been simulated. The discharge voltage, electrode porosities, and species concentrations in electrodes as a function of model parameters and time have been evaluated. It is observed that the model results are consistent with the experiment results considering that the battery operation is limited with zinc concentration. Initial zinc concentration is the major determining factor on discharge duration. Nickel oxyhydroxide concentration affects voltage magnitude. Transfer coefficients have only limited effects on discharge voltage and concentrations.

## ÖZET

### ÇİNKO TABANLI PİLLERİN MODELLENMESİ VE SİMÜLASYONU

Enerji, üretkenliğin ve yaşam kalitesinin belirleyici ögesidir. Elektrik enerjisi en çok kullanılan enerji çeşidi ancak yedeklenmemesi yenilenebilir enerji teknolojilerinin yaygın kullanımını önüyor. Yenilenebilir enerji teknolojilerinde, elektrikli taşıtlarda ve tüketici elektroniğinde gelişmelerin gerçekleşmesi büyük ölçüde akü ve pil teknolojilerindeki ilerlemelere bağlı. Yüksek enerji yoğunluğu, uzun kullanım ömrü, zararsız ve bol bulunan malzemelerden imalat yeni nesil pil ve aküler için çok önemli gereksinimler. Araştırmacılara belli koşullardaki akü ve pil davranışlarını tahmin etmelerini sağlayacak bir model, sistemin matematiksel bir tanımı, geliştirme sürecinin maliyetini ve süresini azaltacak etkili bir araç olacaktır.

Bu çalışmada, ticari nikel elektrot ve kompozit çinko elektrot kullanılarak imâl edilmiş deneysel bir nikel-çinko pilin deşarj esnasındaki davranışı, sonlu eleman metodunu kullanan matematiksel bir model ile simüle edildi. Geliştirilen modelde gözenekli elektrotlar için geçerli olan termodinamik ve kinetik tanımları pil ve akü niteliklerinin konsantrasyon bağımlılıkları da göz önünde bulundurularak kullanıldı.

Başlangıçtaki çinko ve nikel oksihidroksit konsantrasyonlarının ve çinko ve nikel elektrot reaksiyonları anodik transfer katsayılarının pilin elektrokimyasal performansına etkileri simüle edildi. Deşarj gerilimi, elektrot gözenekliliği ve elektrotlardaki malzeme türü konsantrasyonları, model parametrelerine ve zamana bağlı fonksiyonlar olarak hesaplandılar. Model sonuçlarının deneysel pille yapılan deney sonuçlarıyla, çinko konsantrasyonu sınırlı çalışması noktasında uyum gösterdiği gözlemlendi. Elde edilen simülasyon sonuçlarına göre başlangıçtaki çinko konsantrasyonu deşarj süresinde en belirleyici öge. Başlangıçtaki nikel oksihidroksit konsantrasyonu ise deşarj geriliminin büyüklüğünde etkili. Transfer katsayılarının ise deşarj gerilimleri üstünde etkili olduğu, bununla birlikte konsantrasyon değişimlerine etkilerinin çok sınırlı olduğu ve deşarj süresine hiç etkilerinin olmadığı görüldü.

# TABLE OF CONTENTS

LIST OF FIGURES.....	ix
LIST OF TABLES.....	xii
LIST OF SYMBOLS AND ABBREVIATIONS.....	xiii
CHAPTER 1. INTRODUCTION.....	1
1.1. Dimensions and Units.....	1
1.2. Nomenclature.....	2
1.3. Energy and Associated Problems.....	2
CHAPTER 2. ENERGY STORAGE.....	7
2.1. Batteries.....	9
2.1.1. Terminology and Concepts for Battery Specifications.....	9
2.1.1.1. Primary Battery.....	9
2.1.1.2. Secondary Battery.....	10
2.1.1.3. Cell, Module and Pack.....	10
2.1.1.4. Capacity.....	11
2.1.1.5. Energy.....	11
2.1.1.6. C Rate.....	11
2.1.1.7. Power Density.....	12
2.1.1.8. Energy Density.....	12
2.1.1.9. Cycle Life.....	12
2.1.1.10. Self-Discharge.....	12
2.1.1.11. Open-circuit Voltage.....	13
2.1.1.12. Terminal Voltage.....	13
2.1.1.13. Short-circuit Current.....	13
2.1.1.14. State-Of-Health (SOH).....	14
2.1.1.15. State-Of-Charge (SOC).....	14
2.1.1.16. Depth-Of-Discharge (DOD).....	17
2.1.1.17. Depth-Of-Charge (DOC).....	17

2.1.1.18. Nominal Voltage.....	18
2.1.1.19. Cut-off Voltage.....	18
2.1.1.20. Charge Voltage.....	18
2.1.1.21. Charge Current.....	19
2.1.1.22. Float Voltage.....	19
2.1.1.23. Internal Resistance.....	19
2.1.2. Battery Components.....	19
2.1.2.1. Electrodes.....	20
2.1.2.2. Electrolyte Solution.....	21
2.1.2.3. Separator.....	22
2.1.2.4. Current Collectors.....	22
2.1.3. Battery Overview.....	23
2.2. Nickel-Zinc Batteries.....	25
2.2.1. Chemistry of Rechargeable Nickel-Zinc Cell.....	26
2.2.1.1. Nickel-Zinc Thermodynamics.....	28
2.2.1.2. Nickel-Zinc Kinetics.....	34
2.2.1.3. Electrode Porosity.....	41
2.2.2. Issues with Rechargeable Nickel-Zinc Batteries.....	45
 CHAPTER 3. MODELING .....	 46
3.1. Challenges in Modeling a Nickel-Zinc Cell.....	51
3.2. Modeling 1D Nickel-Zinc Battery.....	52
3.2.1. Introduction to Modeling with FEM .....	52
3.2.2. Model Definition.....	53
3.2.3. Electrochemical Reactions.....	53
3.2.4. Physics Setup.....	55
3.2.5. Boundary Conditions.....	57
3.2.6. Model Parameters and Variables.....	57
3.3. Results and Discussions.....	57
3.3.1. Results for Various Zinc Initial Concentrations.....	63
3.3.1.1. Cell Voltage.....	63
3.3.1.2. Zinc and Zinc Oxide Species Concentration Changes.....	64

3.3.1.3. Nickel Oxyhydroxide and Nickel Hydroxide Species Concentration Changes.....	67
3.3.1.4. Porosity Changes.....	70
3.3.2. Results for Various Nickel Oxyhydroxide Initial Concentrations .....	72
3.3.2.1. Cell Voltage.....	72
3.3.2.2. Zinc and Zinc Oxide Species Concentration Changes.....	73
3.3.2.3. Nickel Oxyhydroxide and Nickel Hydroxide Species Concentration Changes.....	76
3.3.2.4. Porosity Changes.....	78
3.3.3. Results for Various Transfer Coefficients for Zinc Electrode Reaction .....	80
3.3.3.1. Cell Voltage.....	81
3.3.3.2. Zinc and Zinc Oxide Species Concentration Changes.....	81
3.3.3.3. Nickel Oxyhydroxide and Nickel Hydroxide Species Concentration Changes.....	83
3.3.3.4. Porosity Changes.....	86
3.3.4. Results for Various Transfer Coefficients for Nickel Electrode Reaction .....	88
3.3.4.1. Cell Voltage.....	88
3.3.4.2. Zinc and Zinc Oxide Species Concentration Changes.....	89
3.3.4.3. Nickel Oxyhydroxide and Nickel Hydroxide Species Concentration Changes.....	91
3.3.4.4. Porosity Changes.....	94
CHAPTER 4. CONCLUSIONS.....	97
REFERENCES.....	99
APPENDIX A. TABLES OF PARAMETERS AND VARIABLES.....	103



# LIST OF FIGURES

<b><u>Figure</u></b>	<b><u>Page</u></b>
Figure 1.1. Energy conversion flowchart .....	3
Figure 2.1. Simple prismatic electrochemical cell structure .....	20
Figure 3.1. 1D geometry of the modeled NiZn battery cell .....	53
Figure 3.2. Geometry of the experimental battery .....	59
Figure 3.3. Discharge voltage test results of the experimental battery .....	61
Figure 3.4. Discharge voltage according to the initial input parameters .....	61
Figure 3.5. Discharge voltage over time for three different initial Zn concentrations .....	64
Figure 3.6. Zn and ZnO concentrations inside NiZn cell for initial Zn concentration of 50 kmol/m <sup>3</sup> .....	65
Figure 3.7. Zn and ZnO concentrations inside NiZn cell for initial Zn concentration of 100 kmol/m <sup>3</sup> .....	66
Figure 3.8. Zn and ZnO concentrations inside NiZn cell for initial Zn concentration of 115.2 kmol/m <sup>3</sup> .....	66
Figure 3.9. NiOOH and Ni(OH) <sub>2</sub> concentrations inside NiZn cell for initial Zn concentration of 50 kmol/m <sup>3</sup> .....	67
Figure 3.10. NiOOH and Ni(OH) <sub>2</sub> concentrations inside NiZn cell for initial Zn concentration of 100 kmol/m <sup>3</sup> .....	68
Figure 3.11. NiOOH and Ni(OH) <sub>2</sub> concentrations inside NiZn cell for initial Zn concentration of 115.2 kmol/m <sup>3</sup> .....	69
Figure 3.12. Porosity changes for initial Zn concentration of 50 kmol/m <sup>3</sup> .....	70
Figure 3.13. Porosity changes for initial Zn concentration of 100 kmol/m <sup>3</sup> .....	71
Figure 3.14. Porosity changes for initial Zn concentration of 115.2 kmol/m <sup>3</sup> .....	71
Figure 3.15. Discharge voltage over time for three different initial NiOOH concentrations .....	73
Figure 3.16. Zn and ZnO concentrations inside NiZn cell for initial NiOOH concentration of 75 kmol/m <sup>3</sup> .....	74
Figure 3.17. Zn and ZnO concentrations inside NiZn cell for initial NiOOH concentration of 150 kmol/m <sup>3</sup> .....	75

Figure 3.18.	Zn and ZnO concentrations inside NiZn cell for initial NiOOH concentration of 300 kmol/m <sup>3</sup> .....	75
Figure 3.19.	NiOOH and Ni(OH) <sub>2</sub> concentrations inside NiZn cell for initial NiOOH concentration of 75 kmol/m <sup>3</sup> .....	76
Figure 3.20.	NiOOH and Ni(OH) <sub>2</sub> concentrations inside NiZn cell for initial NiOOH concentration of 150 kmol/m <sup>3</sup> .....	77
Figure 3.21.	NiOOH and Ni(OH) <sub>2</sub> concentrations inside NiZn cell for initial NiOOH concentration of 300 kmol/m <sup>3</sup> .....	78
Figure 3.22.	Porosity changes for initial NiOOH concentration of 75 kmol/m <sup>3</sup> .....	79
Figure 3.23.	Porosity changes for initial NiOOH concentration of 150 kmol/m <sup>3</sup> ....	79
Figure 3.24.	Porosity changes for initial NiOOH concentration of 300 kmol/m <sup>3</sup> .....	80
Figure 3.25.	Discharge voltage over time for three anodic transfer coefficients for zinc electrode reaction .....	81
Figure 3.26.	Zn and ZnO concentrations inside NiZn cell when the anodic transfer coefficient for zinc electrode reaction is 0.5 .....	82
Figure 3.27.	Zn and ZnO concentrations inside NiZn cell when the anodic transfer coefficient for zinc electrode reaction is 1 .....	82
Figure 3.28.	Zn and ZnO concentrations inside NiZn cell when the anodic transfer coefficient for zinc electrode reaction is 1.5 .....	83
Figure 3.29.	NiOOH and Ni(OH) <sub>2</sub> concentrations inside NiZn cell when the anodic transfer coefficient for zinc electrode reaction is 0.5 .....	84
Figure 3.30.	NiOOH and Ni(OH) <sub>2</sub> concentrations inside NiZn cell when the anodic transfer coefficient for zinc electrode reaction is 1 .....	85
Figure 3.31.	NiOOH and Ni(OH) <sub>2</sub> concentrations inside NiZn cell when the anodic transfer coefficient for zinc electrode reaction is 1.5 .....	86
Figure 3.32.	Porosity changes when the anodic transfer coefficient for zinc electrode reaction is 0.5 .....	87
Figure 3.33.	Porosity changes when the anodic transfer coefficient for zinc electrode reaction is 1 .....	87
Figure 3.34.	Porosity changes when the anodic transfer coefficient for zinc electrode reaction is 1.5 .....	88
Figure 3.35.	Discharge voltage over time for three anodic transfer coefficients for nickel electrode reaction .....	89

Figure 3.36.	Zn and ZnO concentrations inside NiZn cell when the anodic transfer coefficient for nickel electrode reaction is 0.3 .....	90
Figure 3.37.	Zn and ZnO concentrations inside NiZn cell when the anodic transfer coefficient for nickel electrode reaction is 0.5 .....	90
Figure 3.38.	Zn and ZnO concentrations inside NiZn cell when the anodic transfer coefficient for nickel electrode reaction is 0.7 .....	91
Figure 3.39.	NiOOH and Ni(OH) <sub>2</sub> concentrations inside NiZn cell when the anodic transfer coefficient for nickel electrode reaction is 0.3 .....	92
Figure 3.40.	NiOOH and Ni(OH) <sub>2</sub> concentrations inside NiZn cell when the anodic transfer coefficient for nickel electrode reaction is 0.5 .....	93
Figure 3.41.	NiOOH and Ni(OH) <sub>2</sub> concentrations inside NiZn cell when the anodic transfer coefficient for nickel electrode reaction is 0.7 .....	94
Figure 3.42.	Porosity changes when the anodic transfer coefficient for nickel electrode reaction is 0.3 .....	95
Figure 3.43.	Porosity changes when the anodic transfer coefficient for nickel electrode reaction is 0.5 .....	95
Figure 3.44.	Porosity changes when the anodic transfer coefficient for nickel electrode reaction is 0.7 .....	96

## LIST OF TABLES

<b><u>Table</u></b>	<b><u>Page</u></b>
Table 2.1. SOC indication methodologies .....	15
Table 2.2. NiZn battery reactions .....	27
Table A.1. Parameters used in the model .....	103
Table A.2. Variables used in the model .....	105

# LIST OF SYMBOLS AND ABBREVIATIONS

## Abbreviations

BP	Back Propagation
BV	Butler-Volmer
D	Dimensional
DOC	Depth-Of-Charge
DOD	Depth-Of-Discharge
EKF	Extended Kalman Filter
EMF	Electromotive Force
FDM	Finite Difference Method
FEA	Finite Element Analysis
FEM	Finite Element Method
FVM	Finite Volume Method
LPG	Liquefied Petroleum Gas
Mtoe	Million tons of equivalent
NPG	Natural Petroleum Gas
OCV	Open Circuit Voltage
RBF	Radial Basis Function
RDS	Rate Determining Step
SOC	State-Of-Charge
SOH	State-Of-Health
SVM	Support Vector Machine
UPS	Uninterrupted Power Supply

Symbol	Definition	Unit
$\Delta G$	Gibbs free energy	kJ/mol
$\Delta G^\circ$	Gibbs free energy at standard conditions	kJ/mol
$\Delta G^\ddagger$	Free energy of activation	kJ/mol
$\Delta G^\ddagger_\circ$	Standard free energy of activation	kJ/mol
$\Delta G^\ddagger_a$	Anodic free energy of activation	kJ/mol
$\Delta G^\ddagger_c$	Cathodic free energy of activation	kJ/mol
$\Delta S$	Entropy change	J/K

$\Delta S_{\text{surrounding}}$	Entropy change in the surrounding of a system	J/K
$\Delta S_{\text{system}}$	Entropy change in a system	J/K
$\Delta S_{\text{universe}}$	Entropy change in the universe	J/K
$\Delta t$	Time step	s
$A$	Electrode surface area	$\text{cm}^2/\text{cm}^3$
$A_{\text{fq}}$	Frequency factor	
$a_i$	Activation of species i	
$a_{\text{Tf}}$	First Tafel constant	
$Br$	Bruggemann coefficient	
$b_{\text{Tf}}$	Second Tafel constant	
$C$	Binary electrolyte concentration	$\text{mol}/\text{m}^3$
$C_o$	Solvent concentration	$\text{mol}/\text{m}^3$
$C^\circ$	Standard concentration	$\text{mol}/\text{m}^3$
$C_i$	Concentration of species i	$\text{mol}/\text{m}^3$
$C_{i,\text{ref}}$	Reference (or initial) species concentration	$\text{mol}/\text{m}^3$
$C_i^*$	Bulk concentration of species i	$\text{mol}/\text{m}^3$
$C_j$	Concentration of species j	$\text{mol}/\text{m}^3$
$C_{j,\text{eq}}$	Saturated or equilibrium concentration of species j	$\text{mol}/\text{m}^3$
$D$	Chemical diffusivity	$\text{m}^2/\text{s}$
$D^\circ$	Chemical diffusivity at standard conditions	$\text{m}^2/\text{s}$
$E$	Measured potential	V
$e^-$	Electron	
$E^\circ$	Standard electrode potential	V
$E^{\circ'}$	Formal electrode potential at standard conditions	V
$E_{\text{cell}}$	Cell potential	V
$E_{\text{cell}}^\circ$	Cell potential at standard conditions with respect to reference electrode	V
$E_{\text{eq}}$	Equilibrium potential	V
$E_{\text{halfrxn}}$	Potential of half-reaction	V
$E_{\text{halfrxn}}^\circ$	Potential of half-reaction at standard conditions	V
$E_{\text{halfrxn}}^{\circ'}$	Formal half-reaction potential at standard conditions	V
$E_{\text{OCV}}$	Open cell voltage	V
$E_{\text{oxidation}}^\circ$	Potential of oxidation reaction at standard conditions	V

with respect to reference electrode

$E_{\text{reduction}}^{\circ}$	Potential of reduction reaction at standard conditions with respect to reference electrode	V
F	Faraday constant	96485.333 C/mol
f	Activity coefficient	
G	Gibbs free energy	kJ/mol
$G^{\circ}$	Gibbs free energy at standard conditions	kJ/mol
H	Enthalpy	kJ
$H^{\circ}$	Enthalpy at standard conditions	kJ
I	Discharge current	A
$I_{\text{ch}}$	Charging current	A
$I_{\text{cor}}$	Corrected current	A
i	Current density	$\text{A/m}^2$ or $\text{A/cm}^2$
$i_0$	Exchange current density	$\text{A/m}^2$ or $\text{A/cm}^2$
$i_a$	Anodic current density	$\text{A/m}^2$ or $\text{A/cm}^2$
$i_c$	Cathodic current density	$\text{A/m}^2$ or $\text{A/cm}^2$
$i_l$	Superficial current density in electrolyte	$\text{A/m}^2$ or $\text{A/cm}^2$
$i_{\text{loc}}$	Local current density	$\text{A/m}^2$ or $\text{A/cm}^2$
$i_s$	Superficial current density in the solid matrix	$\text{A/m}^2$ or $\text{A/cm}^2$
$i_t$	Total current density of solid matrix and electrolyte current density components in a porous electrode	$\text{A/m}^2$ or $\text{A/cm}^2$
$j_0$	Exchange current density	$\text{A/m}^2$ or $\text{A/cm}^2$
K	Thermodynamic equilibrium constant	
$k^{\circ}$	Standard rate constant	
$k_b$	Backward reaction rate constant	
$k_f$	Forward reaction rate constant	
$k_i$	Experimental constants	
$k_{\text{mod}}$	Modified chemical rate constant	
$M_i$	Molecular weight or molecular mass of species i	g/mol
n	Molar number of transferred electrons	
$n_a$	Number of transferred electrons during RDS	
$n_b$	Number of transferred electrons before RDS	

$N_i$	Average flux density of species i	mol/cm <sup>2</sup> ×s
Oxd	Oxidized species	
pH	Acidity level	
Q	Capacity	Ah or C
$Q_n$	Nominal capacity	Ah or C
$Q_{rxn}$	Reaction quotient	
R	Universal gas constant	8.3143 J/mol×K
Red	Reduced species	
$R_{src,i}$	Reaction source term of species i	
S	Entropy	J/K
$S^\circ$	Entropy at standard conditions	J/K
T	Temperature in Kelvin	K
t	time	s
$t_{ch}$	Charging time	s
$t_{i,o}$	Transport or transference number of species i with respect to the solvent	
$t_i^\sim$	Transport or transference number of species i relative to $v^\sim$	
$v^\sim$	Superficial volume average velocity	cm/s
$W_{electrical}$	Electrical work	W
x	x coordinate	m
$z_i$	Charge number of species i	
$\alpha_a$	Anodic transfer coefficient	
$\alpha_c$	Cathodic transfer coefficient	
$\beta$	Symmetry factor of transfer coefficient for cathodic component of a single step single electron reaction	
$\epsilon$	Porosity or void volume fraction	
$\gamma_i$	Activation coefficient of species i	
$\eta$	Overpotential	V
$\vartheta_b$	Backward reaction rate	mol/cm <sup>2</sup> ×s
$\vartheta_f$	Forward reaction rate	mol/cm <sup>2</sup> ×s
$\vartheta_{net}$	Net reaction rate	mol/cm <sup>2</sup> ×s
$\kappa$	Effective ionic conductivity	S/cm



$\kappa^\circ$	Ionic conductivity at standard conditions	S/cm
$\mu_i$	Chemical or electrochemical potential of the electrolyte	J/mol
$\rho_i$	Density of species i	g/cm <sup>3</sup> or kg/m <sup>3</sup>
$\sigma$	Effective electronic conductivity	S/cm
$\sigma^\circ$	Electronic conductivity at standard conditions	S/cm
$\nu_o$	Stoichiometric coefficient of the solvent	
$\nu_i$	Stoichiometric coefficient of species i	
$\nu_i''$	Stoichiometric coefficient of species i being part of a chronologically second electrode reaction	
$\varphi_i$	Number of moles of produced species i	
$\phi_l$	Electric potential of the electrolyte solution	V
$\phi_s$	Electric potential of the solid matrix	V

### Subscripts

i	Species (vary as: +, -, o, O, R)
j	Secondary species other than species i
+	Positive ions or cations
-	Negative ions or anions
O	Oxidized species
R	Reduced species
o	Solvent

# **CHAPTER 1**

## **INTRODUCTION**

This dissertation focuses to develop a battery model for nickel-zinc chemistry using finite element method based on mathematical models covering thermodynamic and kinetic specifications for oxidation-reduction reactions occurring in porous electrodes.

Having a model in a long lasting period of experiments to solve a problem is a crucial need to diminish the time, effort and cost. Creating a model requires a thorough analysis of the method and associated problems as well as the possible solutions that have been offered until today in order to save modeling time and suggest an alternate but a more advanced and comprehensive model. The reason of the study mentioned in this dissertation is the fact that one of the major energy issues is the electrical storage incapacity and the best candidates to solve this problem is battery technologies. However, battery technologies suffer from many problems and need a breakthrough achievement.

### **1.1 Dimensions and Units**

The definition of a scientific problem and the explanation of its solution require well defined dimensions and precise expressions with units. Dimensions are the independent characteristics of an occurring phenomenon. For instance, when characteristics are length, mass, temperature and time for a mechanical phenomenon their units are meter, kilogram, Kelvin or Celsius and second respectively if the “International System of Units” is being used. The abbreviation of this system is “SI Units”. There are also United States Customary Measurement System and Imperial Units of Measure System which are currently in use. SI Units are used in this dissertation.

## 1.2 Nomenclature

Present study has been made according to the assumption of isothermal process under *the standard conditions* which refers to the ambient temperature of 25 degree of Celcius, ambient pressure of 1 atm (IUPAC 2014, 1435).

Vectoral expressions are differentiated from scalar expressions by using bold type scripts.

## 1.3 Energy and Associated Problems

From the very beginning of the human history, comfort and good living conditions have been related to the availability of energy sources. Use of wood as an energy source for cooking and heating can be considered as one of the earliest examples of using energy to enhance the quality of life. Humankind also used animals such as horses and camels for transportation as well as in agriculture for cultivation which led to an increased productivity of the fields.

The invention of the steam engine by James Watt radically changed the achievable power amount. Thermal energy of coal that was used to heat water and pressure of vaporized water in a constant volume was very powerful. Trains that were manufactured by tons of metals or enormous ships could be moved by the power of pressurized vapor. This power source was also used in manufacturing of goods. The thermal energy obtained from coal was already being used in the metal works. After the steam engine era, the discovery of oil as an energy source and the invention of the refining process of oil led to the inventions of Otto engine, diesel engine, jet engine which are still in use today in automobiles, trucks, planes, ships and in many other kind of vehicles which make life easier, comfortable and more productive. Thermal energy obtained from wood, coal and oil is a result of chemical reactions originated by the chemical energy contained in these sources. Because of their nature, those energy sources are economically very advantageous. They are ready to use, already stored in nature. They can be transported easily. There is no need for specialized sophisticated storage technology to store wood, coal or oil. Wood and coal can be transported with ships or trucks, and oil can be transported in the same ways with barrels, yet there exists another method of transportation for oil which is system of pipelines since oil is in the

liquid phase. Despite the fact that internally combustion engines operate with low rate of efficiency compared to electric engines, they are the dominant engine type for transportation vehicles for over a century, because storing electrical energy is not effective and it is expensive for transportation.

When it comes to two other types of fossil fuels which are “Natural Petroleum Gas” and “Liquefied Petroleum Gas” (NPG and LPG respectively), storage technology gets more sophisticated. These gases can be delivered by ships after liquidification under pressure or as gas with a pipeline network. LPG is being used in thermal power plants, cars, and houses through conversion of chemical energy into thermal energy.

However, there is another form of energy that it is very important for the people and that is the electrical energy. This form of energy is the milestone of today’s technological achievements: Electronics, computers, telecommunication, satellites and many more devices and tools that allow man to create more sophisticated technologies and systems and the ability to control them.

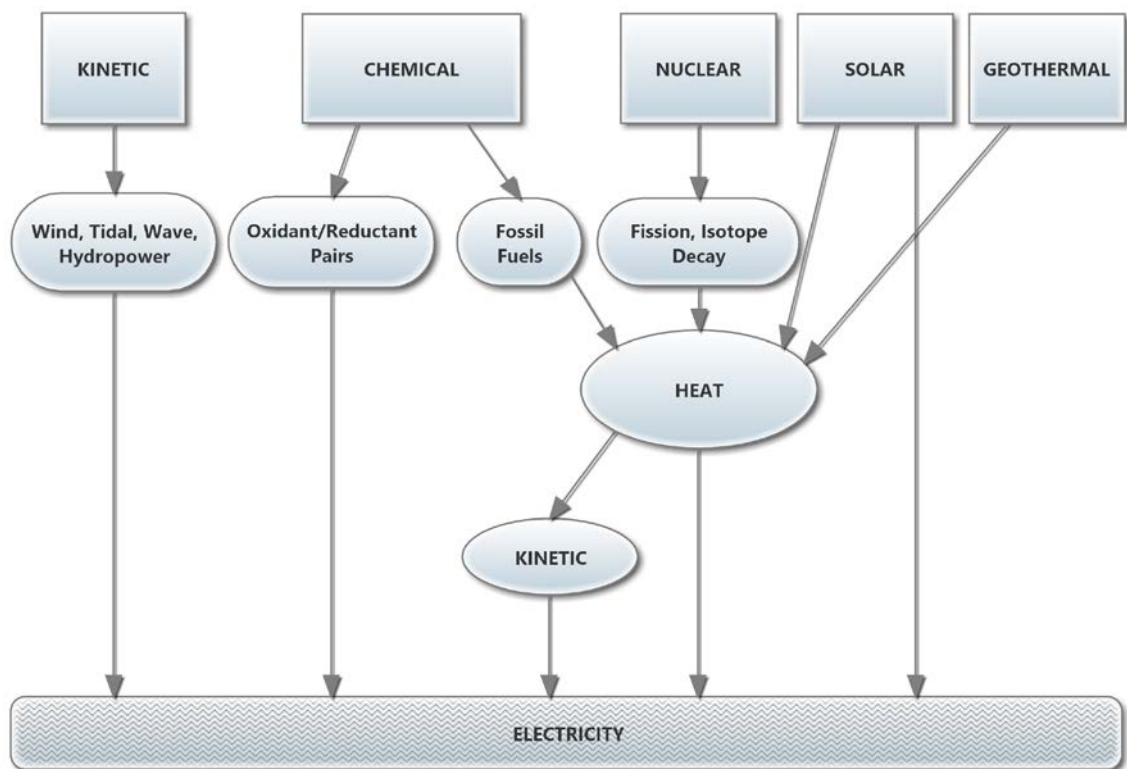


Figure 1.1. Energy conversion flowchart.

The positive aspects of the electricity are that it is clean, easily conductible, very convenient for household utilization in both urban and rural areas, and the possibility to

use it to store or to deliver data. Because of these advantages, electrical energy has the biggest supply chain in the world. Electricity can be generated by chemical reactions or as a result of a conversion process from kinetic, thermal, or solar energy (Walsh 1967).

Figure 1.1 demonstrates a simple flowchart of energy conversion into electrical energy from different forms of energy and the major sources in use for those said different forms. Direct electricity generation from solar energy source is done with photovoltaic cells whereas direct energy conversion from thermal energy to electrical energy is done with devices called thermocouples and thermionics. Conversion of kinetic energy to electrical energy is done with an electric machine called generator. However, generators require rotational force to rotate its mechanical part called rotor. Natural forces are unable to rotate a rotor directly, that is the reason a mechanical process is needed. In this mechanical process, kinetic energy of natural forces are collected and turned into rotational motion by using a machine called turbine which converts fluid motion into rotational motion. As a result, conversion of natural kinetic energy into electrical energy requires two steps; kinetic to kinetic energy, then kinetic to electrical energy. This method is the primary technique to generate electricity. Examples to the source of kinetic energy can be given as wind, tide, marine waves, collected water in dams or convective fluid motion caused by thermal energy transferred into a fluid which is mostly water that it turns to vapor phase after being heated. The source of thermal energy might be nuclear energy, chemical energy of a fossil fuel such as coal, natural gas, oil, organic wastes such as biogas, biomass or household garbage, geothermal energy or concentrated solar beam energy (Walsh 1967; Goswami and Kreith, eds. 2007).

The hydrostatic pressure of collected water and the convective fluid motion are mechanically controllable processes. This brings the facility to engineers and technicians for sustainable electricity generation. Electricity generation from hydrostatic pressure of collected water process happens in dams where the collected water gains potential energy with increasing level and pressure. The potential energy is then converted to kinetic energy when the hatches are opened. Adjusted water flow is channeled into the turbines which convert flow motion into rotational motion to turn the rotor of the generators (Goswami and Kreith, eds. 2007).

Electricity generation from convective fluid motion process contains three steps of conversion and four energy forms which are chemical energy, thermal energy, kinetic energy and electrical energy. The major sources of this process are fossil fuels and

nuclear fuel. Production of biogas, biomass and garbage is very limited. The use of fossil and nuclear fuels causes several environmental problems. Air pollution and the climate change are the results of the use of fossil fuels for decades and radioactive impacts are caused by radioactive wastes and incidents. Vehicles with combustion engines or jet engines do not generate electricity for the grid but they use same energy conversion principles to get the kinetic energy for their motion and the residues of their processes have similar environmental impacts.

The aforementioned environmental problems have resulted in an increased attention and interest towards renewable energy sources such as wind, tide, wave, solar, and geothermal energy technologies. Geothermal power plants use thermal energy of water sources by exchanging the heat of the geothermal water into clean water which changes phase and becomes vapor. This vapor enters a turbine to generate electricity. Alternatively, the clean water does not change phase during the exchange and go into a network of pipes delivering heat to buildings. The performance of this method depends on the amount of geothermal wells, the temperature limits of the wells, and the achievable mass flow rates (DiPippo 2012).

The major problem with the wind, tide, wave and solar energy sources is the lack of constant availability and stability, i.e., the energy source which enters the system is not stable and time to time nothing enters. The electricity generation must be 24/7 when the conditions are normal.

The main problem awaiting a solution with renewable energy technologies is to support those technologies with energy storage options to provide electrical energy all the time. Also those energy sources fluctuate when they enter the system; however, a fluctuating outcome is unacceptable. This is why inverters and rectifiers are commonly used in power electronics. Those devices maintain the output power for use in a power grid; however constant availability requires presence of storage equipment which contains charge controller and battery. In most wind and solar energy applications, multiple batteries are being used to provide electricity in absence of sufficient wind and solar energy.

Lead-acid batteries that are currently in use are heavy, inefficient, have low energy density and have a very negative impact on the environment due to heavy metals and toxic chemicals. However, lead-acid batteries represent the economically cheapest option among commercially available batteries.

Besides grid scale energy storage and batteries for electric vehicles there is another field starving to electrical energy which is consumer electronics covering telecommunication, informatics, data processing, transmission, and storage, and of course electricity storage for portable devices. Portable consumer electronics is a multi-billion dollars market and its growth has been parallel to the development of battery technologies. Cellular phones, notebooks, tablet computers have spread due to the evolution of lithium-ion batteries. Nevertheless, battery technologies need to evolve into better technologies having better specific energy and power density, lighter weight, longer life and being fast chargeable, more secure and environmentally friendly, so that electronic devices can function longer, having more features. In addition, it is important that batteries have low environmental impact and good safety record, but it is crucial for the industry that the batteries are made from abundant materials to meet the increasing global demand considering both the mass production of the final product and the raw material costs.

According to the data of International Energy Agency (2015) the worldwide electricity generation by fuel in 2013 was 23,322,000 GWh. However, the total electrical energy consumption around the world was 1677 Mtoe (IEA 2015) which is equivalent to 19,503,510 GWh. The difference of 3,818,490 GWh is the lost energy. One of the reasons of this loss is the dissipated electrical energy as heat from the transmission lines, i.e., loss in the grid. Efficiency improvements can be done; however, it is impossible to completely eliminate this kind of dissipation with current knowledge and technology. The second reason is that there is not enough storage for electricity. Even though it is not consumed, the generated electrical energy is going to be lost, because of the lack of reserve.

Evidently, there are three fields craving for better electric storage technologies. These fields are renewable energy systems, electrical transportation systems and portable electronic systems.

## CHAPTER 2

### ENERGY STORAGE

Energy storage technologies are expected to have high energy density, high power density, and to be safe, clean and cost efficient.

There are various energy storage methods. Electrochemical storage is the most commonly used one because this storage method has only one step of energy conversion. Electrochemically stored energy is converted into electrical energy via two or more chemical reactions. Single-step conversion makes this method more efficient than others. In addition, electrochemical storage devices and tools tend to be portable, which is not the case for mechanical storage methods such as thermal storage, potential energy storage with a fluid, or pressurized fluid storage (Ter-Gazarian 2011).

There are three electrochemical storage techniques:

- Chemical energy storage for use in fuel cells
- Charge storage in supercapacitors
- Charge storage in batteries

From the 1950s, hydrogen has been considered as the energy source of the future since it is produced from water by electrolysis and the output of electricity generation by a fuel cell using hydrogen is also water. The clean outcome is what makes this technology admirable; however, hydrogen is a very unstable gas. The Hindenburg disaster at May 6th 1937 was a catastrophic event that showed how unsafe was the use of hydrogen. For using hydrogen in fuel cells, a safety method and a technique to decrease the volume of hydrogen without using pressure must be developed, yet fuel cell technology is not effectively in use other than experimental vehicles. Other fuel cell fuels such as methanol are carbon based materials, so their output after the electricity generation is carbon dioxide which is an unwanted output gas because of environmental concerns.

Supercapacitors (also called ultracapacitors or electrochemical double-layer capacitors) are electrochemical storage devices with the ability to charge and discharge very quickly; however, they do not satisfy the need of high energy and high power needs because they are ineffective at high charges. Besides of short shelf life, commonly used electrode material of supercapacitors is ruthenium dioxide, of which



ruthenium is a rare transition metal which is very expensive and toxic. In general terms a metal oxide is a key element to manufacture a supercapacitor and ruthenium dioxide is the most favorable one being used today because of its very good properties in order to meet the required energy and power densities for specific applications (Yu, Chabot and Zhang 2013). Replacing ruthenium dioxide with a cheaper metal oxide and formation of composites of ruthenium with more reasonable amounts are the active research focus for electrochemists in order to make supercapacitors commercially available (Zhao and Zheng 2015).

Today, the supercapacitor's market leader company is Maxwell Technologies, Inc.. Their product range targets both vehicles and integrated electronics. Their products for integrated electronics are aiming to be an alternative to conventional capacitors that has nothing to do with sustainable energy problem. On the other hand their modular products to supply high voltage rates are targeting vehicle market as a complementary part of cranking systems, start/stop systems, regenerative brake systems, and hybrid systems in cars, buses, trucks or trains (Maxwell 2015a). Additional to the vehicle market, the grid storage is also being targeted. Their products' voltage range is between 16 V and 160 V (Maxwell 2015b). For instance, their newest product, a 48 V module with this company's durablue technology aims to be used in hybrid vehicles, rail applications, heavy industrial equipment and UPS (Uninterruptable Power Systems) (Maxwell 2015c). According to the datasheet by Maxwell (2015c), this module's stored energy is 53 Wh which is the combined stored energy of 18 cells with 3.0 Wh energy storage. The 160 V module is to be used in applications of wind turbine pitch control, small UPS and also small industrial systems (Maxwell 2015d). This module provides 21 Wh stored energy, 4 Wh/kg specific energy, 2,500.00 W/kg usable specific power as after the combination of 60 cells that each cell has 0.35 Wh energy storage ability. The 16 V module uses 6 cells that each also having 0.35 Wh energy storage capacity and total stored energy in the module is 2.1 Wh (Maxwell 2015e). Its usable specific power is 2,200 W/kg, and its specific energy is 3.3 Wh/kg.

Despite their usage in the market, supercapacitors cannot be considered as an alternative to batteries, because their benefits satisfy different needs for energy storage. When the fast charge and discharge is required for a limited range of capacities and time, then supercapacitors can be a suitable choice, otherwise there are different types of batteries for high power usage or high energy density needs with reliable shelf life.

The third and the most commonly used electrochemical energy storage devices are batteries.

## **2.1. Batteries**

Battery systems are very important instrument to store energy for later use, mobile usage or back-up utilization. Batteries are categorized under two classes due to the irreversibility and reversibility status of chemical reactions. According to this classification, batteries with irreversible reactions are primary batteries and batteries with reversible reactions are secondary batteries. There exist different chemistries for both classes. The selection of the class and the chemistry for a battery system are mostly dictated by the nature of the problem and economical considerations. For instance silver-zinc batteries are very good; however, they are not in the consumer market because silver is a relatively expensive metal. Molten salt batteries are very effective under harsh operating conditions, so they are preferred in military applications such as cruise missiles. Also same chemistries can be use in both classes of batteries such as primary nickel-zinc and secondary nickel-zinc batteries involving different geometries and different amounts of materials.

### **2.1.1. Terminology and Concepts for Battery Specifications**

The science of a battery system is actually very sophisticated process involving many parameters. As a result, battery scientists and engineers have developed multiple terms and concepts in order to explain the specifications and behavior of the batteries.

#### **2.1.1.1. Primary Battery**

Primary batteries are non-rechargeable batteries. They are operational during one discharge process because their chemical structure leads to irreversible chemical reactions and for that reason it is impossible for primary batteries to return to their initial state (Technical Marketing Stuff of Gates Energy Products 1992; MIT Electric Vehicle Team 2008).

### **2.1.1.2. Secondary Battery**

Secondary batteries are rechargeable batteries. They are also called as storage batteries or accumulator depending on the field of application. The accumulator term is being used for the starter batteries used in vehicles with internal combustion engine. The chemical reaction occurring in these batteries are reversible. However, there are always some thermodynamic irreversibilities which prevent the battery to reinstate its exact initial characteristics (Technical Marketing Stuff of Gates Energy Products 1992; MIT Electric Vehicle Team 2008).

### **2.1.1.3. Cell, Module and Pack**

Any system consisting of electrochemical cells and able to provide electricity can be defined as a battery (Technical Marketing Stuff of Gates Energy Products 1992). In order to explain the distinction there are couple of terms that have to be defined. These are cell, module and pack (MIT Electric Vehicle Team 2008).

A cell or an electrochemical cell is the simplest electrochemical unit. It is the chemical system that converts electrical energy into chemical energy or vice versa. Its voltage depends on the electrochemistry of its components (MIT Electric Vehicle Team 2008). For instance, the open cell voltage for nickel-zinc cell is 1.854 volts and for nickel-cadmium it is 1.3 volts (Vincent and Scrosati 1997).

A module is formed up with more than one cell connected to each other either in series or in parallel (MIT Electric Vehicle Team 2008).

A battery is formed up with one or more cell but it contains also current collectors and necessary insulations to be ready for usage. Generally, the calculations and measurement are made for one cell in the design process and the results are multiplied with the number of total cells to reach the values of the battery (Technical Marketing Stuff of Gates Energy Products 1992).

A pack is the ensemble of modules connected to each other in series or in parallel (MIT Electric Vehicle Team 2008).

#### **2.1.1.4. Capacity**

The capacity is the available amount of electrons for a single use. The availability of electrons per unit time is the definition of a current, so the capacity is the integration of current over the period of time that the battery operates. The unit of the capacity is often ampere-hours (Ah), but Coulomb (C) can also be used. Capacity is related to the amount of active materials inside the battery. There are two types of capacity: theoretical capacity and nominal capacity. Theoretical capacity is a value calculated with the equations obtained via empirical methods. On the other hand, nominal capacity is the capacity in practice. The maximum capacity is defined for certain discharge conditions and indicates the upper limit for the achievable capacity (Linden and Reddy, eds. 2002; MIT Electric Vehicle Team 2008).

#### **2.1.1.5. Energy**

Energy is the integration of power over time and power is the product of voltage and current. The unit of energy is Joules (J) or watt-hours (Wh). Energy of a battery is the available energy of a discharge process or the required energy for a charge process (Linden and Reddy, eds. 2002; MIT Electric Vehicle Team 2008).

#### **2.1.1.6. C Rate**

Because of batteries having different nominal capacities related to chemistry or size, a scaling parameter is a need to determine a certain characteristic of a battery that it is the relation of discharge or charge current with the nominal capacity. 1C is defined as the amount of current to charge or discharge a battery within 1 hour. For instance, for a battery having a nominal capacity of 1 Ah, the 1C current is 1 A. A 2C current is 2 A and 1/10C current is 0.1 A (Technical Marketing Stuff of Gates Energy Products 1992; MIT Electric Vehicle Team 2008).

#### **2.1.1.7. Power Density**

Power density is the achievable power per unit weight or volume from a battery. The units are Watts per kilogram (W/kg) for weight based power density and Watts per liter (W/L) for volume based power density. In certain occasions, instead of liter (L), cubic meter ( $m^3$ ) can be used. Weight based power density is also mentioned as gravimetric power density and the volume based power density is also called as volumetric power density (MIT Electric Vehicle Team 2008).

#### **2.1.1.8. Energy Density**

The definition of energy density is based on weight or volume of the battery and is described as the extractable amount of energy from unit weight or volume. For weight based energy density, the unit is generally Watts-hour per kilogram (Wh/kg) and for volume based energy density, it is Watts-hour per liter (Wh/L). The volume based energy density is also called as volumetric energy density and the weight based is referred as gravimetric energy density (MIT Electric Vehicle Team 2008; Texas Instruments 2011).

#### **2.1.1.9. Cycle Life**

The cycle life is the total number of charge/discharge cycles of a battery until the battery become incapable to deliver its designated performance (MIT Electric Vehicle Team 2008). Batteries are generally considered that they fail to meet their designated performance criteria when their nominal capacity decreases to less than 80% of its rated capacity (Linden and Reddy, eds. 2002; Pop et al. 2008).

#### **2.1.1.10. Self-Discharge**

Self-discharge is the loss of electric potential of a charged battery with time regardless of the battery being in use or not (Technical Marketing Stuff of Gates Energy

Products 1992). This phenomenon occurs due to the interactions of the chemical components of the battery, so the self-discharge rate is related to the chemistry and the temperature (Pop et al. 2008). The loss of electric potential is recoverable for a certain time interval; however, if the battery is not charged for a longtime then the loss becomes unrecoverable. This also means that the battery becomes incapable to store energy because the chemicals have reached their thermodynamic equilibrium. The limit of this duration is called as shelf-life.

#### **2.1.1.11. Open-circuit Voltage**

Open-circuit voltage is the electric potential between anode and cathode terminals of a battery when there is no load placed between them (MIT Electric Vehicle Team 2008).

#### **2.1.1.12. Terminal Voltage**

Terminal voltage is the electric potential between anode and cathode terminals of a battery when an electric load is installed between them (MIT Electric Vehicle Team 2008). Terminal voltage is smaller than the open circuit voltage due to the effects of the load.

#### **2.1.1.13. Short-circuit Current**

The short-circuit current is the current observed when the terminals of a battery are short circuited with a conductor having low resistivity. Short-circuit between battery terminals results in a large charge flux in a short period of time, which exceeds the limits required for the safety and the proper performance of a battery and might lead to a fast over-heating or even explosion in case of high capacity batteries.

#### **2.1.1.14. State-Of-Health (SOH)**

State-Of-Health (SOH) is an indicator for a battery expressing the operational conditions, status in providing the expected electrical properties and the comparison of the final behavior of the battery to its conditions and abilities at the beginning (Pop et al. 2008).

#### **2.1.1.15. State-Of-Charge (SOC)**

State-Of-Charge (SOC) is a percentage expression which momentarily indicates the available capacity of a battery (Pop et al. 2008).

SOC is one of the most used battery term because it is important to know the charge capacity of a battery to predict how long it is going to endure while it is in use. Battery based applications need to use SOC datum for system controlling and dynamic power management of systems. Hybrid electric vehicles, battery efficient communication systems and information technology systems are having the lead on this need (Xiao, Shi, and He 2010). In addition, SOC datum is very useful for modeling and simulation of a battery. However, it is difficult to determine its exact value in practice, so SOC is merely an estimation based on measurements which are sensitive to the non-stabilities of certain parameters, e.g., battery capacitance, battery impedance, temperature (Vairamohan 2002) and cycle life (Chang 2013). Parameters about the battery characteristics can differ even between batteries with same chemistry.

A basic mathematical definition of SOC can be represented as (Chang 2013):

$$SOC = \frac{Q(t)}{Q_n} \quad (2.1)$$

Here,  $Q(t)$  is the current capacity and  $Q_n$  is the nominal capacity which is an information given by the manufacturer and it is the maximum capacity of the battery. The SOC is the proportion of current capacity to nominal capacity and it is shown as a percentage.

There are several mathematical methods to estimate SOC. These methods can be categorized according to their application techniques. These categories are direct

measurement methods, book keeping systems, adaptive systems and hybrid systems (Pop et al. 2008; Chang 2013).

*Direct measurement methodology* aims to measure physical parameters of a battery: electric potential and battery impedance.

*Book keeping systems* measure discharge current and integrates it over time to estimate a SOC value.

*Adaptive systems* are electronic systems using algorithms able to adapt automatically to discharge current in order to estimate SOC. These systems use neural networks or adaptive filters to overcome the nonlinear variations of a battery due to numerous chemical issues (Chang 2013).

*Hybrid systems* use a combination of at least two methods and they aim to optimize the estimation process by eliminating the disadvantages of individual methods.

In Table 2.1 four categories and the methods in these categories are demonstrated (Pop et al. 2008; Chang 2013).

Table 2.1. SOC indication methodologies.

<b>Categories of Methodology</b>	<b>Methods</b>
Direct Measurement	Open circuit voltage (OCV) also known as EMF measurement Terminal potential difference measurement Impedance measurement Impedance spectroscopy investigation
Book keeping systems	Coulomb (Ah) counting Modified Coulomb counting
Adaptive systems	Back propagation (BP) neural network Radial basis function (RBF) neural network Support vector machine (SVM) Fuzzy neural network Kalman filters
Hybrid systems	Coulomb counting & EMF combination Coulomb counting & Kalman filter combination Per-unit system and EKF combination



There are many methods that can be employed to estimate SOC; however, not all of them are applicable for all battery chemistries and all of those methods have specific advantages and disadvantages. Impedance spectroscopy, book keeping systems and adaptive systems are applicable for all battery chemistries. The rest of the methods are applicable particularly for lead and lithium based batteries. Adaptive systems are using adaptive filters such as Kalman filters which are applicable for all battery systems and also for photovoltaic systems; however, applying Kalman filters is difficult because of the complexity of setting an algorithm including all the qualifications for an indication (Pop et al. 2008; Chang 2013). For instance, it requires including abnormalities and nonlinearities into computations (Pop et al. 2008). On the other hand, voltage measurement technique is a simple direct measurement method but it lacks accuracy. Effectiveness and simplicity are essential for SOC indication systems.

Most commonly used technique is Coulomb counting (also known as Ah counting technique) (Pop et al. 2008; Wang et al. 2013) which is a book keeping method. This technique involves measuring the charge flow due time into or out of the battery, collecting the data and when a threshold is reached, using them in an integral calculation to estimate SOC. The mathematical formulation that this method uses (Chang 2013):

$$\text{SOC}(t) = \text{SOC}(t - 1) + \frac{I(t)}{Q_n} \Delta t \quad (2.2)$$

Here  $I(t)$  is the discharge current,  $\text{SOC}(t - 1)$  is the previously estimated SOC value,  $Q_n$  is the nominal charge and  $\Delta t$  is the time step for numerical calculations.

Temperature, discharge current, cycle life and the battery usage has an effective role on the accuracy of this method. Based on this particular method, there is also *modified Coulomb counting method* which uses a corrected current value, a function of discharge current (Chang 2013):

$$I_{\text{cor}}(t) = k_2 I(t)^2 + k_1 I(t) + k_0 \quad (2.3)$$

In this equation  $k_2$ ,  $k_1$ , and  $k_0$  are constants obtained from experiments. After using this corrected current value, the SOC equation becomes:

$$\text{SOC}(t) = \text{SOC}(t - 1) + \frac{I_{\text{cor}}(t)}{Q_n} \Delta t \quad (2.4)$$

The Coulomb counting method is being used in cell phones, laptops and other SOC estimation capable electronic devices and the main role belongs to the specialized integrated circuits made by microelectronic companies such as Texas Instruments and Maxim Integrated (Pop et al. 2008).

There is also another method, a chemical one. It is called *the specific gravity method*, which is based on the measurement of the specific gravity of the electrolyte. For the measurement of the specific gravity, a device called hydrometer is being used. According to this method, the specific gravity and the pH values of the electrolyte are measured and used to estimate SOC value. This method is only applicable to stationary setups, and if the liquid electrolyte of the battery is accessible; hence this method is unusable for sealed batteries (Pang et al. 2001).

#### **2.1.1.16. Depth-Of-Discharge (DOD)**

Most of the rechargeable battery chemistries do not allow using the entire maximum cell capacity; otherwise battery would lose its rechargeability. Depth-of-discharge (DOD) expresses the instantaneous percentage ratio of the used capacity over the maximum capacity. Less than 80% of DOD is considered to be risky for most battery chemistries to keep their rechargeability and 80% DOD and below is called deep-discharge (Pop et al. 2008; MIT Electric Vehicle Team 2008). DOD is the inverse of SOC. When 80% DOD is mentioned this corresponds to 20% SOC. Accordingly 100% DOD corresponds to 0% SOC and 0% DOD to 100% SOC.

#### **2.1.1.17. Depth-Of-Charge (DOC)**

Depth-of-charge (DOC) is the percentage ratio of the charged capacity of a battery referred to its maximum capacity (Pop et al. 2008). DOC is a similar term to SOC but not the same. When SOC is a function of OCV, DOC is the function of the charging current ( $I_{\text{ch}}$ ), the charging time ( $t_{\text{ch}}$ ), and the nominal capacity ( $Q_n$ ) (Snihir et al. 2006):

$$DOC(t) = \frac{I_{ch} \times t_{ch}}{Q_n} \quad (2.5)$$

At the beginning of the charging period the SOC and DOC increase similarly, but after reaching approximately to the half charge they begin to differentiate. At this point SOC increases at slower rate than DOC because of the chemical issues such as side reactions. This difference causes deviations in computations of DOC or SOC (Snihir et al. 2006).

#### **2.1.1.18. Nominal Voltage**

The nominal voltage is the accepted operating electric potential for certain battery chemistry and it is being used as reference voltage with other applications having the same chemistry (Linden and Reddy, eds. 2002; MIT Electric Vehicle Team 2008).

#### **2.1.1.19. Cut-off Voltage**

Batteries begin to be discharged from a certain voltage value and then this value decreases with time and use. There exists a critical voltage value under which the battery stops functioning. This critical voltage is the cut-off voltage. A battery is assumed to be depleted when its cell voltage drops below its cut-off voltage which is determined by the battery chemistry. In reality there are still some capacity keeping the battery rechargeable (Pop et al. 2008).

#### **2.1.1.20. Charge Voltage**

Charging process is actually forcing electrons to move toward the opposite of the direction that they tend to move. Naturally, this forced action requires more electric potential than the discharge potential and it is called the charge voltage.

#### **2.1.1.21. Charge Current**

Battery management system design focuses to the optimization of battery charging and discharging in order to increase the lifetime of the batteries. As a charging method using constant current is another option than using constant voltage. The constant current here is the charge current and the constant voltage is the charge voltage (Hua and Lin 2000).

#### **2.1.1.22. Float Voltage**

The float voltage is the electric potential applied to a battery after its full charge in order to overcome the self-discharge effect and to keep the battery at its full capacity (MIT Electric Vehicle Team 2008).

#### **2.1.1.23. Internal Resistance**

The internal resistance of a battery is the resistivity that the battery components possess against electronic and ionic fluxes. Electronic resistance occurs in solid materials and the ionic resistance occurs in electrolyte solution featuring ions. Their combination is called total effective resistance. (Energizer 2005).

### **2.1.2. Battery Components**

A simple battery with a single cell is a combination of 6 components: negative electrode (anode), positive electrode (cathode), separator, electrolyte solution, negative current collector, and positive current collector.

Batteries can be manufactured with various materials and shapes. There are many possibilities of chemistries; however, few of them can be considered for commercial applications since the main criteria for batteries are to become economically viable and safe. Economical viability suggests that providing effective energy and power densities for aimed range of use while the manufacturing costs of the

battery are reimbursable with profit by the manufacturer and the sell price is acceptable for the consumers.

Batteries do not require any specific shape to work. However, there are some shapes that researchers prefer to work with and industry has some shapes standardized such as AA, AAA. Prismatic and cylindrical cells are easy to work with, and manipulating the geometric features can easily be done. Figure 2.1 represents an exemplary cell with prismatic geometry, which has been used along with the computer model developed for this dissertation.

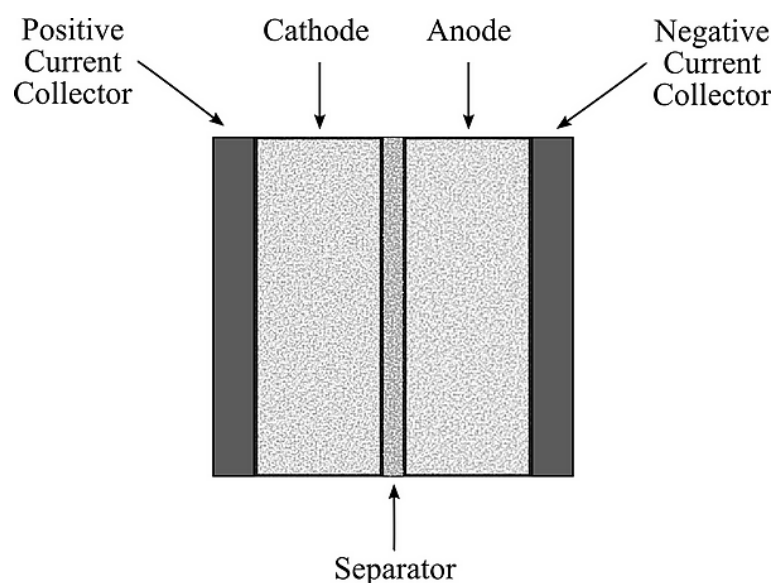


Figure 2.1. Simple prismatic electrochemical cell structure.

The electrolyte solution penetrates into the porosities of the separator and the electrodes if the electrodes are porous. Otherwise electrolyte solution exists only within the separator.

#### **2.1.2.1. Electrodes**

There are at least two electrodes in a battery. One is negative and the other is positive. Polarity of the electrodes is determined according to the location of occurrence of oxidation and reduction reactions.

Negative electrode is where the oxidation reaction occurs. The consequence of an oxidation reaction is the release of electrons from the reactant species, and then the

oxidized reactant species dissolves into the electrolyte solution used with the electrode. For that reason, negative electrode is also called fuel electrode besides being known as anode (Linden and Reddy, eds. 2002). What is expected from an anode material is to be an efficient reducing agent with a high discharge capacity (Ah/g), stability, and high conductivity. In practice, the anode materials are mostly metals. Ease to production and effective cost of the anode substance are important criteria for commercial designs (Linden and Reddy, eds. 2002).

The positive electrode also known as cathode is where the reduction reaction happens. The electrons liberated from the anode travel to the cathode via an electric circuit outside the battery and the current collectors, then they reduce the cathode substance as a consequence of merging with it (Linden and Reddy, eds. 2002).

Being a good oxidizing agent is a necessity for a cathode material. It also has to be stable with the electrolyte solution and to provide a convenient electric potential. Most cathode materials are metal oxides. On the other hand, oxygen, halogenes, oxihalides, sulfur and its oxides can be used to develop battery systems (Linden and Reddy, eds. 2002).

The electrodes can be porous or non-porous. The porous electrodes have a larger surface area for ion dissolution activities and this increases the amount of ions produced in unit time (Linden and Reddy, eds. 2002).

#### **2.1.2.2. Electrolyte Solution**

The electrolyte solution is a mixture which contains one or many kinds of electrolyte salt as solute and similarly solvent. It provides the medium for the transport of chemical species, especially the ions, but not the electrons. The ions travel between electrodes and complete the outside electric circuit. Generally, the electrolyte mixture is in liquid form. The solution of potassium hydroxide in water is the most common alkali solvent for alkaline batteries such as NiMH, NiCd, and NiZn. Sulfuric acid is the electrolyte solution of lead-acid batteries. Lithium-ion batteries use liquid solutions of lithium salts in aprotic organic solvents (Vincent and Scrosati 1997). The electrolyte mixture can also be solid. The expectation from an electrolyte mixture is it to have good ionic conductivity when it is electronically insulating. Additionally, it has to be

nonreactive with the electrode substances and insensitive to minimal change of operating conditions (Linden and Reddy, eds. 2002).

Electrolyte solution is the medium where the ion transport occurs. The dissolved electrolyte substance dissociates into anions and cations (Newman and Thomas-Alyea 2004). The solution determines the ion transport characteristics and some chemical restrictions dependent on electrode substances. The concentration of the electrolyte solution in a battery is important for the battery performance since the solution also takes part in the redox reaction and it affects the chemical reaction rates. Single electrolyte solutions containing two types of charged species, cations and anions, are called binary electrolyte solutions. Binary solutions can also be defined as an electrolyte solution containing just one salt and one solvent (Newman and Thomas-Alyea 2004). They can be symbolized with 1:1 or 1-1. Potassium hydroxide (KOH), sodium hydroxide (NaOH), and potassium chloride (KCl) in pure water are examples for binary solutions (Newman and Thomas-Alyea 2004).

#### **2.1.2.3. Separator**

The separator is a solid object having porosities. It prevents the contact of negative and positive electrodes when the manufacture of a small battery system is the goal. The prevention of the contact of electrodes is a necessity for electronic insulation inside the battery. On the other hand, the porosities are filled with liquid electrolyte material to provide ionic conductivity. A separator is desired to be as porous as it can be to hold maximum amount of electrolyte solution in order to increase battery performance until it starts to fail to prevent contact between electrodes (Linden and Reddy, eds. 2002).

#### **2.1.2.4. Current Collectors**

Current collectors are chosen according to their conductivity and their purpose of use is to maintain electron transfer between the electrodes and the electric circuit. It is essential that the collector material does not decompose or react with anode, cathode and electrolyte materials.

### 2.1.3. Battery Overview

Primary batteries are in the market for a long time. They were the key for portable electronic devices. However, further developments of renewable energy technologies, grid storage systems, portable electronic devices, and hybrid and electric vehicles require rechargeable storage systems. These applications are the primary driving force for secondary battery market and research. Therefore, secondary battery research is mainly focused on the needs of these applications for which the requirements from batteries might greatly differ. An electric vehicle needs a battery having high power density and high energy density, thereby the electric motor of the vehicle runs for a satisfying duration, which is important for an economic efficiency success. A power grid application can be either a short or a long term application, and can have a few or many electrical devices. If this is a backup system, then the most important specifications are its energy density, cycle life, and its shelf life. Since the grid applications are stationary, high power needs are being satisfied with multiple storage units and they do not have to have light weight. On the other hand, consumer electronics desire light weight, high energy density, long life, and long shelf life. There is not one particular system satisfying the needs for every problem. However, there are many options to be considered, researched and developed for creation of a battery system that it is going to become the solution to a specific problem.

Most commonly used battery system is *lead-acid battery* system. This battery system is widely used in vehicles as a starter, and in UPS applications, which is a grid storage system to provide short term backup power. A lead-acid cell provides 2.1 V electric potential. Lead-acid batteries have 30 to 40 Wh/kg specific energy, 60 to 75 Wh/L energy density, and 180 W/kg power density. Their shelf life at 20 °C is 6 to 9 months and its charge/discharge cycles are 200 to 250 (Payer 2014). Since they have lead and sulfuric acid as materials, this battery structure is both non-environmental and unsafe. Heavy weight caused by lead makes these batteries unusable for electrical transportation and also it causes that the ratio of power density to weight becomes very low which is undesirable for any applications. Despite all these, lead-acid system is the most widely used electrochemical energy storage system because it is very cheap and its chemistry is well known.



Another most commonly used battery is *lithium-ion* battery. This battery has started the age of cellular phones and it is nowadays being used for electric vehicles. It has the best performance in the today's market among other batteries. A lithium-ion cell with  $\text{LiCoO}_2$  as its composite porous electrode provides 3.6 V electric potential, with a specific energy of 160 Wh/kg, energy density of 270 Wh/L, and power density of 1800 W/kg. The shelf life of this cell is 9 to 12 months and its life is up to 1000 cycles (Payer 2014). However, the possibility of thermal runaway reactions carries a risk of explosion and fire, which is a serious safety issue.

There exist more secondary battery types such as *nickel metal hydride* (NiMH), *nickel cadmium* (NiCd), and *nickel-zinc* (NiZn) batteries. Those batteries are also called alkaline secondary batteries (Vincent and Scrosati 1997) because their electrolyte is a base solution, usually concentrated KOH. *Zinc-air* batteries are in the metal-air battery class. There are many types of batteries, but in this dissertation only few, related or comparable ones, and the ones in the market, are mentioned.

NiMH batteries have good energy and power density performances. They have 30 to 80 Wh/kg specific energy, 140 to 300 Wh/L energy density, and 250 to 1000 W/kg power density. Their cycle life is 400 to 500 cycles. A cell provides 1.2 V electric potential (Payer 2014). Unfortunately, these batteries suffer from short shelf life because of the phenomenon called self-discharge which occurs with a 4-5 % daily loss. The shelf life of a NiMH cell varies from 3 to 6 months (Payer 2014). Also, the unstable thermal performance and the high costs in the production of these batteries make them inconvenient to be used in electric cars.

NiCd batteries have also good energy and power densities as well as good charge and discharge characteristics. They are reliable, have long life and overcharge capability. Cell voltage of a NiCd cell is 1.2 V, its specific energy is 40 to 60 Wh/kg, its energy density is 50 to 150 Wh/L, and its power density is 150 W/kg. Cycle life of NiCd cell is 400 to 500 cycles. However, its shelf life is short: 3 to 6 months (Payer 2014). In addition, cadmium is an unhealthy and non-environmental material. It is actually a side product of zinc production; as a result, it is an expensive material compared to lead, so the NiCd batteries are also expensive compared to lead-acid batteries (Vincent and Scrosati 1997).

Zinc-air secondary batteries are manageable if they have a small size. Because of this, they are mostly being used in hearing-aid devices. For larger geometries, there are

multiple drawbacks mostly caused by the chemical properties of zinc electrode that those drawbacks occur with the nickel-zinc batteries too.

The nickel-zinc batteries are theoretically excellent batteries. The electrode materials are safe, environmentally friendly, and cheap. These batteries are suitable for utilization with electric vehicle or portable electronics. High energy and power density, light weight, good charge and discharge characteristics, long shelf life and long cycle life make these batteries very advantageous compared to the other batteries. The nominal cell voltage of the nickel-zinc batteries produced by PowerGenix Co. is 1.65 V according to the datasheets of the products having 8, 40 and 80 Ah current capacity (Powergenix 2012a, b, c). Their specific energy is in the range of 60 to 80 Wh/kg, their energy density is 90 to 185 Wh/L, and its power density is 600 to 2000 W/kg, that the power density has inverse proportion with current capacity. A NiZn battery cycle life is more than 500 cycles (Linden and Reddy, eds. 2002). However, NiZn batteries are far from reaching their full potentials due to couple of issues associated with Zn electrodes. Among these issues, the shape change of Zn electrode due to high mobilities of discharge products causing uneven Zn deposition during charging with increasing charge/discharge cycle and short circuiting of the battery electrodes middle of the charging due to dendritic growth of zinc metal are the most commonly encountered issues (Payer 2014).

The aim of this dissertation is to build a modeling tool for nickel-zinc batteries. A well developed model would be useful for better understanding of the behavior of zinc electrode and its interactions with other components. Even this model can provide some insights that the experiments cannot offer because the sealed constitution makes it impossible to do some experiments for certain specifications about the electrochemical reactions. After that, the nickel-zinc model knowledge can be used for similar systems such as zinc-air.

## **2.2. Nickel-Zinc Batteries**

The first appearance of rechargeable nickel-zinc batteries dates back to 1901. In The United States of America, Thomas Edison had manufactured a rechargeable NiZn battery and patented it, and same year, in Russia, Michaelowsky had patented his NiZn battery version. After three decades of silence, in 1932 Dr. James J. Drumm had started

a research with NiZn batteries which are installed in four two-car Drumm railcar sets. This experiment concluded with promising results in 1948; however, the limited charge discharge cycle of NiZn batteries prevented these batteries to be used more widely. After a while, in 1960s, research focused on developing NiZn batteries for replacing silver-zinc batteries in military applications. In 1970s, the idea of using NiZn to energize electric vehicles attracted the interest of researchers. In following years NiZn batteries found use in many applications such as electric lawn, electric scooters and bicycles, trolling motors, deep cycle marine applications, and garden devices. (Payer 2014).

For the last decade two companies have had significant roles with NiZn batteries. PowerGenix Co. of U.S.A. and Pkcell of Republic of China developed their NiZn battery products. PowerGenix provided consumers with rechargeable NiZn batteries having various sizes which were AAA, AA, Sub-C, D and prismatic. Pkcell however only provided with AAA and AA sized rechargeable NiZn batteries. PowerGenix' AA sized batteries had 1500 mAh and the one of Pkcell were 900 mAh capacities. In 2014 PowerGenix terminated AAA and AA products to focus on automotive market with 12 V start-stop battery, 12 V battery and 48 V hybrid battery, and to stationary storage and grid applications. Pkcell is continuing to produce AAA sized batteries with 2500 mAh capacity and 15 g weight, and AA sized ones with 900 mAh capacity and 25 g weight.

### **2.2.1. Chemistry of Rechargeable Nickel-Zinc Cell**

A simple rechargeable electrochemical cell contains two electrodes and an ionic solution between those electrodes. This cell can either be charged if a power source is connected or discharged if a load is connected. Oxidation and reduction reactions happen separately on these electrodes. When oxidation reaction occurs on one electrode then the reduction reaction occurs on the other electrode. As a result of oxidation reaction the electrode loses electrons and as a result of reduction reaction the electrode gains electrons. The oxidized electrode is named positive electrode and the one reduced is named negative electrode. In an electrochemical cell when oxidation happens, reduction also happens or vice versa. This is called as *redox* reaction. When a redox reaction system is evaluated there is an overall reaction that describes the result of the

system. This overall equation is the sum of oxidation and reduction reaction equations and it is the description of the entire system in chemical means (Petrucci et al. 2011).

A nickel-zinc cell contains a nickel electrode, a zinc electrode, an alkaline solution as an electrolyte solution, a separator and two current collectors connected to the electrodes. At the beginning of the discharge process the positive electrode is the nickel electrode. The nickel electrode contains the oxidized form of nickel which is called nickel oxyhydroxide with the chemical formula NiOOH. The negative electrode is zinc, which symbolized with Zn. Nickel oxyhydroxide molecules gain electrons and merge with hydrogen atoms of the water during the discharge of the cell, thereby NiOOH molecules are reduced. As a result of this they turn into nickel hydroxide (Ni(OH)<sub>2</sub>) molecules. In the other electrode, the metallic zinc (Zn) atoms are oxidized. They merge with hydroxide ions (OH<sup>-</sup>) then zincate ions (Zn(OH)<sub>4</sub><sup>2-</sup>) are being formed. Then zincate ions turn into zinc oxide (ZnO) molecules by releasing hydroxide ions and water (H<sub>2</sub>O). This reaction is an acid-base reaction which is different than the others. In the charge process, these molecular and atomic transformations occur in reverse direction. ZnO turns into Zn(OH)<sub>4</sub><sup>2-</sup> then Zn and Ni(OH)<sub>2</sub> turns into NiOOH. So the oxidation reaction happens in the nickel electrode and the reduction reaction happens in the zinc electrode. In both nickel and zinc electrodes, some additives are being added in order to adjust some material properties and manipulate chemical behavior of the electrodes. Neglecting that they contribute to reactions, simplified representative reaction equations can be represented as (Linden and Reddy, eds. 2002; Torabi and Aliakbar 2012):

Table 2.2. NiZn battery reactions.

Discharge		E <sub>ocv</sub>	
Positive Electrode	$2 \text{ NiOOH} + 2 \text{ H}_2\text{O} + 2 \text{ e}^- \rightarrow 2 \text{ Ni(OH)}_2 + 2 \text{ OH}^-$	0.49 V	(2.6)
Negative Electrode	$\text{Zn} + 4 \text{ OH}^- \rightarrow \text{Zn(OH)}_4^{2-} + 2 \text{ e}^-$	-1.305 V	(2.7)
	$\text{Zn(OH)}_4^{2-} \rightarrow \text{ZnO} + 2 \text{ OH}^- + \text{ H}_2\text{O}$		(2.8)
Overall Reaction	$\text{Zn} + 2 \text{ NiOOH} + \text{ H}_2\text{O} \rightarrow \text{ZnO} + 2 \text{ Ni(OH)}_2$	1.795 V	(2.9)
Charge			
Overall Reaction	$2 \text{ Ni(OH)}_2 + \text{ ZnO} \rightarrow 2 \text{ NiOOH} + \text{ H}_2\text{O} + \text{ Zn}$	-1.795 V	(2.10)

In Table 2.2  $E_{OCV}$  is the open cell voltage, and it is 1.795 V for the entire cell. This value is theoretical. In practice, it is around 1.65 V. These reactions are simplified; however, in reality the process is much more complex and there are a few side reactions with low effect in both electrodes.

### **2.2.1.1. Nickel-Zinc Thermodynamics**

The redox reactions, which govern an electrochemical cell, occur due to the electrical potential difference between the anode and the cathode. As a result of the chemical reactions, an electrochemical work is generated if the anode and the cathode are connected electrically outside of the cell. When the electrodes are not electrically connected externally or the potential difference between electrodes is null, reactions do not take place and the system is in electrochemical equilibrium state. Electrochemical equilibrium means that the total of the all electrochemical potentials is zero (Rubinstein, ed. 1995) and with the definition the electrochemical equilibrium concept differs from the chemical equilibrium concept. Chemical equilibrium concept is based on reaction rates and it suggests that the equilibrium state occurs when the net reaction rate is zero which is when the forward and backward reaction rates became equal to each other. So a charged battery at open circuit is at electrochemical equilibrium but not at chemical equilibrium because electrodes are ready to react once the circuit becomes closed. But a depleted battery is at both electrochemical and chemical equilibrium. Battery behavior in either chemical or electrochemical equilibrium can be understood and expressed through thermodynamics. Otherwise, the electrode kinetics studies must be used to understand and express the reactions occurring in the electrodes, at the interfaces and in the electrolyte solution. It is very important to note that the necessary initial and boundary conditions for kinetic expressions are obtained with the principles of thermodynamics.

Reversibility is an important concept in chemical thermodynamics and it refers to the chemical reactions are able to occur in both forward and backward directions. Reversibility of an electrochemical reaction of a cell allows charging that cell and it is essential for rechargeability. On the other hand, chemical irreversibility means that a chemical reaction happens in only one direction and it is impossible to have the backward reaction. Non-rechargeable cells possess chemically irreversible processes.

When there is no electric load connected to the terminals of the cell, the voltage between terminals is the open circuit voltage (OCV) or also known as electromotive force (EMF) of the cell (Vincent and Scrosati 1997). The EMF of the cell is the potential of the overall redox reaction and it is theoretically equal to 1.795 V for NiZn cells under standard conditions which refers to 25 °C ambient temperature and 1 atm ambient pressure.

The occurred chemical reactions in the discharge process are spontaneous reactions. Spontaneous means that this reaction has the natural tendency to occur without requiring any intervention from outside of the system once it begin to react. As a thermodynamical concept, entropy indicates the possibilities of energy distribution of a system into micro energy states. When there is a spontaneous change in the system, the interaction of the entropy change of the system and the surroundings with the entropy change of the universe can be stated as (Petrucchi et al. 2011):

$$\Delta S_{\text{universe}} = \Delta S_{\text{system}} + \Delta S_{\text{surrounding}} > 0 \quad (2.11)$$

The complexity of using Equation 2.11 to determine the spontaneity of a process, had been overcome by a function called Gibbs free energy:

$$G = H - TS \quad (2.12)$$

Here, G is the Gibbs free energy, H is the enthalpy, S is the entropy and T is the absolute temperature. Gibbs free energy change is expressed as:

$$\Delta G = \Delta H - T\Delta S \quad (2.13)$$

At constant temperature and pressure, if  $\Delta G$  of a process is negative then the change is spontaneous, if it is positive then the change is non-spontaneous, and if it is equal to zero then the system is in chemical equilibrium. Accordingly, the expectations about a battery processes are that the discharge process has a negative  $\Delta G$ , charge process has a positive  $\Delta G$ , and  $\Delta G$  becomes zero when the chemical equilibrium has been reached at end of the discharge process. An important fact is that the  $-\Delta G$  is equal to the available energy from a process.

Thermodynamic properties are the functions of temperature and pressure. The notation of Equation 2.13 for standard conditions can be expressed as:

$$\Delta G^{\circ} = \Delta H^{\circ} - T\Delta S^{\circ} \quad (2.14)$$

The relation between the general Gibbs free energy change ( $\Delta G$ ) and the standard Gibbs free energy change ( $\Delta G^{\circ}$ ) is expressed as:

$$\Delta G = \Delta G^{\circ} + RT \ln Q_{\text{rxn}} \quad (2.15)$$

Here,  $R$  is the universal gas constant and  $Q_{\text{rxn}}$  is the reaction quotient which is replaced by the thermodynamic equilibrium constant,  $K$ , when there is chemical equilibrium.  $\Delta G$  is also equals to zero in chemical equilibrium, thus the relation between standard Gibbs free energy change and the thermodynamic equilibrium constant:

$$\Delta G = \Delta G^{\circ} + RT \ln K \quad (2.16)$$

$$0 = \Delta G^{\circ} + RT \ln K \quad (2.17)$$

$$\Delta G^{\circ} = -RT \ln K \quad (2.18)$$

An electrochemical cell has a cell potential delivered by oxidation and reduction reactions that both reaction have electric potentials. These potentials are also the electrode potentials. The potential of an electrode can be determined as a result of measurements based on a reference electrode and done at standard conditions which are 1 atm of pressure, 25 °C of temperature, and 1 M (molar) of solution concentration. Usually the reference electrode is a hydrogen electrode which is called *the standard hydrogen electrode*. The cell potential at standard conditions is noted as  $E_{\text{cell}}^{\circ}$  and used as reference value in calculations. Its relation with oxidation and reduction potentials is:

$$E_{\text{cell}}^{\circ} = E^{\circ}_{\text{reduction}} - E^{\circ}_{\text{oxidation}} \quad (2.19)$$

The work done by electrons in an electrochemical cell having a reversible process is defined for standard conditions in Equation 2.20.

$$w_{\text{electrical}} = nFE_{\text{cell}}^{\circ} \quad (2.20)$$

Here,  $n$  is the molar number of electrons,  $F$  is the Faraday constant and  $E_{\text{cell}}^{\circ}$  is the cell voltage. Electrical work is the available work of the cell and it is equal to  $-\Delta G^{\circ}$ .

$$\Delta G^{\circ} = -nFE_{\text{cell}}^{\circ} \quad (2.21)$$

By using the relation of standard Gibbs free energy change with cell potential given in Equation 2.21, a relation between thermodynamic equilibrium constant and cell potential can be established with the use of standard Gibbs free energy definition given in the Equation 2.18.

$$E_{\text{cell}}^{\circ} = \frac{RT}{nF} \ln K \quad (2.22)$$

Cell potential expression has to be rearranged for nonstandard conditions and non-equilibrium state. Instead of thermodynamic equilibrium constant  $K$  the reaction quotient  $Q_{\text{rxn}}$  is needed to be used. This expression is also known as the Nernst equation:

$$E_{\text{cell}} = E_{\text{cell}}^{\circ} - \frac{RT}{nF} \ln Q_{\text{rxn}} \quad (2.23)$$

A general reaction has reactants and products that these species have stoichiometric coefficients determined depending on the molar ratios of the transformed reactants into the products. A general expression for a chemical reaction can be defined as



where;  $\alpha$ ,  $\beta$ ,  $\psi$ , and  $\delta$  are the stoichiometric coefficients,  $A$  and  $B$  are the reactant species, and  $C$  and  $D$  are the produced species. Reaction quotient  $Q_{\text{rxn}}$  is the ratio of the activations of products and reactants and it can be defined as



$$Q_{\text{rxn}} = \frac{(a_C(x, t))^{\psi} (a_D(x, t))^{\delta}}{(a_A(x, t))^{\alpha} (a_B(x, t))^{\beta}} \quad (2.25)$$

where;  $a_i$  is the activation of species  $i$  (Zuhmdahl and Zumdahl 2010). Activations are time dependent since the concentration is time dependent and activation is a function of concentration. Activation definition of a solute  $i$  is (Bard and Faulkner 2001):

$$a_i = \gamma_i^{v_i} \left( \frac{C_i(x, t)}{C^\circ} \right)^{v_i} \quad (2.26)$$

where;  $\gamma_i$  is the activation coefficient of species  $i$ ,  $v_i$  is the stoichiometric coefficient of species  $i$ ,  $C_i(x, t)$  is the  $x$ -coordinate and time dependent concentration of species  $i$ , and  $C^\circ$  is the standard concentration. Standard concentration is generally 1 M, and it is assumed 1 M in this dissertation. Based on this assumption, Equation 2.26 becomes (Bard and Faulkner 2001):

$$a_i = (\gamma_i C_i(x, t))^{v_i} \quad (2.27)$$

The source of the electromotive force generated by an electrochemical cell is a pair of oxidant and reductant species. Oxidant species are the reduced species and reductant species are the oxidized species in a redox reaction. A general expression for a redox reaction can be defined as



where;  $n$  is the molar number of the transferred electrons, Oxi stands for oxidized species and Red for reduced species. Subscripts O and R of the stoichiometric coefficient,  $v$ , refer to the oxidized and reduced species' stoichiometric coefficients. The Equation 2.28 describes reduction reaction from left to right direction and it also describes oxidation reaction from right to left direction. Since the components of a redox reaction are oxidation and reduction reactions, oxidation reaction and reduction reaction can be separately expressed and they are called half reaction.

Concentration dependency is a significant factor in zinc based batteries. The Nernst equation can be derived into a concentration dependent form to calculate electrode potential for a reduction reaction which is a half reaction:

$$E_{\text{half rxn}} = E_{\text{half rxn}}^{\circ} - \frac{RT}{nF} \ln \frac{(\gamma_R C_R(x, t))^{v_R}}{(\gamma_O C_O(x, t))^{v_O}} \quad (2.29)$$

The activity coefficients are mostly unknown parameters and they have to be determined experimentally. The method found to overcome this problem is to merge the activity coefficients with the standard potential. The newly emerging concept which emerges is called formal potential. It is defined as (Bard and Faulkner 2001):

$$E_{\text{half rxn}}^{\circ'} = E_{\text{half rxn}}^{\circ} - \frac{RT}{nF} \ln \frac{(\gamma_R)^{v_R}}{(\gamma_O)^{v_O}} \quad (2.30)$$

The electric potential of a half reaction can be rearranged by using formal potential definition. After applying Equation 2.30 into Equation 2.29 the electric potential of a half reaction definition becomes (Bard and Faulkner 2001):

$$E_{\text{half rxn}} = E_{\text{half rxn}}^{\circ'} - \frac{RT}{nF} \ln \frac{(C_R(x, t))^{v_R}}{(C_O(x, t))^{v_O}} \quad (2.31)$$

The activity coefficients of the species are assumed to be equal to 1 for the electrolyte solution. This assumption is valid for dilute solutions but not for the concentrated ones. Additionally, alkaline battery electrolyte solutions are not very concentrated. The preferred ratio of solute to solvent is generally 40 wt% (weight percent) for KOH and pure water solution in NiZn batteries. This is also valid for other alkaline battery chemistries with KOH electrolyte or any other aqueous electrolyte solutions. Thus, aqueous electrolyte solutions can be assumed as dilute solutions. Based on this assumption electric potential of a half reaction can be rearranged into:

$$E_{\text{half rxn}}^{\circ'} = E_{\text{half rxn}}^{\circ} \quad (2.32)$$

$$E_{\text{half rxn}} = E_{\text{half rxn}}^{\circ} - \frac{RT}{nF} \ln \frac{(C_R(x, t))^{v_R}}{(C_O(x, t))^{v_O}} \quad (2.33)$$

Equation 2.33 is the Nernst equation for a half reaction or it can be said as the Nernst equation for the half cell. The Nernst equation for the entire cell given in Equation 2.23 can be rearranged with concentration dependent terms:

$$E_{\text{cell}} = E_{\text{cell}}^{\circ} - \frac{RT}{nF} \ln \frac{(C_R(x, t))^{v_R}}{(C_O(x, t))^{v_O}} \quad (2.34)$$

Nernst equation gives the electric potential at electrochemical equilibrium (Rubinstein, ed. 1995). For that reason, left hand side term is sometimes mentioned as equilibrium potential and noted as  $E_{\text{eq}}$ . It is the theoretical open circuit voltage as a function of standard potential, temperature, transferred electrons, and time dependent concentrations of oxidized and reduced species. Species concentrations can also be considered as bulk concentrations at electrochemical equilibrium. Consequently, it is convenient to write Nernst equation as

$$E_{\text{eq}} = E_{\text{cell}}^{\circ} - \frac{RT}{nF} \ln \frac{(C_R^*)^{v_R}}{(C_O^*)^{v_O}} \quad (2.35)$$

where;  $C_i^*$  is bulk concentration of species  $i$  and  $E^{\circ}$  is the standard potential. Nernst equation is one of the fundamental equations in electrochemical thermodynamics. It is important to remember that a kinetic expression for electrodes should reduce into the Nernst equation at electrochemical equilibrium (Bard and Faulkner 2001).

#### 2.2.1.2. Nickel-Zinc Kinetics

Every chemical reaction has a rate when it occurs. This rate is called the reaction rate. A reversible chemical reaction involves two rates which are forward and backward reaction rates even when the reaction is spontaneous. This realization is also valid for oxidation and reduction reactions. Considering the general expression for oxidation reaction:



where;  $k_f$  is the forward reaction rate constant and  $k_b$  is the backward reaction rate constant. These constants are mostly unknown in practice because forward process and backward process occurs simultaneously and they are inseparable, for that reason no measurement can be done to estimate these values separately. But in theory, the forward and backward reaction rates having molar per second (M/s) as unit are defined as (Crow 1974):

$$\vartheta_f = k_f(C_O(x, t))^{\nu_O} \quad (2.37)$$

$$\vartheta_b = k_b(C_R(x, t))^{\nu_R} \quad (2.38)$$

The difference of the forward and the backward reaction rates is the net rate which is the measurable reaction rate. Its definition is:

$$\vartheta_{\text{net}} = k_f(C_O(x, t))^{\nu_O} - k_b(C_R(x, t))^{\nu_R} \quad (2.39)$$

At the end of the reaction process, when the chemical equilibrium state has occurred, net rate becomes zero. Then forward and backward reaction rates become equal to each other:

$$k_f(C_O(x, t))^{\nu_O} = k_b(C_R(x, t))^{\nu_R} \quad (2.40)$$

The ratio of the forward reaction rate constant to backward reaction rate constant is equal to the ratio of the reduced species concentration to the oxidized species concentration and to the thermodynamic equilibrium constant:

$$\frac{k_f}{k_b} = \frac{(C_R(x, t))^{\nu_R}}{(C_O(x, t))^{\nu_O}} = K \quad (2.41)$$

This equality is a requirement for a kinetic expression. All kinetic processes end at chemical equilibrium. Therefore, every kinetic expression must collapse into a

thermodynamic expression because the equilibrium state is expressed with thermodynamics. In order to validate the kinetic expression of an electrochemical cell, the expression must satisfy the equality in Equation 2.41, and also it must collapse into Nernst equation which is Equation 2.35, and it also must satisfy the Tafel equation which will be discussed.

Reaction rates at the electrode surface can be expressed according to the components of the current. These components are cathodic current for reduction reaction, which is the forward process, and the anodic current for oxidation reaction, which is the backward process. Cathodic current is proportional to forward reaction rate and anodic current is proportional to backward reaction rate. The x component of the concentration is equal to zero at the electrode surface. Then the reaction rates are:

$$\vartheta_f = k_f(C_O(0, t))^{v_o} = \frac{i_c}{nFA} \quad (2.42)$$

$$\vartheta_b = k_b(C_R(0, t))^{v_R} = \frac{i_a}{nFA} \quad (2.43)$$

where;  $i_c$  and  $i_a$  are respectively the cathodic and anodic currents,  $A$  is the electrode surface area. Current density passing through the electrode is the difference between cathodic and anodic current components and also it is related to net reaction rate:

$$i = i_c - i_a \quad (2.44)$$

$$\vartheta_{\text{net}} = k_f(C_O(0, t))^{v_o} - k_b(C_R(0, t))^{v_R} = \frac{i}{nFA} \quad (2.45)$$

According to the surface concentration and the rate constants the total current can be defined by arranging the Equation 2.45:

$$i = nFA\{k_f(C_O(0, t))^{v_o} - k_b(C_R(0, t))^{v_R}\} \quad (2.46)$$

These expressions are valid for homogeneous reactions that the nickel-zinc reactions are assumed to be homogeneous.

It has been mentioned for a cell or a half cell that the equilibrium potential (or open circuit potential) for reversible reaction can be calculated by using its relation to

the Gibbs free energy change or by using the Nernst equation. Since a half cell is a single electrode, the equilibrium potential can be defined for a single electrode having an electrode potential,  $E^\circ$ , like it is defined for a half cell (Gileadi 1993).

$$E_{eq} = -\frac{\Delta G}{nF} = E^\circ - \frac{RT}{nF} \ln Q_{rxn} \quad (2.47)$$

However, in practice, the measured potential value may be significantly different than the calculated and the expected potential value due to the polarization of the electrode. The magnitude of this difference is related to its polarization level (Gileadi 1993). This difference is called overpotential and it is symbolized with  $\eta$ . Its mathematical definition is:

$$\eta = E - E_{eq} \quad (2.48)$$

Here,  $E$  is the measured electrode potential. Tafel equation reveals the overpotential behavior with current. A kinetic expression for an electrode must explain this behavior. This is the second requirement for a viable kinetic expression after the collapse of the kinetic expression to the Nernst equation at electrochemical equilibrium. The Tafel equation indicates this behavior as a relation between the overpotential and the logarithm of the current density in a general expression using two constants  $a_{Tfl}$  and  $b_{Tfl}$  dependent on the battery behavior (Gileadi 1993; Bard and Faulkner 2001):

$$\eta = a_{Tfl} + b_{Tfl} \log i \quad (2.49)$$

Forward and backward rate constants can be expressed using standard rate constant,  $k^\circ$ , with a symmetry factor symbolized with  $\beta$  (Noel and Vasu 1990).

$$k_f = k^\circ e^{\left(\frac{-\beta nF \eta}{RT}\right)} \quad (2.50)$$

$$k_b = k^\circ e^{\left(\frac{(1-\beta)nF \eta}{RT}\right)} \quad (2.51)$$

$\beta$  is a value varying between 0 and 1. It is the ratio of the potential effect of activation energy to the free energy of the overall reaction. Moreover, it is called *transfer*

*coefficient* (Bard and Faulkner 2001). The sum of the cathodic component and the anodic component must be 1 for a single step process. The symmetry factor  $\beta$  is also stands for the cathodic component.

The Arrhenius equation relates the activation energy, the temperature, and the universal gas constant to chemical rate constant. Its general expression with free energy of activation term is:

$$k^\circ = A_{fq} e^{\left(-\frac{\Delta G^\ddagger}{RT}\right)} \quad (2.52)$$

where;  $A_{fq}$  is frequency factor which is unitless and  $\Delta G^\ddagger$  is the standard free energy of activation in kJ/mol.  $\Delta G^\ddagger$  is the internal energy required for a chemical process to occur at standard conditions. The free energy of activation can be considered as a combination of two components resulting in the forward and backward processes of an electrochemical reaction: anodic and cathodic components (Bard and Faulkner 2001).

$$\Delta G_c^\ddagger = \Delta G_c^{\ddagger\circ} + \beta nF(E - E^\circ) \quad (2.53)$$

$$\Delta G_a^\ddagger = \Delta G_a^{\ddagger\circ} - (1 - \beta)nF(E - E^\circ) \quad (2.54)$$

where;  $\Delta G_c^{\ddagger\circ}$  and  $\Delta G_a^{\ddagger\circ}$  are the standard cathodic and anodic free energies of activation when the electric potential of the electrode is equal to formal potential  $E^\circ$ .  $\Delta G_c^\ddagger$  is the cathodic free energy of activation or also called as cathodic or reduction barrier.  $\Delta G_a^\ddagger$  is the anodic free energy of activation and it is also called anodic or oxidation barrier.  $\Delta G_c^\ddagger$  and  $\Delta G_a^\ddagger$  are the free energies of activation when the electrode potential is  $E_{eq}$  and they can also be used to define forward and backward reaction rate constants in Arrhenius equation form (Bard and Faulkner 2001):

$$k_f = A_{fq,f} e^{\left(-\frac{\Delta G_c^\ddagger}{RT}\right)} \quad (2.55)$$

$$k_b = A_{fq,b} e^{\left(-\frac{\Delta G_a^\ddagger}{RT}\right)} \quad (2.56)$$

After substituting Equations 2.53 and 2.54 into 2.55 and 2.56 an important relation is obtained. This relation is the current-potential relation and mostly mentioned as *Butler-Volmer Kinetics*. This relation combines faradaic current, electrode potential, concentration of oxidized and reduced species (Bard and Faulkner 2001; Noel and Vasu 1990).

$$i = nFAk^o \left[ C_O(0, t) e^{-\frac{\beta nF}{RT}(E - E^{\circ'})} - C_R(0, t) e^{\frac{(1-\beta)nF}{RT}(E - E^{\circ'})} \right] \quad (2.57)$$

An important fact about this expression is that it is valid only for single step processes with transfer of  $n$  electrons.

The net reaction rate and the current is zero at the electrochemical equilibrium. The concentrations are also bulk concentrations and the electrode potential is equal to equilibrium potential. Then, the current-potential relation becomes:

$$i = nFAk^o \left[ C_O^* e^{-\frac{\beta nF}{RT}(E_{eq} - E^{\circ'})} - C_R^* e^{\frac{(1-\beta)nF}{RT}(E_{eq} - E^{\circ'})} \right] = 0 \quad (2.58)$$

$$nFAk^o \left[ C_O^* e^{-\frac{\beta F}{RT}(E_{eq} - E^{\circ'})} \right] = nFAk^o \left[ C_R^* e^{\frac{(1-\beta)F}{RT}(E_{eq} - E^{\circ'})} \right] \quad (2.59)$$

Even though the output current of the cell is zero, a faradaic activity still occurs inside the cell with balance between electrodes. This activity is mentioned as *the exchange current* and it is symbolized with  $i_0$ . The magnitude of the exchange current is equal to the cathodic and anodic currents which form the output current  $i$ .

$$i_0 = nFAk^o \left[ C_O^* e^{-\frac{\beta nF}{RT}(E_{eq} - E^{\circ'})} \right] \quad (2.60)$$

After the substitution of the Nernst Equation which is Equation 2.35 into Equation 2.60, exchange current expression becomes:

$$i_0 = nFAk^o \left[ C_O^{*(1-\beta)} C_R^{*\beta} \right] \quad (2.61)$$



The importance of the exchange current is its proportion to the standard rate constant  $k^\circ$ . This information makes possible to substitute  $k^\circ$  with a proper definition of  $i_0$ . The exchange current can be normalized to obtain exchange current density in unit area:

$$j_0 = \frac{i_0}{A} \quad (2.62)$$

The current-potential relation can be improved by using exchange current and overpotential. As a result of this improvement, the current-overpotential equation for one step processes is obtained (Bard and Faulkner 2001; Noel and Vasu 1990):

$$i = i_0 \left[ \frac{C_O(0, t)}{C_O^*} e^{-\frac{\beta n F}{RT} \eta} - \frac{C_R(0, t)}{C_R^*} e^{\frac{(1-\beta) n F}{RT} \eta} \right] \quad (2.63)$$

Here,  $\eta = E - E_{eq}$ . By using overpotential instead of  $E_{eq} - E^{\circ'}$ , the formal electrode potential is avoided. The error caused by this evasion can be tolerated within the exchange current formulation, which is an advantage of using exchange current instead of standard rate constant (Bard and Faulkner 2001).

In practice, most reactions occur as a result of multiple steps. Every step is a redox reaction by itself and has its own forward and backward reaction rates, as well as its own net reaction rate. The slowest net rate determines the overall rate. For that reason, the step with the slowest net rate is called in literature as *Rate Determining Step* (RDS) (Bard and Faulkner 2001). At each step, electrons are moving over and in terms of current-potential definition, the number of transferred electrons during rds gain importance than the overall number of transferred electrons. This fact makes the symmetry factor used for single-step processes inadequate. Instead, the terms of anodic and cathodic transfer coefficients have to be used. These coefficients' values are functions of the number of transferred electrons in overall process, number of total number of electrons transferred before RDS ( $n_b$ ), number of transferred electrons during RDS ( $n_a$ ), the stoichiometric coefficients ( $\nu$ ), and the symmetry factor ( $\beta$ ). The relation of these parameters for cathodic and anodic transfer coefficients is expressed by Noel and Vasu (1990):

$$\alpha_c = \frac{n_b}{v} + n_a \beta \quad (2.64)$$

$$\alpha_a = \frac{n - n_b}{v} - n_a \beta \quad (2.65)$$

In single step processes the sum of the cathodic component and the anodic component of the transference must be 1, but not necessary for multi-step processes (Bard and Faulkner 2001).

After implementing these coefficients into current-potential formulation, it becomes (Bard and Faulkner 2001):

$$i = i_0 \left[ \frac{C_O(0, t)}{C_O^*} e^{-\frac{\alpha_c n_a F}{RT} \eta} - \frac{C_R(0, t)}{C_R^*} e^{\frac{\alpha_a n_a F}{RT} \eta} \right] \quad (2.66)$$

Equation 2.66 is the mathematical expression useful for conducting electrochemical cell investigations based on concentration dependent kinetics. This expression also gives the ease to define an electrochemical reaction having either a multi-step or a single step mechanism with  $n$  molar number of transferred electrons.

### 2.2.1.3. Electrode Porosity

In battery applications, porous electrodes are much preferable to plane electrodes because porous electrodes provide greater area of contact between active electrode material and the electrolyte solution, which causes higher reaction rates (Gu, Bennion, and Newman 1976). The increase in rates leads to increase in amount of current in unit time.

The most accurate mathematical model has been developed by Newman et al. and their works had been published in a book (Newman and Thomas-Alyea 2004) along with several papers (Newman and Tobias 1962; Newman and Tiedemann 1975; Gu, Bennion, and Newman 1976). The governing mathematical equations for a porous electrode were given in these publications.

Physical structure of a porous electrode has voids between solid active material particles. Those voids are filled with electrolyte solution in an electrochemical system. Solid active material is commonly a composite material to prevent some chemical

events or improve the electrode's characteristics. This mixed structure of solid matrix and the heterogeneous geometric structure of the voids affect conductivity, reaction rate, diffusivity parameters and some other ones (Newman and Tiedemann 1975). The complexity of the geometric structure leads the investigators to develop a model that it allows them to ignore geometric details.

Solid matrix of the porous electrode provides a current  $i_s$  and the electrolyte solution filling the voids provides a current  $i_l$ . The total current that the porous electrode provides is  $i_t$ . Solid matrix current density is given by:

$$\mathbf{i}_s = -\sigma \nabla \Phi_s \quad (2.67)$$

Here,  $\sigma$  is the effective conductivity of solid matrix and  $\Phi_s$  is the electric potential of the solid matrix.

The pore phase current density through a binary electrolyte solution and a solid material interface can be expressed as (Newman and Tiedemann 1975):

$$\mathbf{i}_l = -\kappa \nabla \Phi_l - \left( \frac{v_+}{\varphi_+ n} + \frac{t_{+,o}}{z_+ \varphi_+} - \frac{v_o C}{n C_o} \right) \kappa \frac{\nabla \mu_l}{F} \quad (2.68)$$

Here,  $\kappa$  is the effective conductivity of the electrolyte solution,  $\Phi_l$  is the electric potential of the electrolyte solution,  $v_+$  is the stoichiometric coefficient of cations in the electrolyte,  $\varphi_+$  is number of moles of produced cations due to the dissociation of one mole of electrolyte,  $n$  is the number of transferred electrons,  $t_{+,o}$  is the transport number of cations with respect to the solvent,  $z$  is the charge number,  $v_o$  is the stoichiometric coefficient of the solvent,  $C$  is the binary electrolyte concentration,  $C_o$  is solvent concentration and  $\mu_l$  is the chemical potential of the electrolyte. This relation can also be expressed as (Lai and Ciucci 2011):

$$\mathbf{i}_l = -\kappa \nabla \Phi_l - \frac{2\kappa RT}{F} (1 - t_{+,o}) \left( 1 + \frac{\partial \ln f}{\partial \ln C} \right) \nabla \ln C \quad (2.69)$$

Here;  $f$  is the activity coefficient. For simplifying the calculations  $\partial \ln f / \partial \ln C$  term can be assumed equal to zero.

The porosity is symbolized with  $\epsilon$ . It is also referred to as the void volume fraction (Newman and Tiedemann 1975) or electrolyte volume fraction. The change of porosity over time can be defined as:

$$\frac{\partial \epsilon}{\partial t} = \frac{1}{nF} (\nabla \cdot \mathbf{i}_t) \sum_{\text{solid phases}} \left( \frac{v_i M_i}{\rho_i} \right) \quad (2.70)$$

where;  $M_i$  is the molecular weight,  $\rho_i$  is the density of solid phase, and  $v_i$  is the stoichiometric coefficient of species  $i$ .

Porosity and tortuosity are physical factors affecting diffusivity and conductivity parameters of the electrolyte solution. These effects create diversities between the parametric values of the electrolyte solution and the actual values that those diversities are needed to be corrected. The most appreciable method to fulfil this purpose is to use Bruggeman correction coefficients (Newman and Thomas-Alyea 2004; Lai and Ciucci 2011). Then, the definitions of the effective conductivities and the effective chemical diffusivity become:

$$\sigma = \sigma^\circ \epsilon^{\text{Br}} \quad (2.71)$$

$$\kappa = \kappa^\circ \epsilon^{\text{Br}} \quad (2.72)$$

$$D = D^\circ \epsilon^{\text{Br}} \quad (2.73)$$

Here,  $\kappa_0$  is the electrolyte conductivity at out of the pores,  $D^\circ$  is the chemical diffusivity of the electrolyte out of the pore, and Br is the Bruggeman coefficient. This coefficient is determined empirically and generally it is accepted as 1.5 (Lai and Ciucci 2011).

Material balance of a porous electrode can be expressed as (Sunu and Bennion 1980):

$$\frac{\partial \epsilon C_i}{\partial t} = -\nabla \cdot \mathbf{N}_i - \frac{v_i}{nF} \nabla \cdot \mathbf{i}_i + R_{\text{src},i} \quad (2.74)$$

Here;  $\mathbf{N}_i$  is the average flux density of species  $i$  in the solution filling the pores (Newman and Tiedemann 1975) and  $R_i$  is the reaction source term. This term represents the produced or consumed species  $i$  during the electrode reaction.

$$R_{src,i} = -\frac{v_i}{nF} \nabla \cdot \mathbf{i}_1 + v_i'' a k_{mod} (C_j - C_{j,eq}) \quad (2.75)$$

where,  $C_j$  describes the concentration of species  $j$ ,  $C_{j,eq}$  represents the saturated or equilibrium concentration of the species  $j$ . In a zinc electrode reaction of a nickel-zinc cell these species  $j$  are zincate ions ( $Zn(OH)_4^{2-}$ ) (Sunu and Bennion 1980). Additionally,  $a$  is the specific surface area per unit volume of the electrode that the electrolyte solution and the solid matrix are in contact. Furthermore,  $k_{mod}$  is a rate constant, which is the modified form of the chemical rate constant for precipitated species such as zinc oxide for zinc electrode, by taking into consideration the mass transfer of species  $j$  moving from the bulk solution in the pores to the solid matrix surface where the reactions occur (Sunu and Bennion 1980).  $v_i$  and  $v_i''$  are the stoichiometric coefficients of species  $i$  in the first and second electrode reaction respectively. It is important to note that Equation 2.75 is for an electrode having two reaction mechanisms.

The expression of the average flux density of species  $i$  in the existence of a multicomponent diffusion in a binary electrolyte is given in the work of Jain and Weidner (1999):

$$\mathbf{N}_i = -D \nabla C_i + \frac{\mathbf{i}_1 t_i}{F} + C_i \mathbf{v} \quad (2.76)$$

Here, species  $i$  can be cations, anions or solvent.  $\mathbf{v}$  is the superficial volume average velocity and  $t_i$  is the transport number of species  $i$  relative to  $\mathbf{v}$ . Superficial volume average velocity is a function of partial molar volume of the electrolyte solution and it diverges to zero while the partial molar volume of the electrolyte solution is constant (Newman and Thomas-Alyea 2004). The partial molar volume of KOH electrolyte solution can be assumed constant in porous nickel and zinc electrodes, thus the average flux density is expressed as:

$$\mathbf{N}_i = -D \nabla C_i + \frac{\mathbf{i}_1 t_i}{F} \quad (2.77)$$

Since the average flux density occurs in a cross sectional area of the porous electrode consisting of solid matrix and aqueous binary electrolyte solution with low concentration, this assumption is not expected to be diversionary.

### **2.2.2. Issues with Rechargeable Nickel-Zinc Batteries**

The non-expensive active materials, safe chemistry, environmentally friendly materials, high energy and power densities, and the convenience for deep cycle applications are the main advantages of rechargeable nickel-zinc batteries. However, these batteries suffer from short life besides some other drawbacks. The reason of the short life is that the shape of zinc electrode changes after several charge/discharge cycles. With each cycle, the shape of the electrode changes more, because the zinc atoms begin to dissolve from the edges of the electrode with discharge, but with charge they rejoin to the electrode at the center of the electrode and most of the zinc atoms pile on each other. When the battery dies most of the zinc from the edges are piled at the center of the electrode while there are so few left on the edges (Vincent and Scrosati 1997).

Another important problem arising with zinc electrode is the dendritic grow. During charging, the zinc atoms might rejoin to other zinc atoms in a way to cause a dendritic expansion from zinc electrode to the nickel electrode. These dendrites expand through the separator and form a short circuit with nickel electrode which eliminates the electric potential difference between electrodes. This phenomenon only occurs depending on certain conditions (Vincent and Scrosati 1997).

If a nickel-zinc battery is charged very rapidly then it is more likely that it would not feed any electric circuit due to the non-conductive zinc oxide layer covering the surface of the zinc electrode and inhibiting the dissolution of zinc atoms at discharge process. The prevention of the dissolution of the zinc species results in the reduction reaction not taking place and this leads to the stagnation of electron transfer (Payer 2014).

All these issues lead to the fact that zinc morphology is problematic like many scientific or engineering achievements once were, before they were solved with the light of experiments and computations.

## **CHAPTER 3**

### **MODELING**

An engineering system passes from several steps to become a product from an idea. Firstly, the idea leads to the determination of goals, and then it determines the specifics of the system which is going to be designed. The specifics reveal the boundaries of the system and the researchers. After a survey has been done, a raw design becomes a solid object. Afterwards, experiments follow each other to understand how distant this design to meet the researchers' expectations. If it is beyond to be tolerated, then more experiments follow to improve the system, and most of the time, nearly every first engineering design requires modification and improvements happening with trial-and-error process. This process needs loads of resources such as time and material. More time and material expenses mean that the experimental process will cost more. There is a methodology to diminish those expenses it is to model and simulate the system. There exist various methods of modeling and these methods vary accordingly to the focused problem's nature (Ramadesigan et al. 2012).

When the focused system is a battery, then first thing to be investigated would be the market level, the system level and the electrochemical cell of this battery. Here, investigation at the market level is to determine a consumer profile and their expectations along with the price, safety and lifetime. The investigations focus on the problems of the system at the system level. For instance, these system problems are deformation, densification and passivation of zinc electrode, and dendritic growth on zinc electrode with nickel-zinc battery. In electrochemical cell level or also named sandwich level in the work of Ramadesigan et al. (2012), simplest structure with anode, cathode, separator and electrolyte, has to be understood by researchers in order to develop a solution for system problems.

First step of designing is to match anode and cathode materials to each other in terms of capacity. Second step is to understand the effects of geometry and porosity of both active and additional materials (Ramadesigan et al. 2012). Then, an economically viable production and selling plan can be made. Next step is to investigate the thermal behavior and to balance it in a tolerable range. Following step is to work with detailed

microscopic models in order to reveal more unknown to apprehend the true nature of the system and to optimize its functions by replacing one or few values of parameter at a time (Ramadesigan et al. 2012).

The aim of modeling is to decrease experimental expenses and accelerate the design process. Due to the problems dealt with, the modeling methods can be simple or complex. Simple models are fast and easily affordable, yet their predictability is poor. On the other hand, complex and high scale multiphysics models have high rank of predictability, but they are very expensive and hard to be built. Consequently, model development process begins from simple state, and then it is improved by additions of dimensions and physics until the model reaches a sufficient accuracy with experimental results. When the model is accepted that it is working well, it is applied to other situations before an experiment has been done. Couple of simulations based on the model supply better clues before changing the parameter values, and they provide opportunity to choose new parameter values more wisely in order to find accurate ones (Ramadesigan et al. 2012).

In battery modeling, according to Ramadesigan et al. (2012), models can be classified under 4 categories which are empirical, electrochemical engineering, multiphysics, molecular or atomistic models.

Empirical models neglect physical chemistry and use the data of former experiments to predict battery behaviors under changed circumstances. These models can be run very easily due to their simple formulation. However, their ability of prediction is far from being good and they are useless to be used for another battery's electrochemistry.

Electrochemical engineering models cover electrode kinetics and transport phenomena principles. Continuum models based on these principles provide more accuracy on predictions than empirical models. Electrochemical models have some levels of complexity within itself. Single-particle model uses only the transport phenomena principles with a basic approach and only applies in a narrow range of conditions. Ohmic porous electrode model is more sophisticated than single particle model by considering the porous structure of the electrodes and their interrelation with the electrolyte solution. It neglects the concentration changes in the geometry but it considers Tafel equations, linear or exponential kinetic equations defining the reactions happening between electrodes and electrolyte solution. Pseudo-two-dimensional (Pseudo 2D) model takes ohmic porous electrode model one step ahead. It additionally



includes Butler-Volmer kinetic equation and the diffusion of active materials occurring in electrolyte solution and electrodes. This model is based on physics and it is the most preferable modeling method among battery researchers. It is able to solve concentrations of species and electric potentials in an electrolyte solution and electrodes by employing electrochemistry, thermodynamics and transport phenomena principles. Involvement of many parameters with the computations increases the prediction ability along with the modeling cost (Ramadesigan et al. 2012).

Multiphysics model is being used to understand the relation between electrochemical and other physical behaviors of a battery. This model has multiple scale, dimension and computation ability to solve coupled equations. For instance, thermal model involves mass transport and heat transfer equations. As a result of this, thermal behavior of the battery can be understood and it can be managed by researchers. It is important that batteries operate with reasonable temperatures. Otherwise, reactions can get out of control and this might cause a fire, an explosion or a toxic gas or liquid release. Even if these situations do not occur, heated battery loses its performance, its voltage decreases and this is an unwanted incident. Another multiphysics model is stress-strain and particle distribution model which is useful to model intercalating particles in solid and liquid phase. Another one is mesoscale model which simulates morphological properties of the electrodes. Variation of particle size and shape with space and time are the targets which are added in this model. Stack model is used to understand cell behaviors when multiple cells are functioning together. It is important to understand radical cell behaviors inside a stack that can be resulted in fire or explosion after a thermal runaway, and since it is very difficult and not practical to measure each cell in a stack, using a model is very convenient (Ramadesigan et al. 2012).

Molecular or atomistic models are based on a method called Kinetic Monte Carlo, which is able to predict discharge characteristics in an intercalation process, diffusions of active materials, cell behavior relations with species concentrations, thermodynamics of a cell, and phenomena at interfaces. Molecular dynamics aims to improve the understanding on molecular level phenomena. Furthermore, density function theory provides an improved vision about the structure and the functionality of a material being investigated for its convenience to become an electrode (Ramadesigan et al. 2012).

Simulations are based on analytical calculations or numerical methods. Analytical calculations give exact results; however, they can be performed only for

simple problems. Most of the engineering and scientific problems involve partial equations with 2 or more unknowns. The practical way to solve them is to use numerical methods. In modeling and simulating processes, models are built to be solved either analytically as in empirical models which are non-effective or with numerical methods that the rest of the aforementioned models are built to be solved numerically. The speed and the precision ability of a numerical method depend on the complexity of the equations and the number of iterations. The number of unknown parameters, boundary conditions, and the algorithm of numerical operations define the equations and the decided error tolerance determines the iteration number. Most common numerical methods are the finite difference method (FDM), finite element method (FEM) and finite volume method (FVM). These methods can be applied with a computer program created by a code compiler such as Fortran, Matlab, Python, Visual Basic, C++. The selection of the code platform has to be done due to the advantages and disadvantages of the compiler. For instance, Matlab is a strong tool to build a computation program in a short time period; however, a computation program building in C++ takes more time. On the other hand, a computation process takes more time with Matlab compared to the process time of a program created with C++. These numerical methods can also be used by modeling software such as Comsol Multiphysics. Comsol Multiphysics is a modeling and simulation interface using finite element method (also called finite element analysis (FEA)) (COMSOL 2015) allowing to its users to build a model by determining its domains, parameters, geometry, boundary conditions, and it also allows to select physics, and then it solves the FEM (FEA) equations. This kind of modeling and simulation interfaces eliminate the code writing, thus they save a lot of time and make modeling simpler for very complex systems such as electrochemical systems (Ramadesigan et al. 2012).

The dimensions of a model are needed to be chosen carefully. The model can have 1, 2 or 3 spatial dimensions. It can be time-dependent or stationary. It can also be frequency dependent. An electrochemical model is needed to be time-dependent when the charge and discharge characteristics are predicted. Number of spatial dimension is very effective on the computation duration. Hence, the beginning step is 1D models which are the simplest models for the researchers to understand that they are on the right track. When the 1D models become accurate with experimental results, it is logical to move on to the 2D models. Since most of the modeling process is generally based on assumptions and iterations, the only reliable and effective way is to proceed step-by-

step. After obtaining a 2D accurate model, it can be proceeded to 3D modelling. However, 3D modelling is generally unnecessary for battery systems due to the fact that the complexity and the increased computation durations improve the results so less in term of accuracy. The physical forces which are able to drive charge transportation are effective on two spatial dimensions for a prismatic or cylindrical cell. Besides, experimental results are obtained as electrical outputs gathered from current collectors that these collectors have infinitely large surfaces compared to their thickness, thus they are considered that they have only two dimensions. The results obtained from the collectors are needed to be compared with the model predictions to understand model's accuracy. Since the experimental results are based on two dimensions, a 3D model of a battery usually unnecessary. Actually, eliminating the 3rd dimension is assuming that the ions are transported homogeneously along one axis. This assumption also means that the ion concentration on that axis is homogeneous and simplifies the model without causing an effective error in the simulations (Ramadesigan et al. 2012).

Modeling and simulation are very powerful tools in a research. They give the insight to design experimental conditions. They shape the expectations from the experiments or the applications. They allow predicting the behaviors or the failures of a system. They also allow testing the system under certain conditions that cannot be done as an experiment. They make possible to reach some conclusions in a shorter time with lesser costs compared to fully experimental work. Naturally, modeling and simulation are based on experiments and it is impossible to eliminate the experimentation but modeling and simulation aim to optimize it. Doing experiments is a requirement in order to solve a problem but modeling and simulation can minimize the required number of these experiments by increasing the effectivity of design process of the experiments and the researcher can progress faster with the results through his evolved ability of interpretation and prediction.

This dissertation is based on the results of a modeling and simulation process using FEM to predict the discharge behavior of a rechargeable nickel-zinc cell. A literature survey revealed that there are few studies of modelling NiZn cells with FEM. This study aims to provide an understanding about the zinc electrode nature, to fill the gap in the literature and to provide a modeling and simulating tool for further studies on NiZn cells and batteries. Additionally, this study can be referred to further studies involving zinc as an electrode. For instance, silver-zinc, zinc-air, and zinc-magnesium

battery systems can be modeled by using this kind of a modeling tool as a basis (Ramadesigan et al. 2012).

### **3.1. Challenges in Modeling a Nickel-Zinc Cell**

A mathematical model of a nickel-zinc cell has many parameters. Some of these parameters require experimental data based on SOC and DOD characteristics which are important to predict accurate results; however, it is difficult to obtain reliable SOC and DOD due to practical limitations of electronic measurements or high sensitivity of chemical measurement processes. It is experimentally almost impossible to observe chemical processes inside of a battery; therefore, every level of modeling is actually based on assumptions and speculations. These assumptions are needed to be based on well-educated-guesses. This is why the measured experimental data have to be very accurate. For instance, ionic conductivity and pH of an electrolyte solution vary with the change of electrolyte salt concentration, and with temperature. Ionic conductivity defines the velocity of charged particles and this velocity has a very significant role on battery performance.

Another problem with NiZn cell is the complex zinc electrode kinetics. Nickel electrode's kinetics are well known; however, the zinc electrode's kinetics are not. The problems lying with zinc electrode in practice also reveal themselves during modelling. The formation of zincate as a middle product and its behavior are not quite understood. Passivation and dendritic growth are also issues in modeling and are very difficult to simulate due to lack of experimental data (Payer 2014).

Eventually, modeling process is the numerical analysis process of mathematical expressions based on mathematical definitions of fundamental concepts. These mathematical expressions must include all physical aspects; however, due to lack of understanding of kinetics or experimental data, almost all models and simulations are also based on some assumptions.

Since obtaining experimental data related to reaction kinetics is nearly impossible from a solid state battery system, the mathematical expressions developed for pouch cells are sometimes used. It is likely that solid state batteries are working slightly different than pouch cells. One of its differences is the distance between electrodes. The distance between electrodes in a pouch cell are up to 1000 times longer

than the distance in a solid state battery and this difference is important to model a cell accurately with numerical methods.

As a result of these problems, the encountered situations are needed to be overcome with a trial-and-error process in order to build an accurate mathematical model of nickel-zinc cell, which is the very aim of this dissertation.

## **3.2. Modeling 1D Nickel-Zinc Battery**

Electrochemistry is a science studying chemical reactions involving electron transfer, with the aspects of thermodynamics and kinetics, and also studying the transport of the charged particles taking part in these reactions. A mathematical model of an electrochemical system is based on the analytical electrochemistry theorems.

In this dissertation, electrochemistry of the Ni-Zn battery system was modeled and simulated. One-dimensional Ni-Zn model involves mathematical expressions defining the chemical reactions, the electrochemical thermodynamics and kinetics of the cell components, and the transport phenomena of the charged particles. The model solves these mathematical expressions numerically by applying finite element method. It also allows doing parametric sweep which is a useful feature to visualize the effects of a set of selected parameters on model output.

### **3.2.1. Introduction to Modeling with FEM**

The model uses the finite element method (FEM) as a numerical analysis method. It covers the thermodynamic and kinetic theories defined for the binary electrolytes because the electrolyte of nickel-zinc battery is potassium hydroxide (KOH) which is a binary electrolyte disassociating into 2 ions which are  $K^+$  and  $OH^-$  cation and anion respectively. Electrochemical reactions in the electrodes cause variations in species concentration and porosity of the electrodes that those variations affect power density, energy density, charge/discharge cycles, cell voltage, and short circuit amperage, briefly everything about a battery.

Also this model allows changing and simulating according to those changes, any parameter; unless that change of value or expression causes any divergence in the computations.

### 3.2.2. Model Definition

A one dimensional, isothermal, ready-to-discharge cell of nickel-zinc battery is presented with this model. The model is considered that when the cell is charged and it simulates only the first discharge of the cell. The positive porous electrode is composed of nickel oxyhydroxide (NiOOH) and the negative porous electrode is zinc (Zn) metal powder pasted on a current collector. Between the electrodes the electrical insulation is provided by a separator material. In order to obtain ionic conductivity, porous electrodes and the separator are soaked with the liquid electrolyte which is potassium hydroxide (KOH).

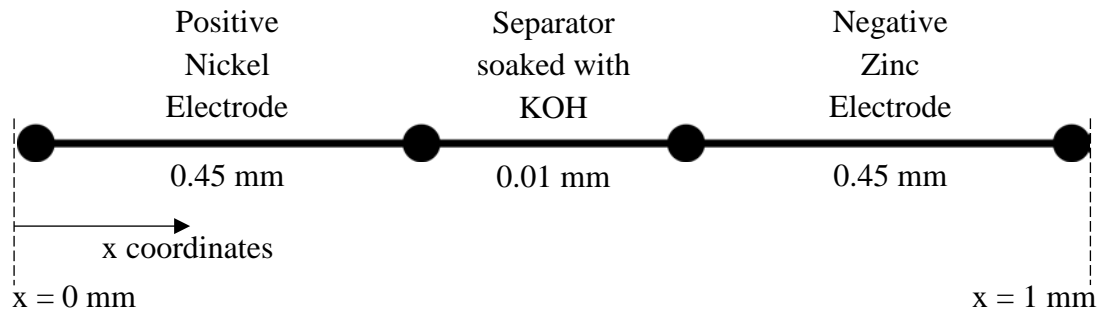


Figure 3.1. 1D geometry of the modeled NiZn battery cell.

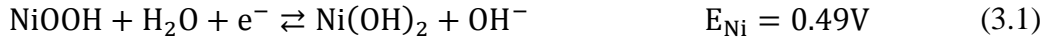
In Figure 3.1, one-dimensional geometry of the model is presented. There are three domains which are the positive porous electrode (NiOOH), the separator, and the negative porous electrode (Zn) from left to right. The thicknesses of the layers are adjustable as parameters.

### 3.2.3. Electrochemical Reactions

The processes of charge and discharge include couple of electrochemical reactions. Those reactions are also called *redox* reaction where *redox* stands for

reduction and oxidation. As a result of a reduction reaction the reactant gains electron and it becomes electrically more negative. On the other hand, at the end of an oxidation reaction the reactant loses electron and it becomes electrically positive. This happens generally for reactants by combining with an oxygen atom or atoms.

For the positive nickel electrode, it has been considered following reaction equation without charge balancing with the zinc electrode reaction:



In the negative zinc electrode, the equation for the considered electrochemical reaction is:



Equation 3.2 expresses that zinc atoms transform into zinc oxide molecules by neglecting the zincate formation which is assumed that it has no contribution to the electrochemical kinetics in terms of electrical characteristics. Electrode kinetic reactions for nickel-zinc battery are arranged as it follows respectively to the Equation 3.1 and 3.2.

$$i_{\text{loc,Ni}} = i_{0,\text{Ni}} \left\{ \left( \frac{C_{\text{OH}^-}}{C_{\text{OH}^-,\text{ref}}} \right) \left( \frac{C_{\text{Ni(OH)}_2}}{C_{\text{NiOOH},\text{ref}}} \right) \exp \left( \frac{n\alpha_{\text{a,Ni}} F \eta_{\text{Ni}}}{RT} \right) - \left( \frac{C_{\text{NiOOH}}}{C_{\text{NiOOH},\text{ref}}} \right) \exp \left( \frac{-n\alpha_{\text{c,Ni}} F \eta_{\text{Ni}}}{RT} \right) \right\} \quad (3.3)$$

$$i_{\text{loc,Zn}} = i_{0,\text{Zn}} \left\{ \left( \frac{C_{\text{OH}^-}}{C_{\text{OH}^-,\text{ref}}} \right)^2 \left( \frac{C_{\text{Zn}}}{C_{\text{Zn},\text{ref}}} \right) \exp \left( \frac{n\alpha_{\text{a,Zn}} F \eta_{\text{Zn}}}{RT} \right) - \left( \frac{C_{\text{ZnO}}}{C_{\text{Zn},\text{ref}}} \right) \exp \left( \frac{-n\alpha_{\text{c,Zn}} F \eta_{\text{Zn}}}{RT} \right) \right\} \quad (3.4)$$

In these kinetic expressions;  $i_{\text{loc}}$  is the local current density,  $i_0$  is the exchange current density,  $C_i$  is the species concentration,  $C_{i,\text{ref}}$  is the reference species concentration at the beginning,  $n$  is the transferred electrons number,  $\alpha_{\text{a}}$  and  $\alpha_{\text{c}}$  are

anodic and cathodic transfer coefficients,  $F$  is Faraday's constant,  $\eta$  is the overpotential,  $R$  is the gas constant, and  $T$  is the temperature in Kelvin.

The overpotential is calculated from electric potential of electrodes ( $\Phi_s$ ), the potential of electrolyte ( $\Phi_l$ ) and the equilibrium potential ( $E_{eq}$ ). The relation of these variables is given in the following equation.

$$\eta = \Phi_s - \Phi_l - E_{eq} \quad (3.5)$$

Once the overpotentials for electrodes are computed, local current densities can be found by using concentration dependent Butler-Volmer kinetics equations which are Equation 3.3 and 3.4.

### 3.2.4. Physics Setup

There are 4 physical processes which are the electronic current conduction in the porous electrodes, ionic charge transport in the electrolyte solution which fills the pores of the porous electrodes and the separator, material transport in the electrolyte solution, and the electrochemical reaction kinetics in the porous electrodes.

It is considered with this model that the particles are non-intercalating and the electrode kinetics are concentration driven. Bruggeman correction factor is used to improve effective electrolyte salt diffusivity in the separator and the porous electrodes. Equation 3.6 is used to calculate the effective electrolyte conductivity.

$$\sigma_{l,eff} = \frac{\epsilon_l F^2}{RT} (D_{K^+} + D_{OH^-}) C_l \quad (3.6)$$

In this equation  $\epsilon_l$  is the porosity,  $C_l$  is the electrolyte salt concentration, and  $D_i$  is the diffusion coefficient of species  $i$ . The effective electrical conductivity of the porous electrodes is calculated with Equation 3.7.

$$\sigma_{s,eff} = \sum_i m_i^{1.5} \sigma_{s,i} \quad (3.7)$$



In Equation 3.7,  $\sigma_{s,i}$  is the electrical conductivity and  $m_i$  is the mass fraction of species  $i$  in the solid phase of the porous electrode.

The difference between the reactants and the products of electrochemical reactions causes the change in porosity. Porosity change in positive nickel electrode can be formulated as:

$$\frac{\partial \epsilon_l}{\partial t} = -\frac{1}{2F} \left( \frac{M_{\text{NiOOH}}}{\rho_{\text{NiOOH}}} - \frac{M_{\text{Ni(OH)}_2}}{\rho_{\text{Ni(OH)}_2}} \right) a_{\text{Ni}} i_{\text{loc,Ni}} \quad (3.8)$$

In this equation  $a_{\text{Ni}}$  is the active specific surface area of the nickel electrode,  $M_i$  stands for the molecular weight of species  $i$  and  $\rho_i$  stands for the density of species  $i$ . The porosity change equation for the negative zinc electrode is:

$$\frac{\partial \epsilon_l}{\partial t} = \frac{1}{2F} \left( \frac{M_{\text{Zn}}}{\rho_{\text{Zn}}} - \frac{M_{\text{ZnO}}}{\rho_{\text{ZnO}}} \right) a_{\text{Zn}} i_{\text{loc,Zn}} \quad (3.9)$$

The concentration changes of species of both positive and negative electrodes are:

$$\frac{\partial c_{\text{NiOOH}}}{\partial t} = \frac{1}{2F} a_{\text{Ni}} i_{\text{loc,Ni}} \quad (3.10)$$

$$\frac{\partial c_{\text{Ni(OH)}_2}}{\partial t} = -\frac{1}{2F} a_{\text{Ni}} i_{\text{loc,Ni}} \quad (3.11)$$

$$\frac{\partial c_{\text{Zn}}}{\partial t} = -\frac{1}{2F} a_{\text{Zn}} i_{\text{loc,Zn}} \quad (3.12)$$

$$\frac{\partial c_{\text{ZnO}}}{\partial t} = \frac{1}{2F} a_{\text{Zn}} i_{\text{loc,Zn}} \quad (3.13)$$

To compute porosity and concentration variations in the electrodes, Equation 3.8 to 3.13 are arranged to be computed simultaneously with the porous electrode equations for binary electrolyte.

### 3.2.5. Boundary Conditions

The electric ground is defined at the negative electrode current collector where the electric potential is 0 V. The positive electrode current collector is where the discharge current is applied. This discharge current is formulated to be uniform or non-uniform with time, or a pulse. The selection is up to the objectives of the simulation.

Beside of the discharge current, a parametric study is provided for different initial concentration of zinc in the negative electrode.

The study stops when the minimum voltage limit is reached defined as a condition in the model.

It is assumed that the mass transport stops at the external boundaries of the porous electrodes. That means there is no mass flux from cell's porous electrodes to current collectors.

### 3.2.6. Model Parameters and Variables

Within the model user-defined parametric values and descriptions were preferred in order to satisfy the needs of a parametric modeling. These parameters are referred to the experimental data and literature survey. In the model there are two sets of data that one is called "Parameters" and the other is called "Variables". *Parameters* data set consist constant values for the variable of the equations that they were mentioned in early sections. Besides that, *Variable* data set include varying values according to certain mathematical expressions that these varying parameters are for describing mass fractions of electrode materials and effective ionic and electrical conductivities. Parameters and variables data sets are given respectively in Table A.1 and Table A.2 in Appendix A.

## 3.3. Results and Discussions

A one-dimensional nickel-zinc cell model has been built and simulated with finite element analysis method. The analytic electrochemistry methods and porous electrode kinetics had been applied numerically and behavior of the important cell

characteristics according to the amount of zinc and nickel oxyhydroxide initial concentrations and magnitude of transfer coefficients of redox equations are resulted in graphics when a constant discharge current density of  $0.05 \text{ A/cm}^2$  has been applied to the cell. Cell voltage, species concentrations in both electrodes and porosity changes along the battery due time at discharge process have been computed for various zinc initial concentrations, nickel oxyhydroxide initial concentrations, and for various values of transfer coefficients for both nickel and zinc electrodes by adding a parametric sweep option.

The development of the model, the geometric and concentration related parameters are based on an experimental battery. This battery contains two porous zinc electrodes at sides and one porous nickel electrode in the middle. Between them there are separators. Figure 3.2 shows the geometry of this battery. The electrodes and the separators are soaked with 7 molar KOH solution with pure water. The battery is prepared in discharged situation. This means that the zinc electrode was initially zinc oxide (ZnO) powder. 6 grams of zinc oxide powder were mixed with some additives and 7 molar electrolyte solution, and then it had a paste form. This paste had spread on a single side of a current collector, and then covered with the separator which is already soaked with electrolyte solution. The other zinc electrode had prepared with same steps. The zinc electrodes were having 0.45 mm of thicknesses. 10 grams of nickel oxide ( $\text{Ni(OH)}_2$ ) were mixed with additives and electrolyte solution, and then it was spread on both sides of a current collector. The nickel electrode was having 0.45 mm of thickness at each side. After this manufacture process, the battery was charged, and then it was ready for a discharge test. At this point it is assumed that the all zinc oxide turns into zinc metal and the zinc electrode was consisting of only zinc metal. Same assumption is considered for the nickel electrode too. Then the volumes and the molar concentration values of the electrodes were calculated. The battery was having 4 cm of height and 4 cm of depth that these make  $16 \text{ cm}^2$  of cross sectional area. Multiplying this area with electrode thickness gives the volume of the electrode. Excluding the current collectors, each side of the nickel electrode and the zinc electrode were having 0.045 cm of thicknesses. As a result, the volumes of the electrodes are  $7.2 \times 10^{-7} \text{ m}^3$  for each.

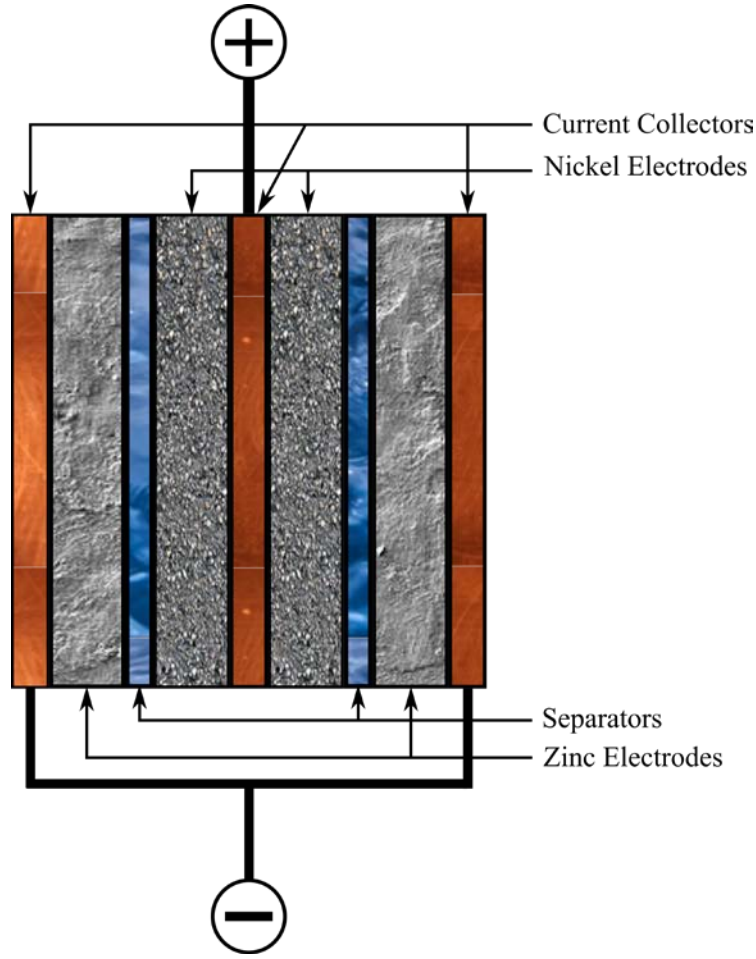


Figure 3.2. Geometry of the experimental battery.

The molecular weight of ZnO is 81.408 g/mol and the molecular weight of Ni(OH)<sub>2</sub> is 92.707 g/mol. 6 g of ZnO is 0.0737 mol. 10 g of Ni(OH)<sub>2</sub> is 0,1079 mol. It can be seen in the reaction equations given in Table 2.2 that 1 mol of ZnO turns into 1 mol of Zn and 1 mol of Ni(OH)<sub>2</sub> turns into 1 mol of NiOOH as result of charging. It was assumed that the all initial substances are transforming so there are no molar losses. At the end of charge process there are 0.0737 mol of Zn and 0,108 mol of NiOOH. The molar concentration of a substance is the ratio of its mol over its volume. The initial concentrations of Zn and NiOOH before the discharge process are:

$$C_{\text{Zn,init}} = \frac{0.0737 \text{ mol}}{7.2 \times 10^{-7} \text{ m}^3} = 102.361 \frac{\text{kmol}}{\text{m}^3} \quad (3.14)$$

$$C_{\text{NiOOH,init}} = \frac{0.1079 \text{ mol}}{7.2 \times 10^{-7} \text{ m}^3} = 149.861 \frac{\text{kmol}}{\text{m}^3} \quad (3.15)$$

These concentration values are used in the model as initial concentrations with a little approximation. Because of the symmetric geometry only the half of the actual battery is modeled. The model contains one side of the nickel electrode, one zinc electrode and one separator between them. Graphical results are obtained as a conclusion of a matching process. This process was done by using discharge test results of the experimental battery.

Figure 3.3 shows multiple discharge voltage curves as results of a series of discharge test with the experimental battery. A discharge test apparatus had been used for this test. This apparatus was connected to battery terminal, it applied a constant discharge current of  $0.05 \text{ A/cm}^2$ , and it collected the discharge voltage data, and then it delivered this data into computer. There is a cycle of charge/discharge going on but only the discharge curves are relevant for the model because the model is only able to simulate the discharge process. As the charge/discharge cycle count increases battery capacity decreases as expected. The kinetics of the charge process are not similar to the discharge process. This is why modeling the charge process requires a different approach and combining charge and discharge processes in a single model is a very difficult task. The aim of this dissertation is to develop a model which simulates the discharge behavior of a nickel-zinc cell and the experimental results are giving the control sample for a comparison.

Figure 3.4 is the model result which shows the discharge voltage when all the parameters are constant without a parametric sweep. Here, initial zinc concentration is  $100 \text{ kmol/m}^3$ , initial nickel oxyhydroxide concentration is  $150 \text{ kmol/m}^3$ , anodic transfer coefficient for zinc electrode reaction is 0.5, and anodic transfer coefficient for nickel electrode reaction is 0.6. The discharge voltage curve of the model is converged to the discharge curve obtained from the test of the experimental battery by manipulating the assumed parameters which are transport number, exchange current densities, specific surface areas of porous electrodes.

According to comparison of Figures 3.3 and 3.4 the convergence has been made but not perfectly. Especially the model used in the simulation predicts 10-20% higher capacity compared to the actual battery. The main reason for this difference is the omission of zincate ion formation during discharge process, which is expressed with Equation 2.8. Instead, it is assumed in the model that zinc species transform into zinc oxide species directly, yet it is able to give an approximated discharge voltage behavior.

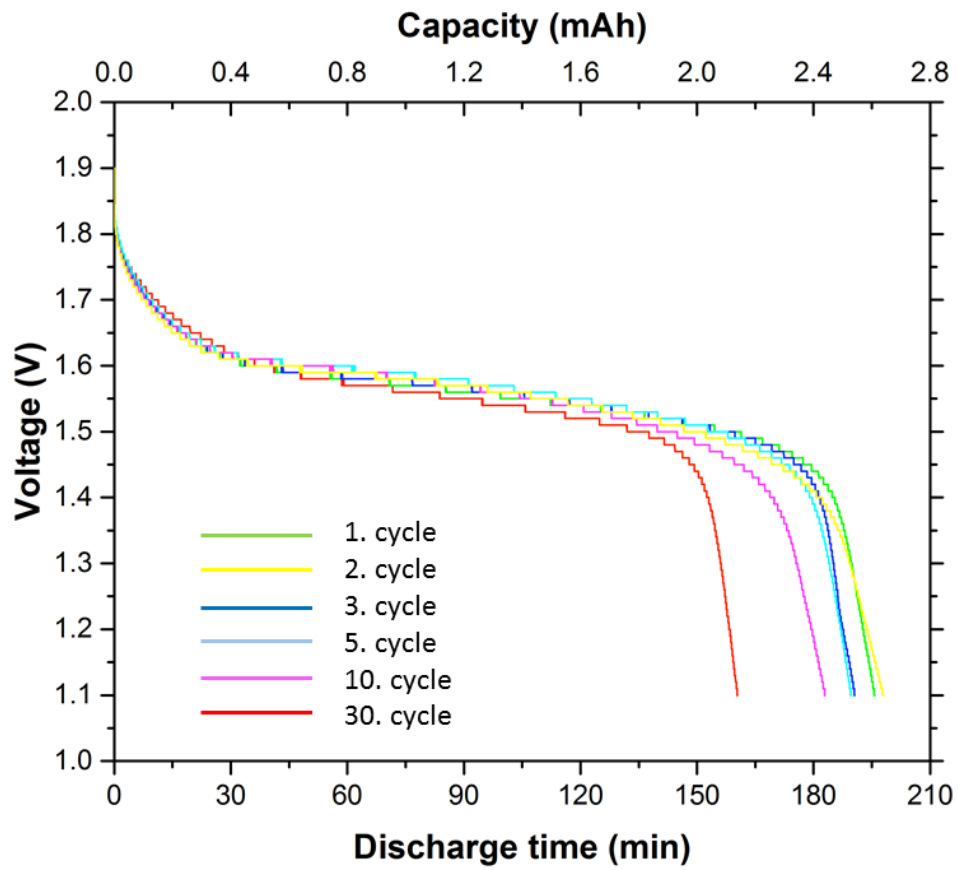


Figure 3.3. Discharge voltage test results of the experimental battery.

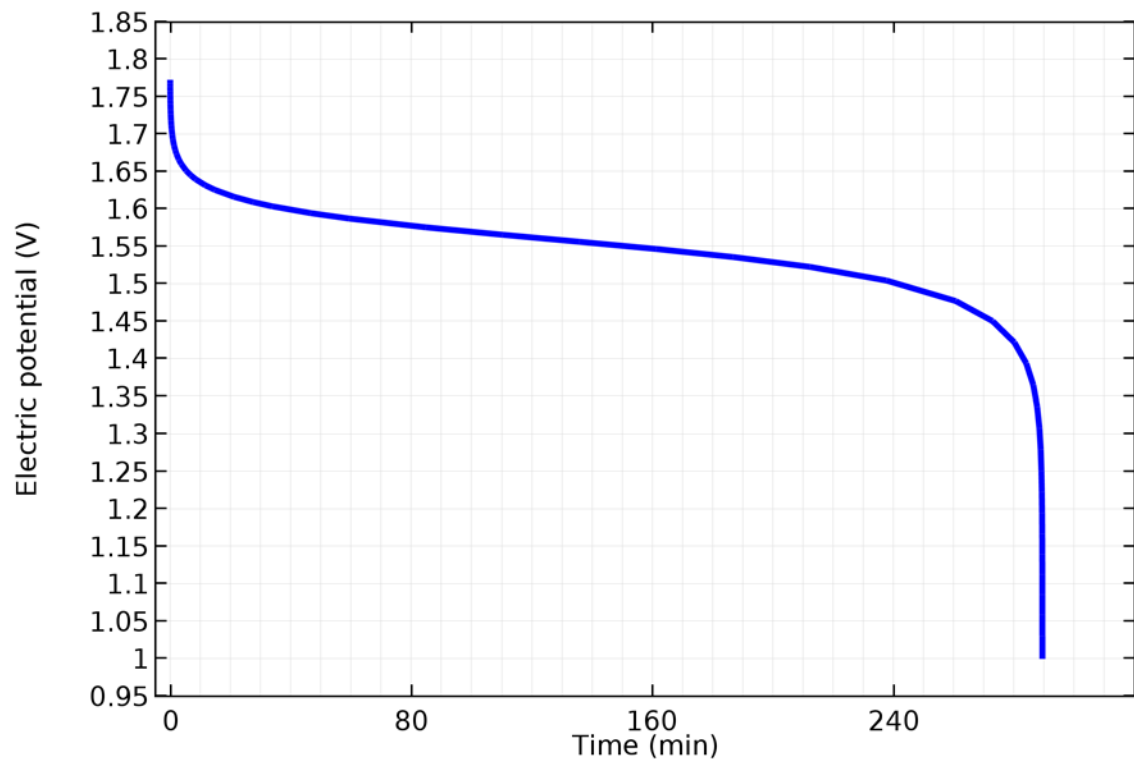


Figure 3.4. Discharge voltage according to the initial input parameters.

Some unknown but assumed parameters of the model such as exchange current densities for electrode reactions, transport number, transfer coefficients, active surface areas are manipulated in order to obtain similarity with experimental results of the nickel-zinc battery. The initial zinc concentration is approximately 100 kmol/m<sup>3</sup> and the initial nickel oxyhydroxide concentration is 150 kmol/m<sup>3</sup> for the experimental cell. These concentration values are used as input values in the parameter table of the model. Three levels of concentration have been chosen for each initial concentration parameter for parametric sweep that those levels are indicated with factors such as 0.5, 1, and 1.152 for initial zinc concentration and 0.5, 1, and 2 for nickel oxyhydroxide concentration. According to these factors the initial zinc concentrations are 50, 100 and 115.2 kmol/ m<sup>3</sup>, and initial nickel oxyhydroxide concentrations are 75, 150, and 300 kmol/ m<sup>3</sup>. Moreover, the effects of transfer coefficients of the electrode reactions on the discharge voltage, species concentrations and porosity variations were investigated. Three different coefficients have been tried out for the anodic transfer coefficients of each electrode reaction. These coefficients are 0.5, 1, and 1.5 for zinc electrode reaction and 0.3, 0.5, and 0.7 for nickel electrode reaction. Since the sum of the anodic and the cathodic transfer coefficients are equal to the molar number of the transferred electrons, the cathodic transfer coefficients can be calculated as a subtraction of the anodic transfer coefficient from the molar electron number. This relation was used to define the cathodic transfer coefficients to perform the parametric sweep for anodic transfer coefficients. The molar numbers of zinc and nickel electrode reactions are respectively 2 and 1.

$$\alpha_{a,Zn} + \alpha_{c,Zn} = 2 \quad (3.17)$$

$$\alpha_{c,Zn} = 2 - \alpha_{a,Zn} \quad (3.18)$$

$$\alpha_{a,Ni} + \alpha_{c,Ni} = 1 \quad (3.19)$$

$$\alpha_{c,Ni} = 1 - \alpha_{a,Ni} \quad (3.20)$$

Here;  $\alpha_{a,Zn}$ ,  $\alpha_{c,Zn}$ ,  $\alpha_{a,Ni}$ , and  $\alpha_{c,Ni}$  are standing for anodic and cathodic transfer coefficient for zinc and nickel electrodes. Subscripts a and c indicates the terms of anodic and cathodic.

The computations are operated for an applied discharge current density of 0.05 A/m<sup>2</sup>, until the discharge voltage drops below 1 V.

Four sets of results were obtained with parametric sweeps for initial zinc concentration, initial nickel oxyhydroxide concentration, anodic transfer coefficient for zinc electrode reaction, and anodic transfer coefficient for nickel electrode reaction. The input values for these parameters before the sweep are respectively 100 kmol/m<sup>3</sup>, 150 kmol/m<sup>3</sup>, 0.5, and 0.6. During parametric sweep of a single parameter, initial values of all other parameters, which are given in Appendix A, were used for the simulation.

### **3.3.1. Results for Various Zinc Initial Concentrations**

Determining the right amount of electrode material is important for matching the electrodes and the optimization of consumption time of the stored energy. The effects of various zinc initial concentrations over cell voltage, species concentration in porous electrodes and porosity changes are resulted and illustrated for selected time intervals. In the model three levels of initial concentration for zinc metal has been considered. Those levels are based on the zinc metal concentration in experimental battery. In the experimental battery there is approximately 100 kmol/m<sup>3</sup> of zinc metal. In the model the computations took into considerations half of this value and the 1.152 times of it along with itself. So the initial concentrations that the computations include are 50, 100, and 115.2 kmol/m<sup>3</sup>. The last concentration value is the upper limit for convergence of the numerical analysis. When the factor become 0.153 the computations does not converge because it does not match with nickel oxyhydroxide concentration.

#### **3.3.1.1. Cell Voltage**

Most important information about an electrochemical cell is that how much potential it provides and for how long it is providing. Figure 3.5 shows three functions of discharge voltage over time for 50 kmol/m<sup>3</sup>, 100 kmol/m<sup>3</sup>, and 115.2 kmol/m<sup>3</sup> initial concentration of zinc metal in the negative electrode.



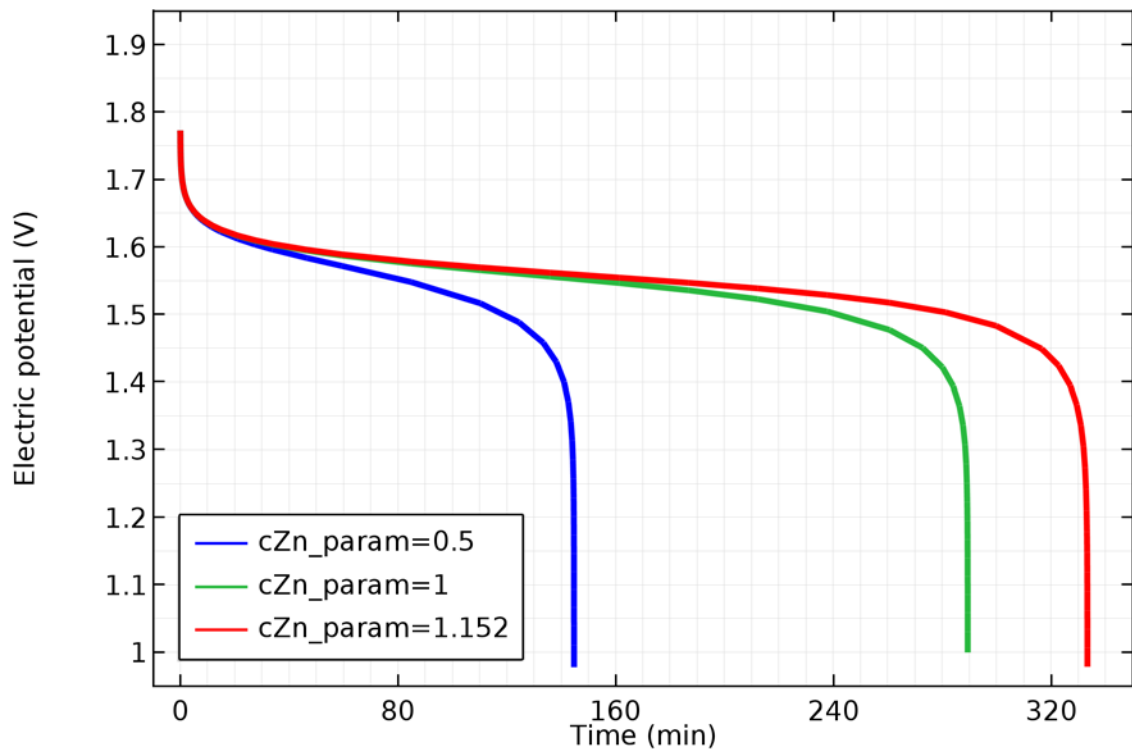


Figure 3.5. Discharge voltage over time for three different initial Zn concentrations.

In Figure 3.5,  $cZn\_param$  values are the factors for  $100 \text{ kmol/m}^3$  concentration which is the concentration value of zinc metal in the experimental battery. The direct effect of zinc concentration onto cell endurance can be seen in this figure. Of course this effect is dependent on the initial nickel oxyhydroxide concentration which is  $150 \text{ kmol/m}^3$  during the parametric sweep for zinc initial concentrations. The duration of the electricity generation above 1 V of electrical potential is 144 minutes for  $50 \text{ kmol/m}^3$ . It is 289 minutes for  $100 \text{ kmol/m}^3$  and 333 minutes for  $115.2 \text{ kmol/m}^3$ .

### 3.3.1.2. Zinc and Zinc Oxide Species Concentration Changes

Zinc is the active material and the main material of the negative electrode. During discharge process an oxidation reaction happens in the porous zinc electrode. As a result of this reaction zinc atoms make a bond with oxygen atoms and forms zinc oxide molecules. This is a very simple explanation based on omission of multiple reaction mechanisms and any side reaction happening in the zinc electrode. Concentration change of zinc and zinc oxide species are expected to affect on battery performance.

Figure 3.6, 3.7, and 3.8 demonstrate the variations of concentration of zinc and zinc oxide species at three distinct moment of time which are the beginning, middle, and end of discharge process.

Since the model is built based on the ideal conditions which means it only covers the simple one step reaction mechanism isothermally without any side effects such as zincate formation. For that reason, in Figure 3.6, 3.7, and 3.8 all the zinc material is turned into zinc oxide at the end of discharge. In the middle of discharge process, the steady and linear consumption of zinc material during the oxidation reaction can be observed. Also it can be observed that the zinc species dissolve a little bit faster at the zinc electrode/separator interface ( $x = 0.55$  mm) compared to the dissolution at the deeper zone of the porous electrode.

The curves indicate that the zinc species transformation behavior into zinc oxide species over time is happening steadily and independent from the initial concentration.

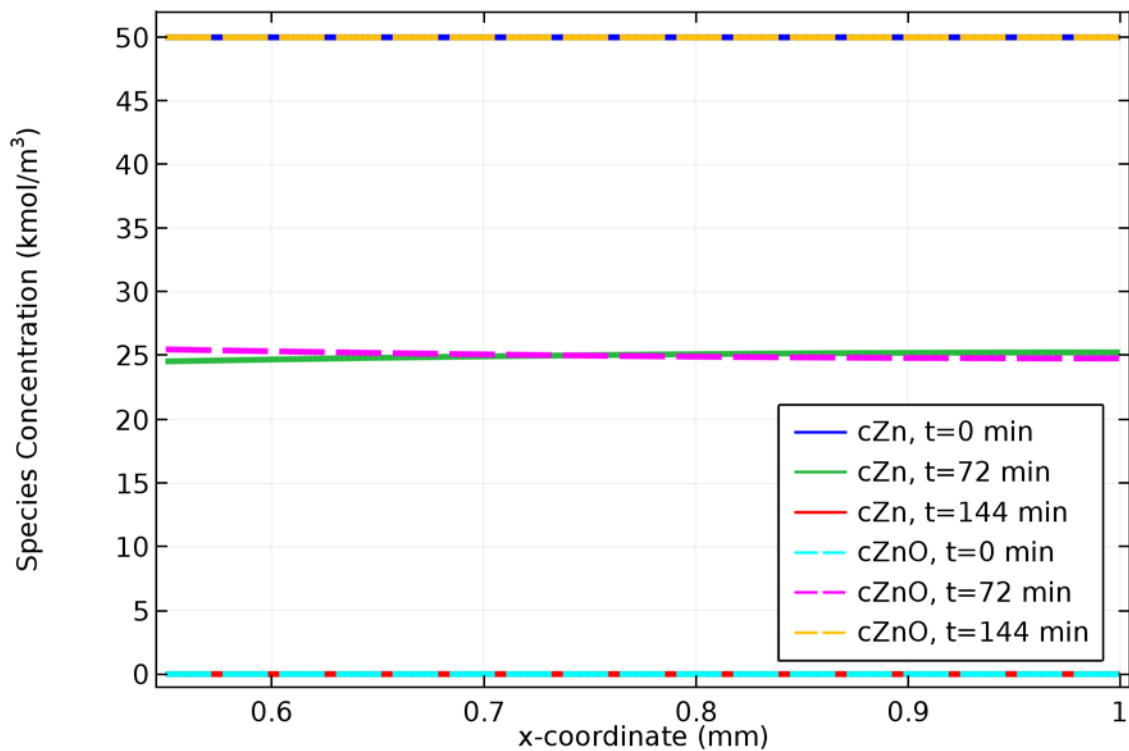


Figure 3.6. Zn and ZnO concentrations inside NiZn cell for initial Zn concentration of  $50 \text{ kmol/m}^3$ .

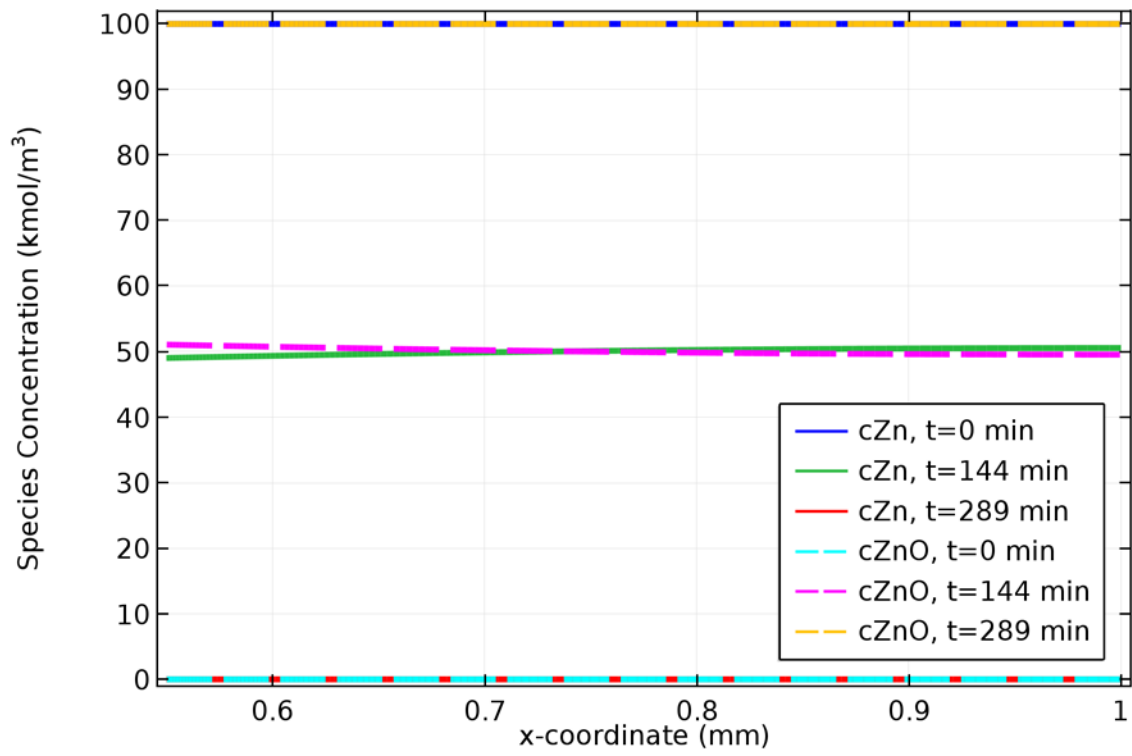


Figure 3.7. Zn and ZnO concentrations inside NiZn cell for initial Zn concentration of 100 kmol/m<sup>3</sup>.

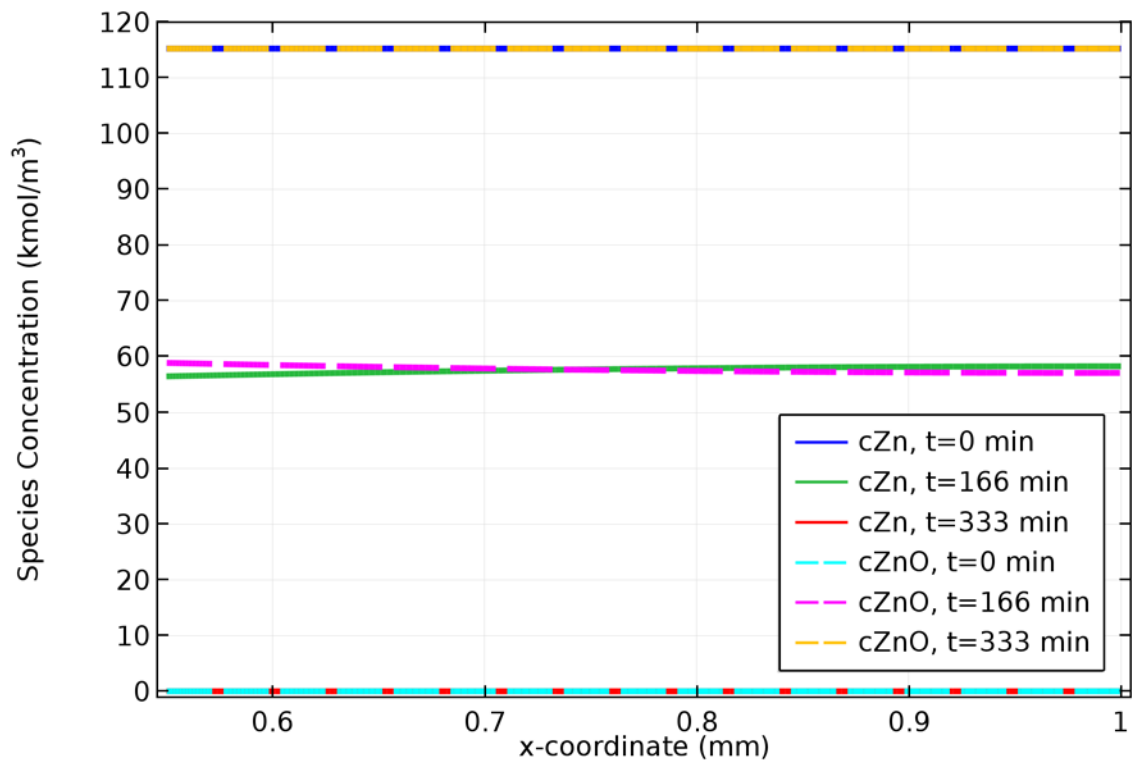


Figure 3.8. Zn and ZnO concentrations inside NiZn cell for initial Zn concentration of 115.2 kmol/m<sup>3</sup>.

### 3.3.1.3. Nickel Oxyhydroxide and Nickel Hydroxide Species Concentration Changes

At the beginning of discharge, positive nickel electrode is majorly formed by nickel oxyhydroxide species. During the discharge, reduction reaction takes place in the positive electrode and nickel oxyhydroxide molecules transform into nickel hydroxide molecules after catching a hydrogen cation.

Figure 3.9, 3.10, and 3.11 reveal the species concentrations of nickel oxyhydroxide and nickel hydroxide for initial zinc concentrations of 50, 100, and 115.2  $\text{kmol/m}^3$  at the beginning, middle and end of discharge.

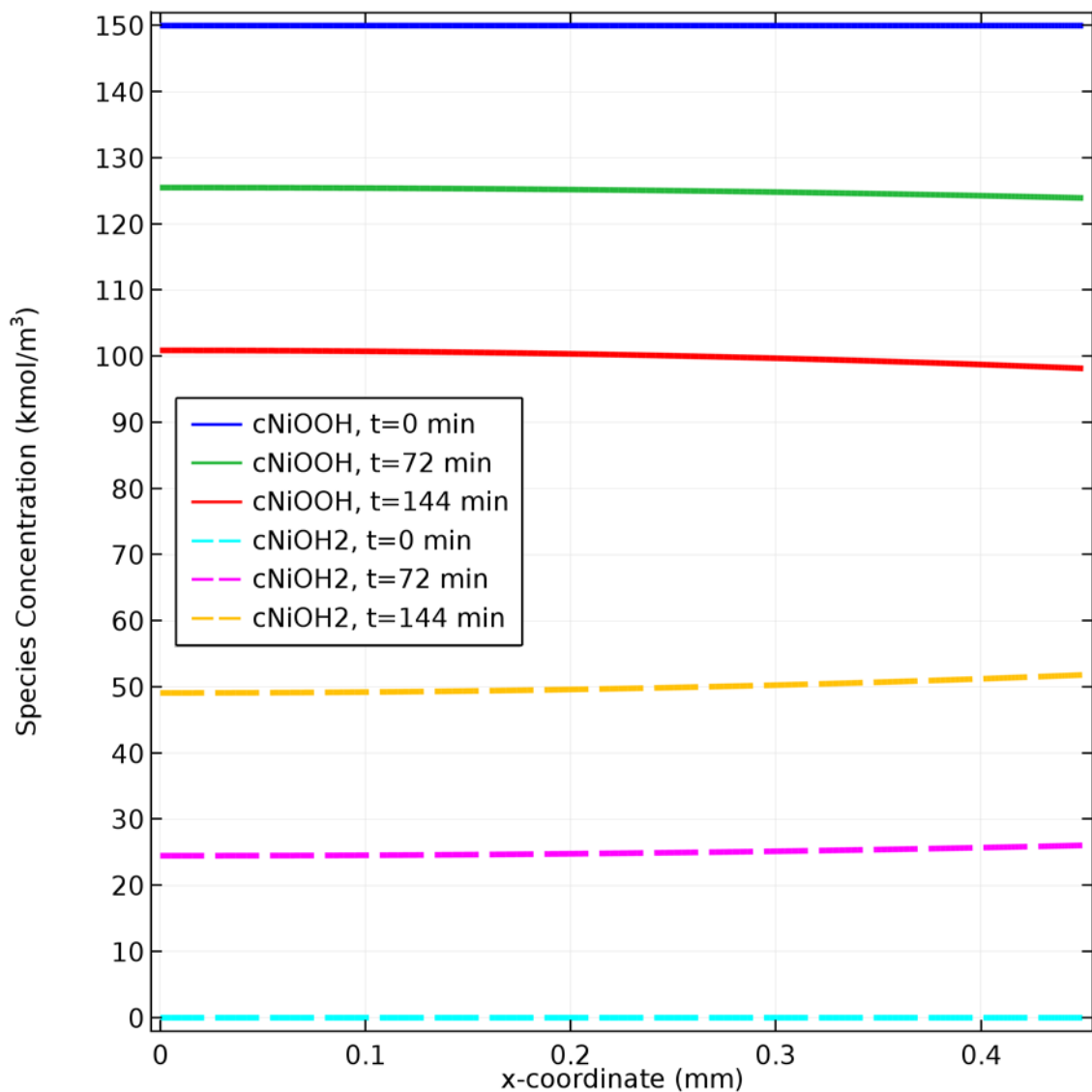


Figure 3.9. NiOOH and Ni(OH)<sub>2</sub> concentrations inside NiZn cell for initial Zn concentration of 50  $\text{kmol/m}^3$ .

Figure 3.9 and 3.10 show that the initial zinc concentration has a great effect on nickel oxyhydroxide consumption during the reduction reaction. When the zinc concentrations are 50 and 100 kmol/m<sup>3</sup> nickel oxyhydroxide transformations are steady and all the species are not consumed, this means that the battery operates as zinc limited just like the experimental battery did before. In those figures the slight difference of dissolving velocity of nickel oxyhydroxide species at the separator interface ( $x=0.45$  mm) and at the deep of the porous nickel electrode can be seen.

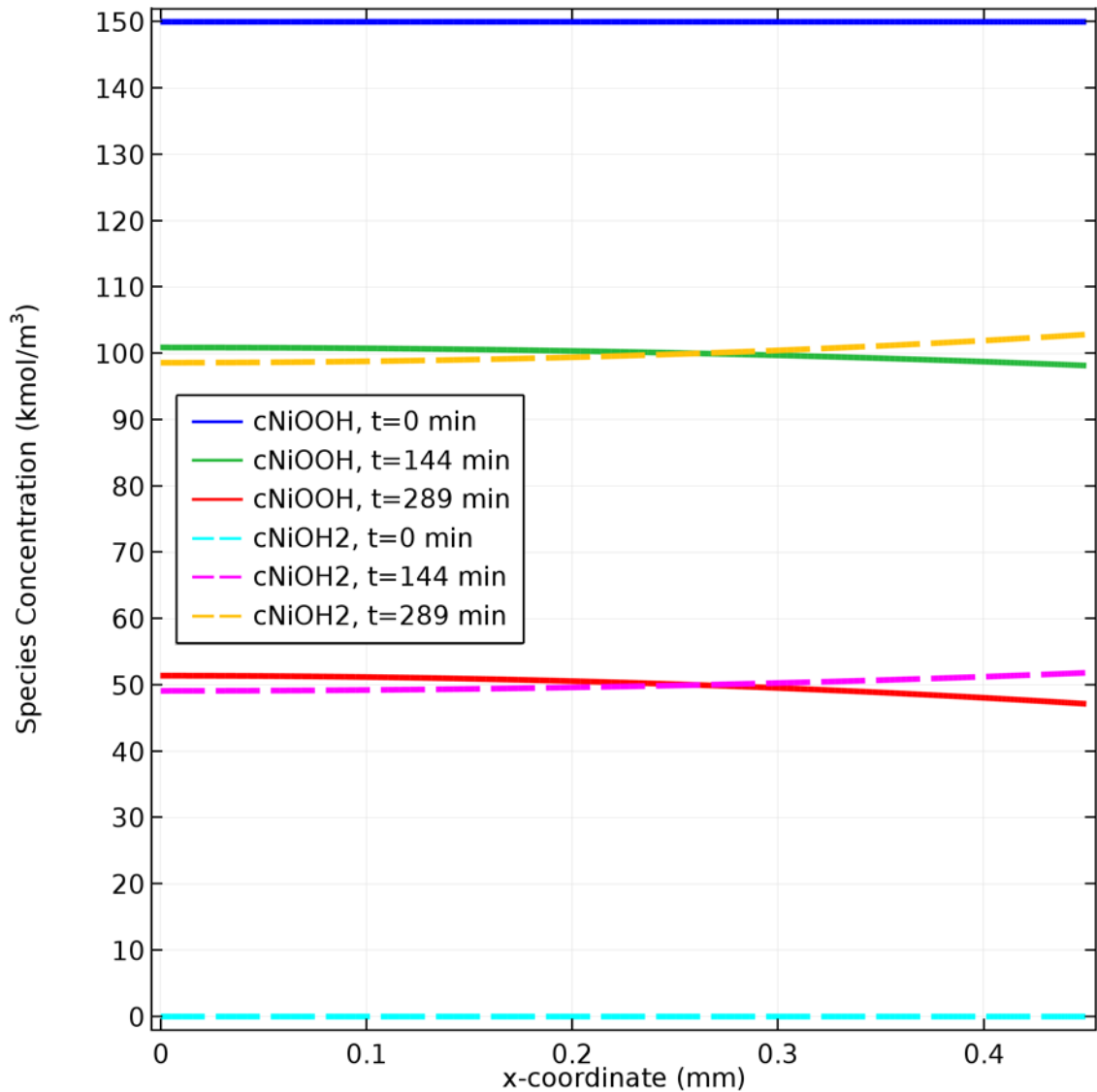


Figure 3.10. NiOOH and Ni(OH)<sub>2</sub> concentrations inside NiZn cell for initial Zn concentration of 100 kmol/m<sup>3</sup>.

On the other hand, Figure 3.11 shows that when the initial zinc concentration is  $115.2 \text{ kmol/m}^3$ , the nickel oxyhydroxide consumption suddenly increases at the separator interface when the cell is getting closer to be depleted. This initial concentration value is the upper limit for convergence of the numerical calculations.

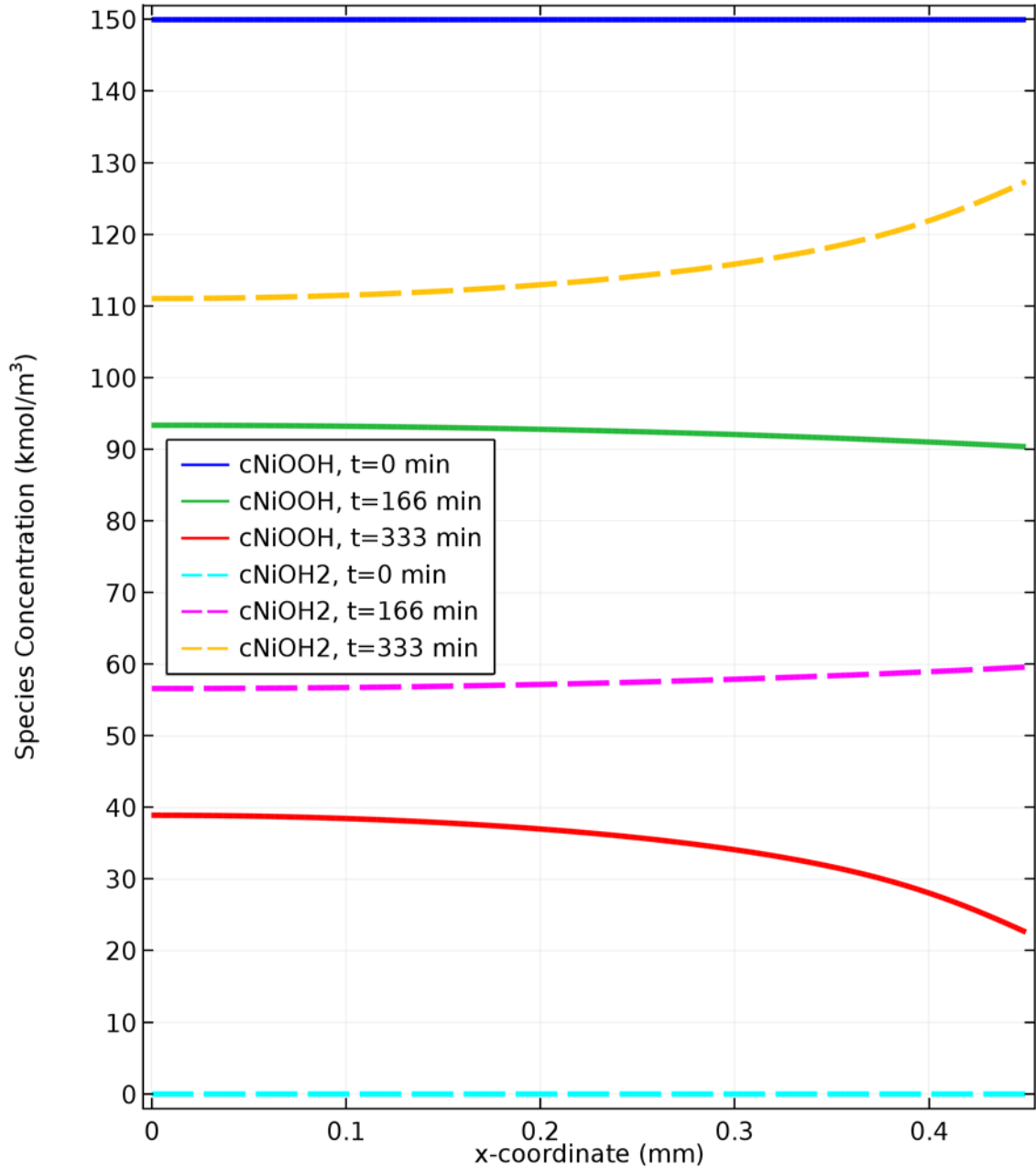


Figure 3.11.  $\text{NiOOH}$  and  $\text{Ni(OH)}_2$  concentrations inside NiZn cell for initial Zn concentration of  $115.2 \text{ kmol/m}^3$ .

### 3.3.1.4. Porosity Changes

Porosity changes while a battery operates. The changed porosity eventually influences the battery behavior and performance. Figure 3.12, 3.13, and 3.14 shows the porosity changes for initial zinc concentrations of 50, 100, and 115.2 kmol/m<sup>3</sup>. The initial porosities of zinc and nickel electrodes are 0.731 and 0.5 respectively. The porosity of the separator is 0.5.

As a result of the electrode reactions during the discharge process, porosities of the both electrodes decrease with time. The porosity of the separator remains intact. In Figure 3.12 shows that the porosity deformation is greater at the separator interfaces due to electrode reactions. The porosity of the zinc electrode (between  $x=0.55$  mm and  $x=1$  mm) decreases faster than the nickel electrode and it becomes approximately 0.47 when the all zinc species transformed to zinc oxide species all over the  $x$ -coordinates. At this final moment porosity of nickel electrode at the current collector side is nearly 0.349 and 0.34 at the separator side.

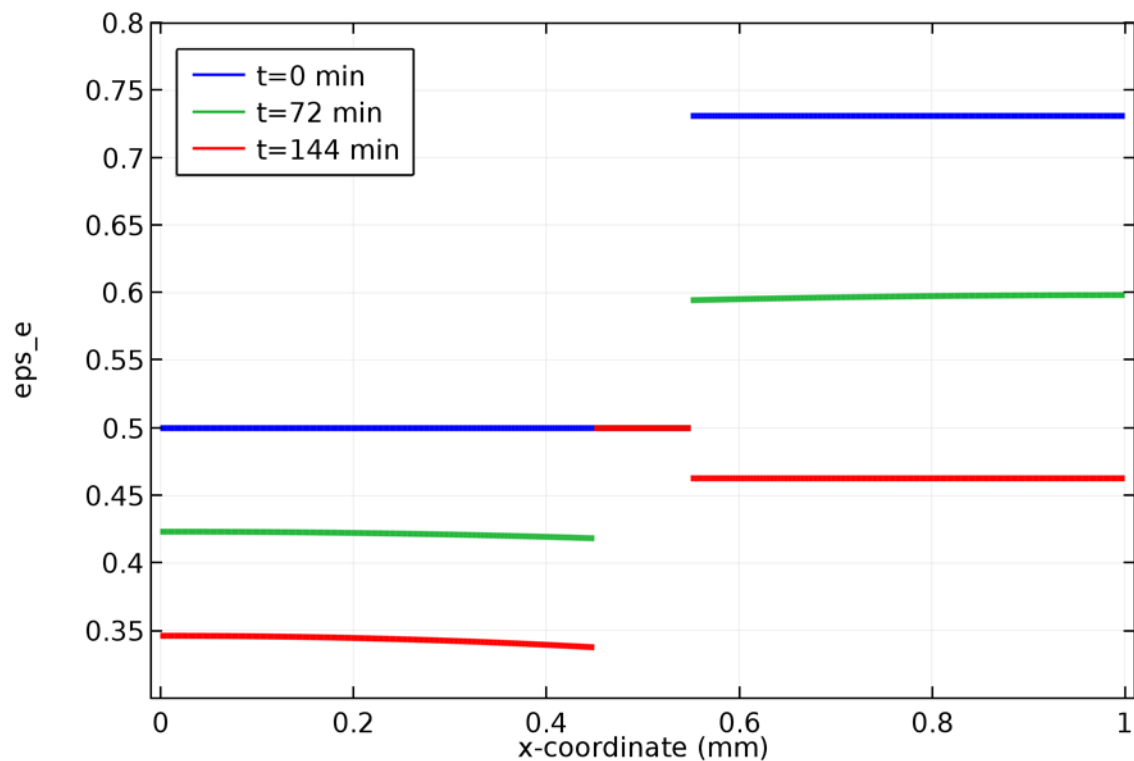


Figure 3.12. Porosity changes for initial Zn concentration of 50 kmol/m<sup>3</sup>.

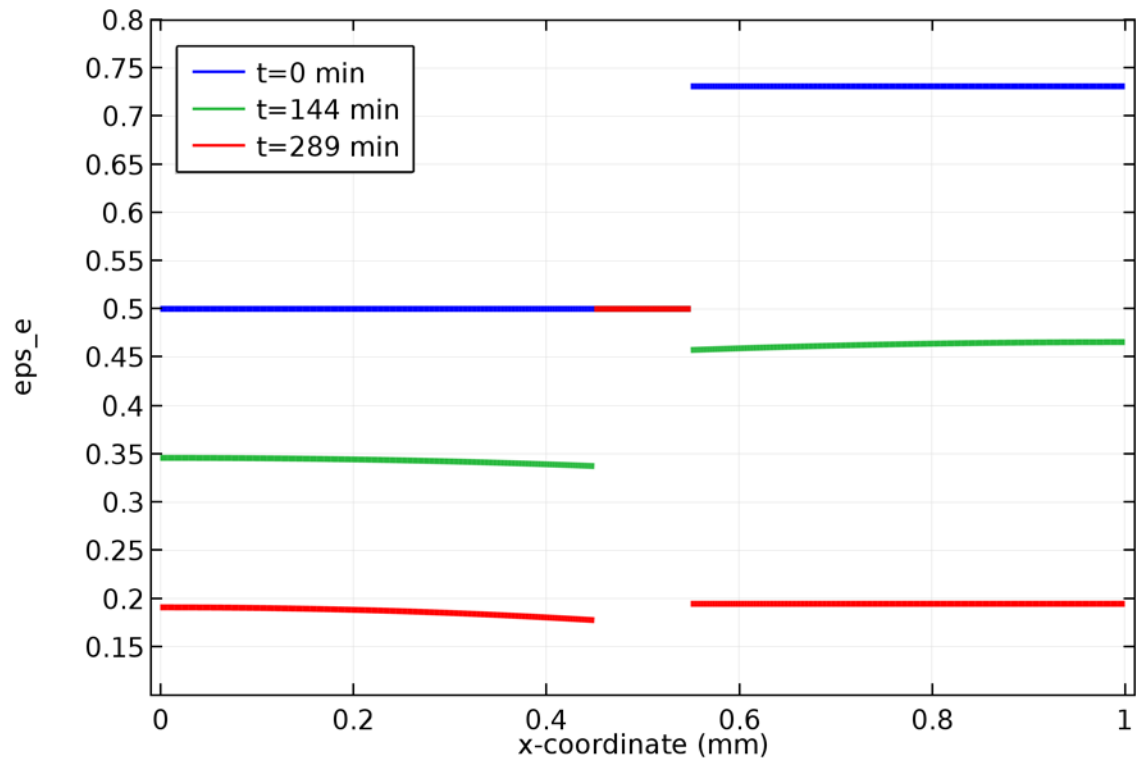


Figure 3.13. Porosity changes for initial Zn concentration of 100 kmol/m<sup>3</sup>.

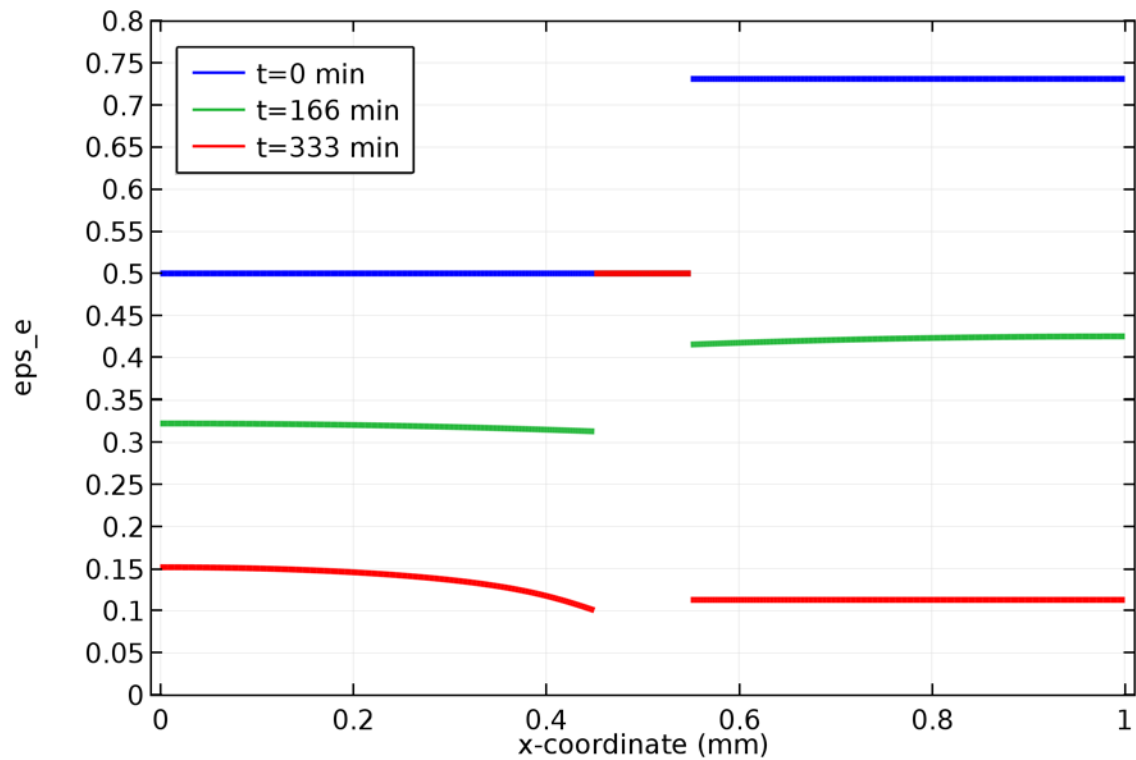


Figure 3.14. Porosity changes for initial Zn concentration of 115.2 kmol/m<sup>3</sup>.



Figure 3.13 indicates that the increase in initial zinc concentration concluded with more decrease of porosities in the electrodes. For nickel electrode collector current side porosity is 0.19 and separator side porosity is 0.17 at the final moment when the zinc species are fully transformed into zinc oxide. In Figure 3.14, the porosity curves for the final moment shows that the porosity change velocity at the separator side of the nickel electrode increases near to the depletion of zinc species when the initial zinc concentration is  $115.2 \text{ kmol/m}^3$ . This behavior looks similar to the nickel oxyhydroxide species concentration behavior when the level of initial zinc concentration is the same.

### **3.3.2. Results for Various Nickel Oxyhydroxide Initial Concentrations**

Another parametric sweep similar to the initial zinc concentration study has been done for initial nickel oxyhydroxide concentration. Three levels of concentration have been applied. The original concentration is  $150 \text{ kmol/m}^3$  which is obtained from the experimental battery. The other two levels are the half of this value and the double of it, so the concentrations which are swept are 75, 150, 300  $\text{kmol/m}^3$ .

#### **3.3.2.1. Cell Voltage**

In Figure 3.15, three discharge voltage curves are being seen. When the half of the original concentration of nickel oxyhydroxide is used the duration of the electricity generation above 1 V of electric potential is 217 minutes. For 150 and 300  $\text{kmol/m}^3$  it is 289 minutes. Here the curves indicate that initial nickel oxyhydroxide concentrations are no longer any effect on cell duration after a moment since it is zinc limited cell case. However, the amount of concentration of nickel oxyhydroxide has an effect on the cell voltage and the plain of the voltage curve contrary to the initial zinc concentration.

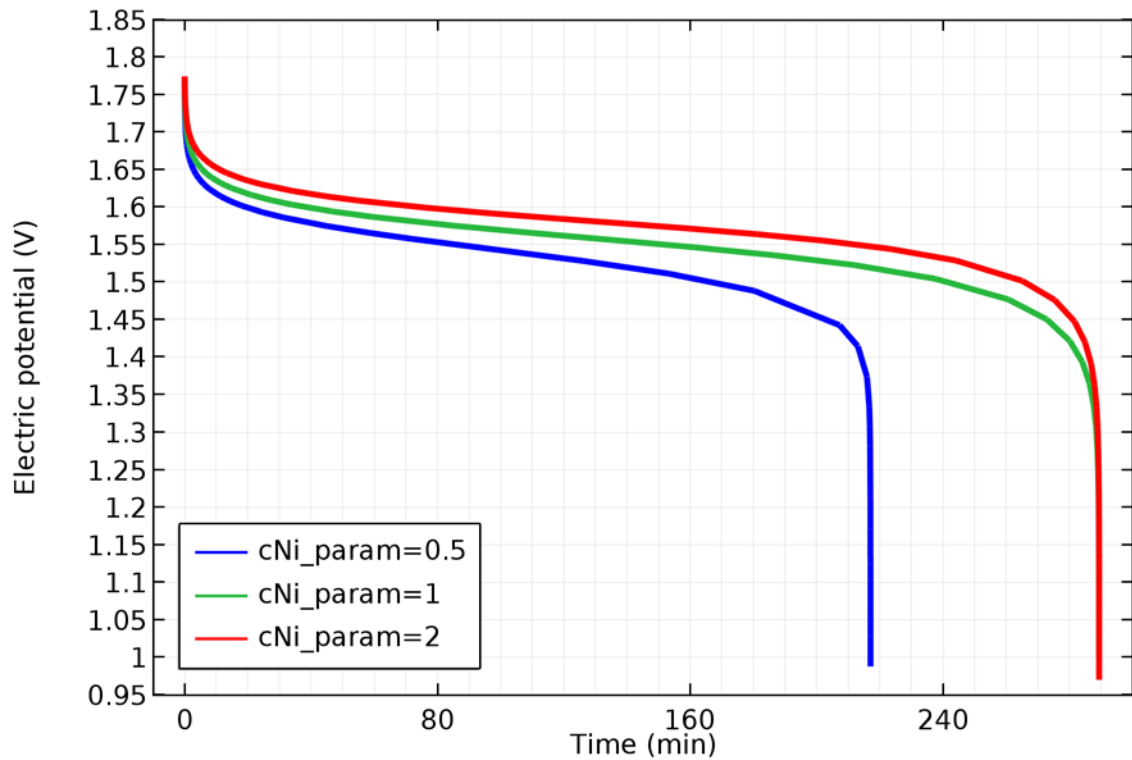


Figure 3.15. Discharge voltage over time for three different initial NiOOH concentrations.

In this plot, the influence of zinc electrode to discharge duration is obvious after taking into consideration the previous section about initial zinc concentration.

### 3.3.2.2. Zinc and Zinc Oxide Species Concentration Changes

In Figure 3.16 the initial nickel oxyhydroxide concentration is  $75 \text{ kmol/m}^3$ . First of all, this figure reveals that the nickel oxyhydroxide species are depleted before than the zinc species. More than  $20 \text{ kmol/m}^3$  zinc species do not involve in the oxidation reaction. Since the 1 mol of zinc transform into 1 mol of zinc oxide the species concentration curves vary linearly over time.

Figure 3.17 and 3.18 demonstrate the variation in concentration of zinc and zinc oxide species at three distinct moment of time for  $150$  and  $300 \text{ kmol/m}^3$  initial nickel oxyhydroxide concentrations. For both concentrations the discharge durations are the same so is the zinc and zinc oxide species distributions and zinc species are depleted completely at the end of both computations.

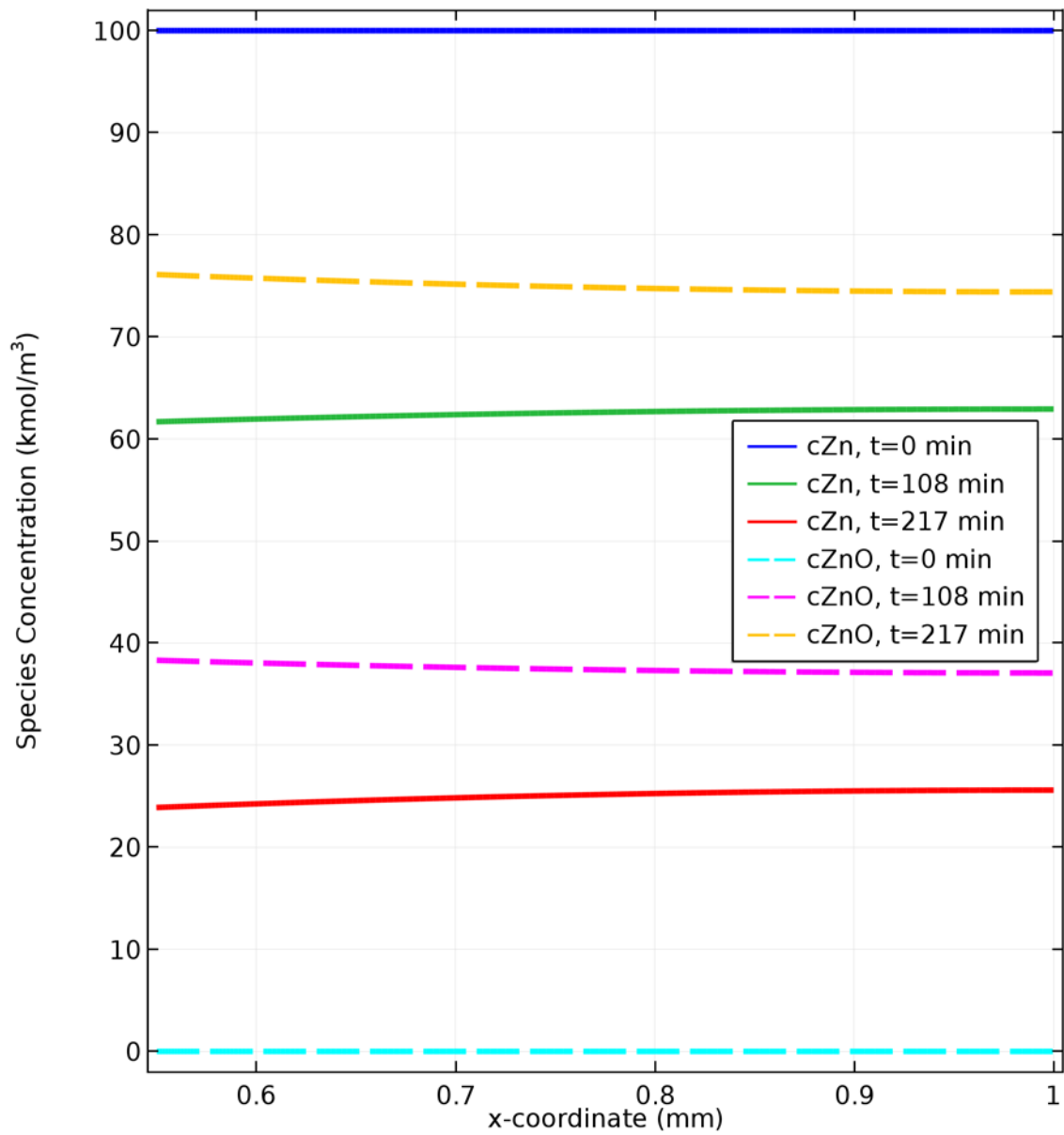


Figure 3.16. Zn and ZnO concentrations inside NiZn cell for initial NiOOH concentration of  $75 \text{ kmol/m}^3$ .

Even though the initial nickel oxyhydroxide concentrations are affecting the cell voltage and the plateau of the curve; they have no effect on zinc and zinc oxide species distributions according to Figure 3.17 and 3.18.

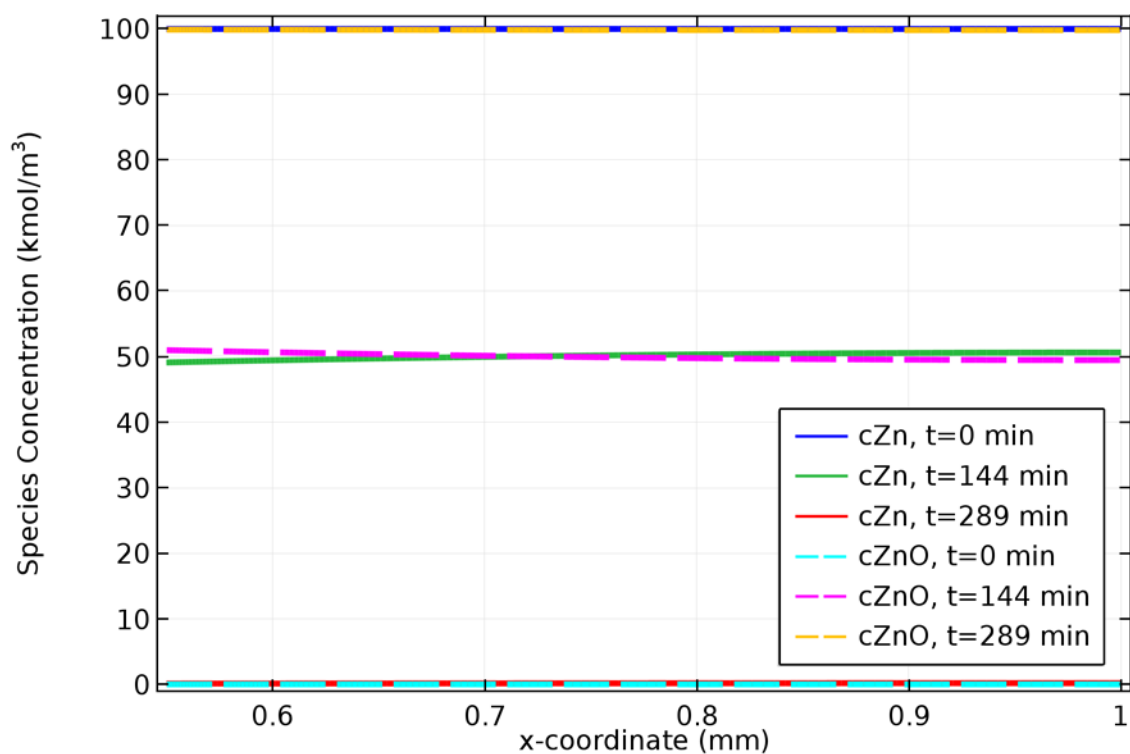


Figure 3.17. Zn and ZnO concentrations inside NiZn cell for initial NiOOH concentration of 150 kmol/m<sup>3</sup>.

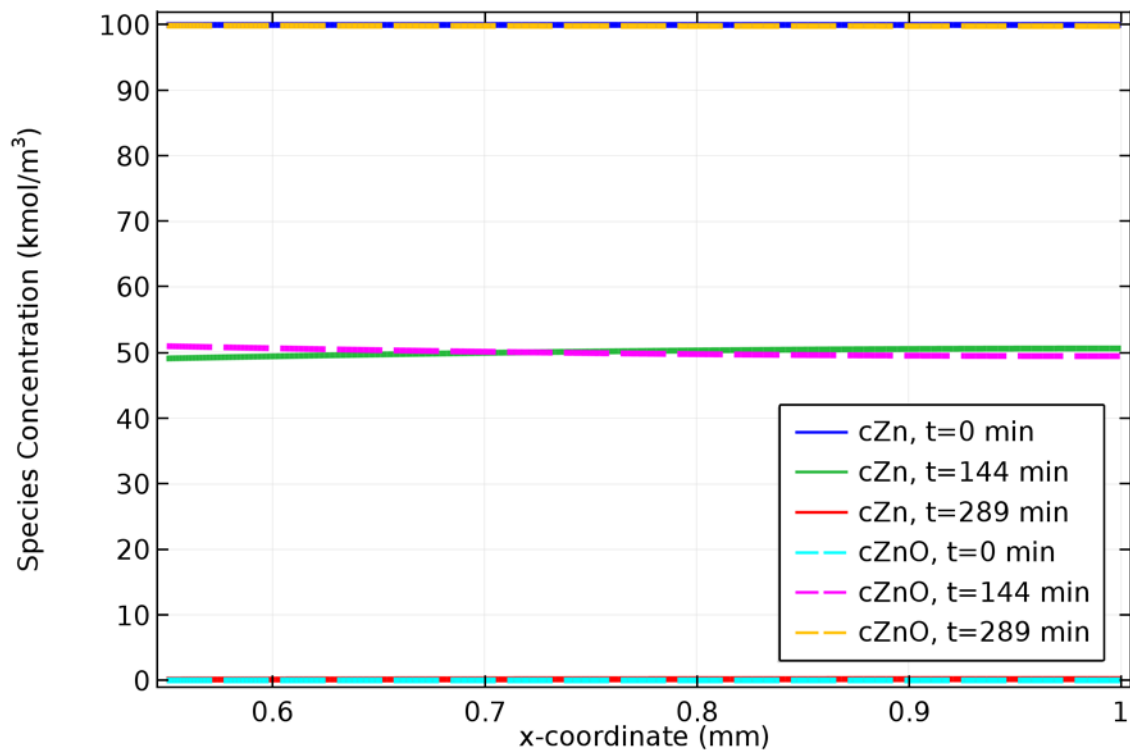


Figure 3.18. Zn and ZnO concentrations inside NiZn cell for initial NiOOH concentration of 300 kmol/m<sup>3</sup>.

### 3.3.2.3. Nickel Oxyhydroxide and Nickel Hydroxide Species Concentration Changes

Figure 3.19 demonstrates that the nickel oxyhydroxide reserve is completely depleted after a discharge which takes 217 minutes when its initial concentration is  $75 \text{ kmol/m}^3$ .

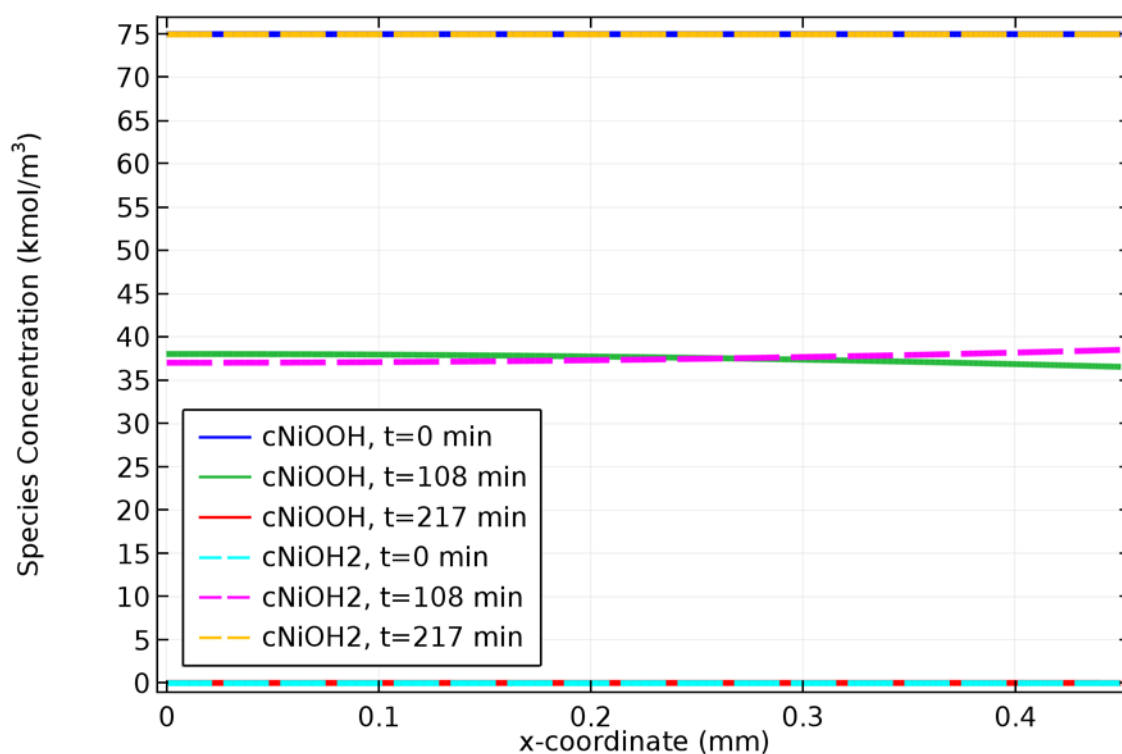


Figure 3.19. NiOOH and Ni(OH)<sub>2</sub> concentrations inside NiZn cell for initial NiOOH concentration of  $75 \text{ kmol/m}^3$ .

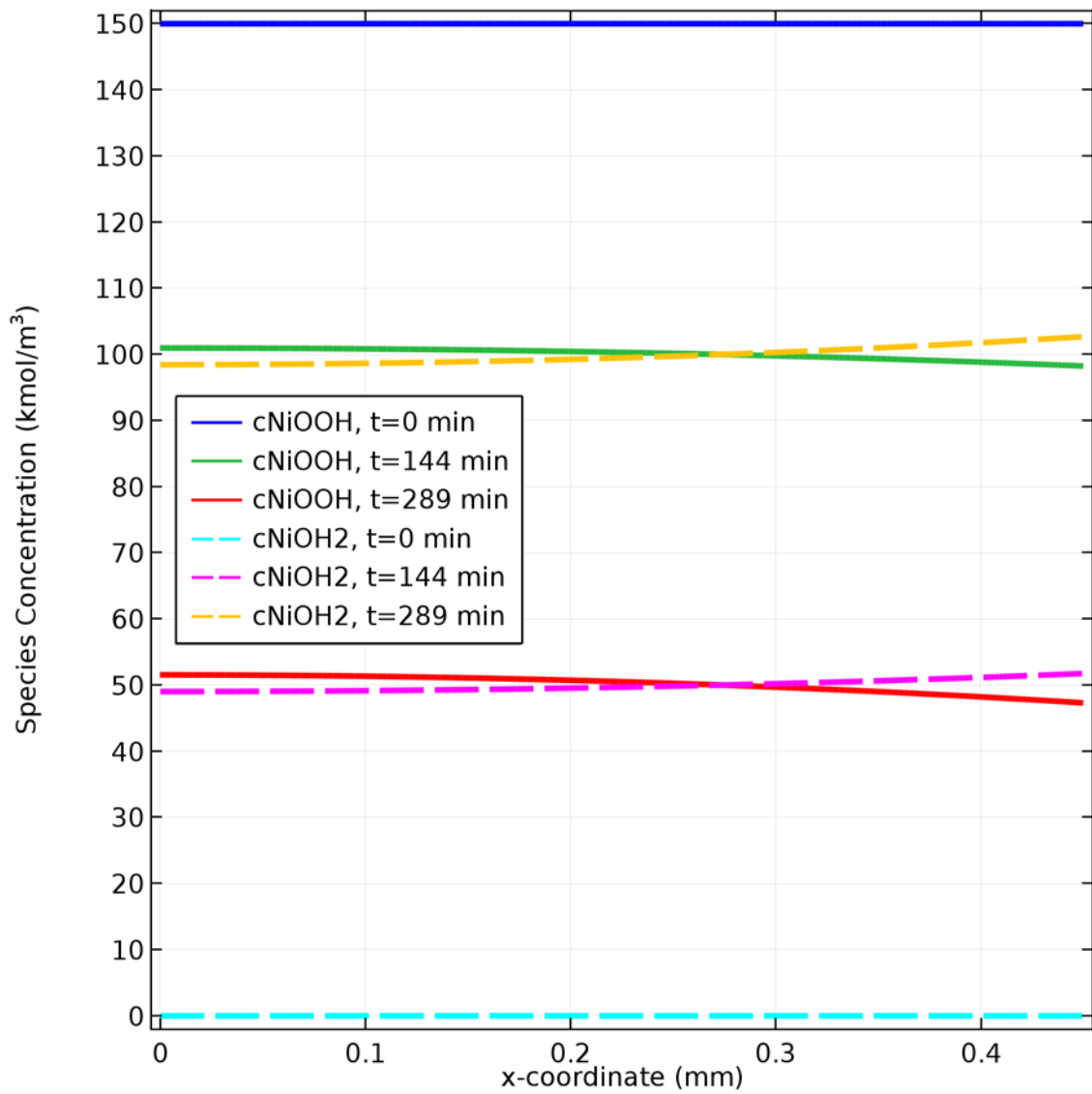


Figure 3.20. NiOOH and Ni(OH)<sub>2</sub> concentrations inside NiZn cell for initial NiOOH concentration of 150 kmol/m<sup>3</sup>.

Figure 3.20 shows that the initial nickel hydroxide concentration of 150 kmol/m<sup>3</sup> is more than enough. There is an excess nickel oxyhydroxide material having 50 kmol/m<sup>3</sup> concentration at the end of discharge. The excess material concentration is 200 kmol/m<sup>3</sup> when the initial concentration is 300 kmol/m<sup>3</sup> according to Figure 3.21.

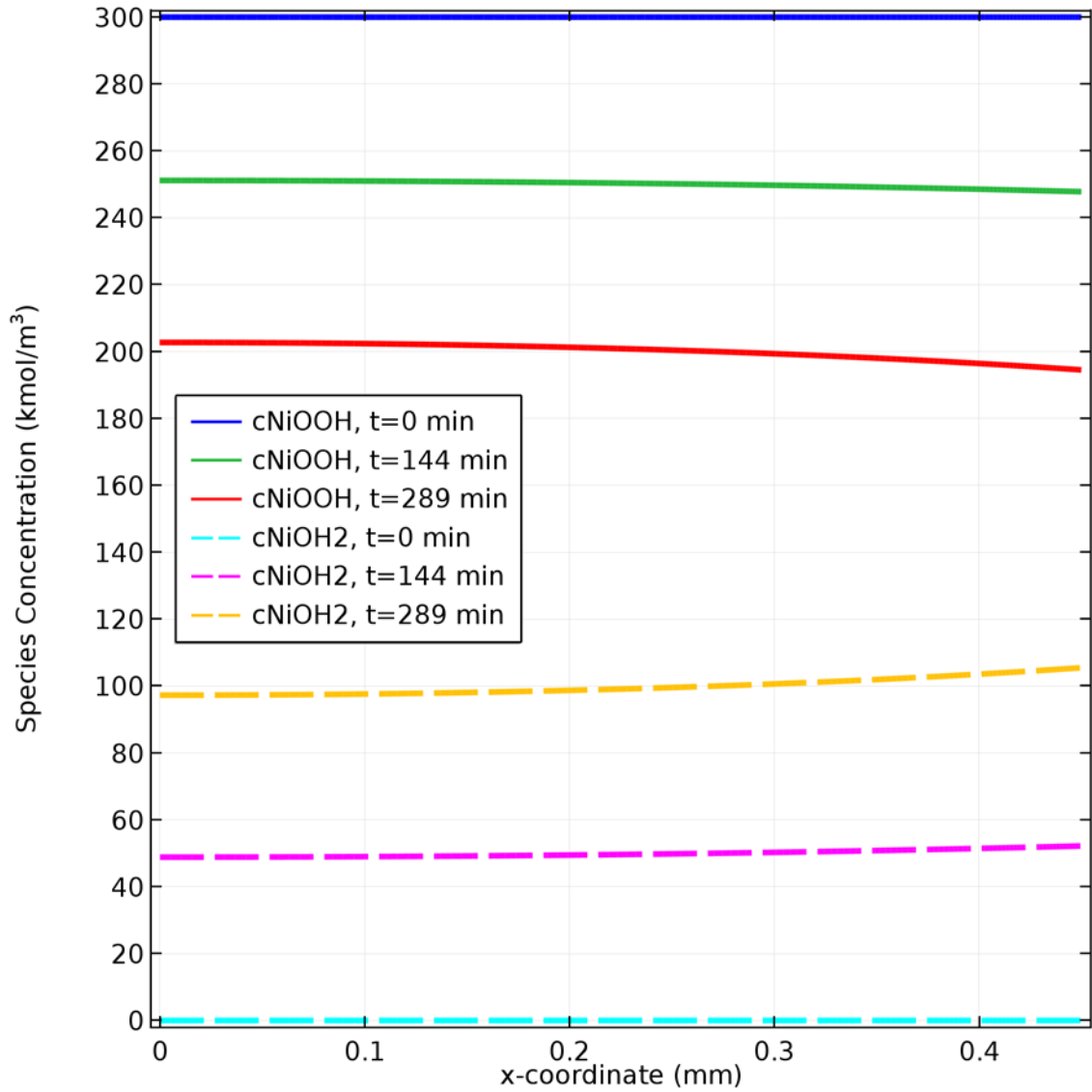


Figure 3.21. NiOOH and Ni(OH)<sub>2</sub> concentrations inside NiZn cell for initial NiOOH concentration of 300 kmol/m<sup>3</sup>.

#### 3.3.2.4. Porosity Changes

Figure 3.22, 3.23, and 3.24 indicate that the porosity change is related with the duration. As discharge times get longer with increasing NiOOH concentration the porosities of both electrodes decrease more.

The porosity values for zinc electrode are similar in Figure 3.23 and 3.24. In these figures the discharge processes have the same length of time and all the zinc species involve into the reaction.

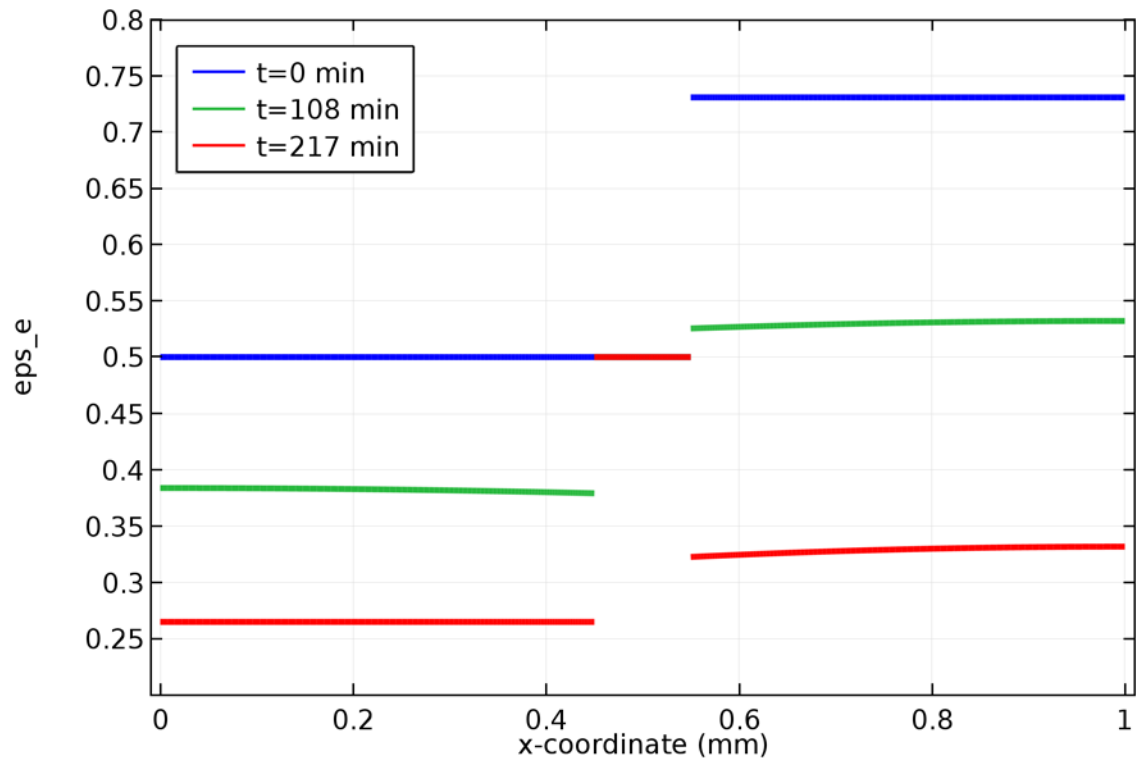


Figure 3.22. Porosity changes for initial NiOOH concentration of 75 kmol/m<sup>3</sup>.

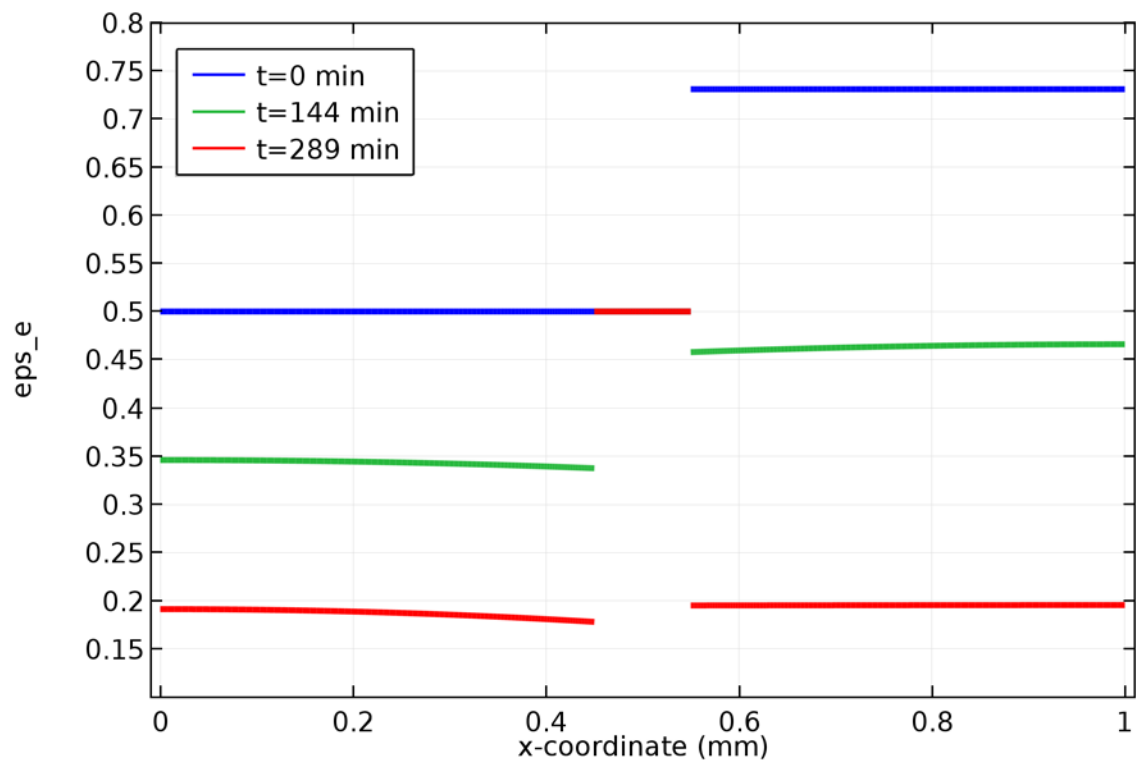


Figure 3.23. Porosity changes for initial NiOOH concentration of 150 kmol/m<sup>3</sup>.



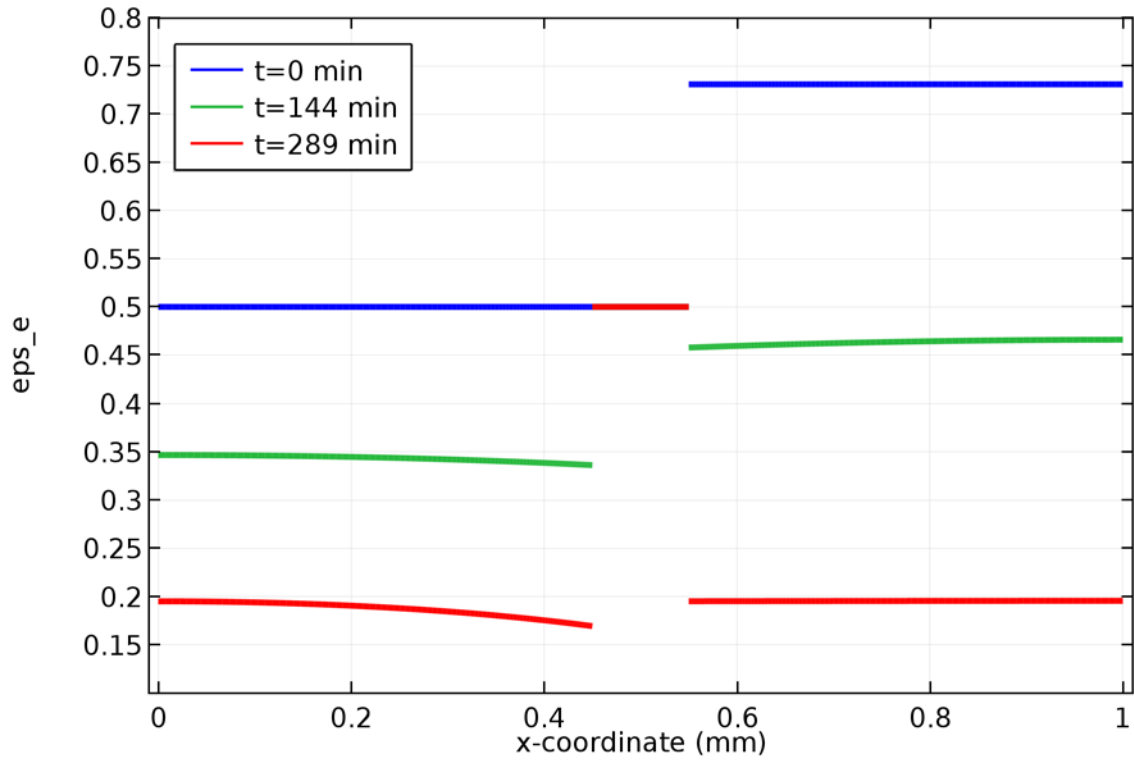


Figure 3.24. Porosity changes for initial NiOOH concentration of 300 kmol/m<sup>3</sup>.

Nickel electrode porosities have the same values at the current collector side, yet there are little differences at the separator side. Higher initial concentration causes more decrease in porosity closer to the separator as the battery drains.

### 3.3.3. Results for Various Transfer Coefficients for Zinc Electrode Reaction

Transfer coefficients of an electrode reaction are very difficult parameters to calculate. In this model, single mechanism of reaction approach has been used. For that reason, the anodic and cathodic transfer coefficients are the components of total number of electrons transferred during the reaction. Three values are accepted for anodic transfer coefficient that those are 0.5, 1, and 1.5. The transfer coefficients for nickel electrode are constants and it is 0.5, so the sum of the anodic and cathodic transfer coefficients is 1 because there is one electron transferred in the nickel electrode reaction. The initial zinc and nickel oxyhydroxide concentrations are 100 and 150 kmol/m<sup>3</sup> respectively. According to parametric sweep, cell voltage, species concentrations and porosity changes are computed and illustrated.

### 3.3.3.1. Cell Voltage

Figure 3.25 shows clearly that the transfer coefficients of zinc electrode reaction affect the cell voltage magnitude and the transition on the edges when the voltage drops drastically and the cell becomes depleted. Transfer coefficients are exponentials in the Butler-Volmer kinetics. This is why there is not a linear increase in the cell voltage magnitude as transfer coefficients are increased.

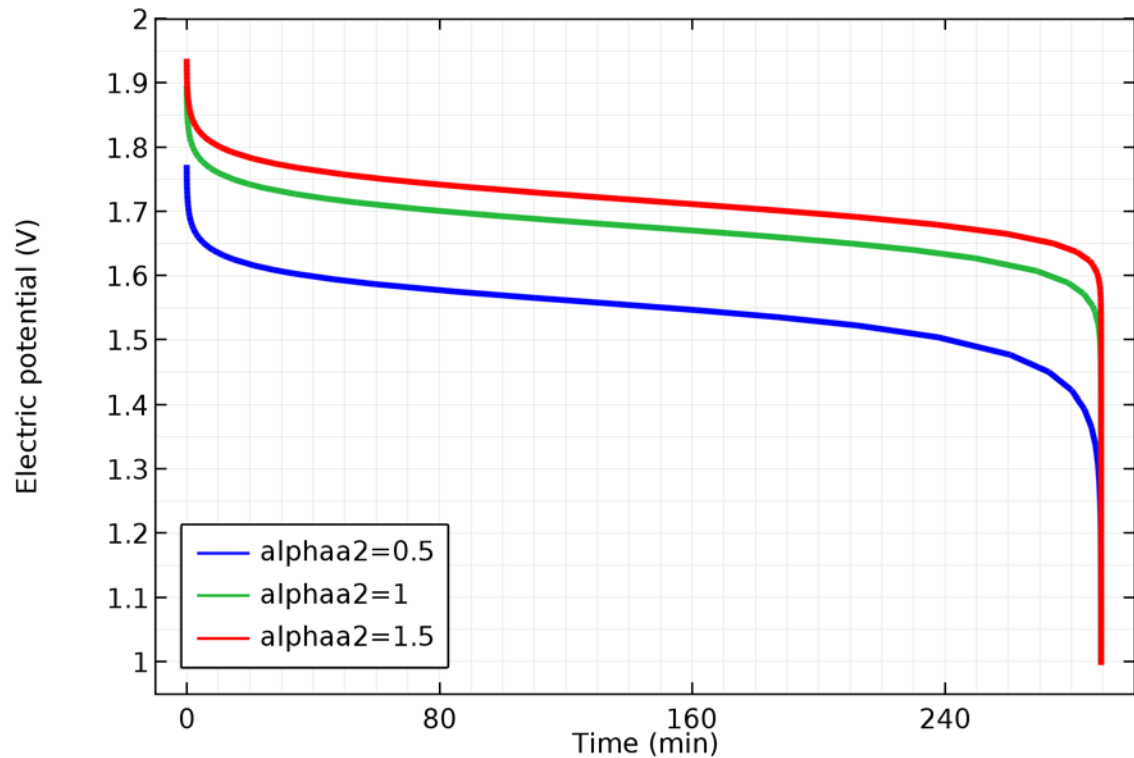


Figure 3.25. Discharge voltage over time for three anodic transfer coefficients for zinc electrode reaction.

### 3.3.3.2. Zinc and Zinc Oxide Species Concentration Changes

Figure 3.26, 3.27, and 3.28 shows that the all zinc species are used in the zinc electrode reaction.

Another indication is that the anodic transfer coefficient might have a relation with the zinc species dissolution at the separator interface. The concentration differences between Zn and ZnO slightly increases with increased anodic transfer coefficient at the separator interface.

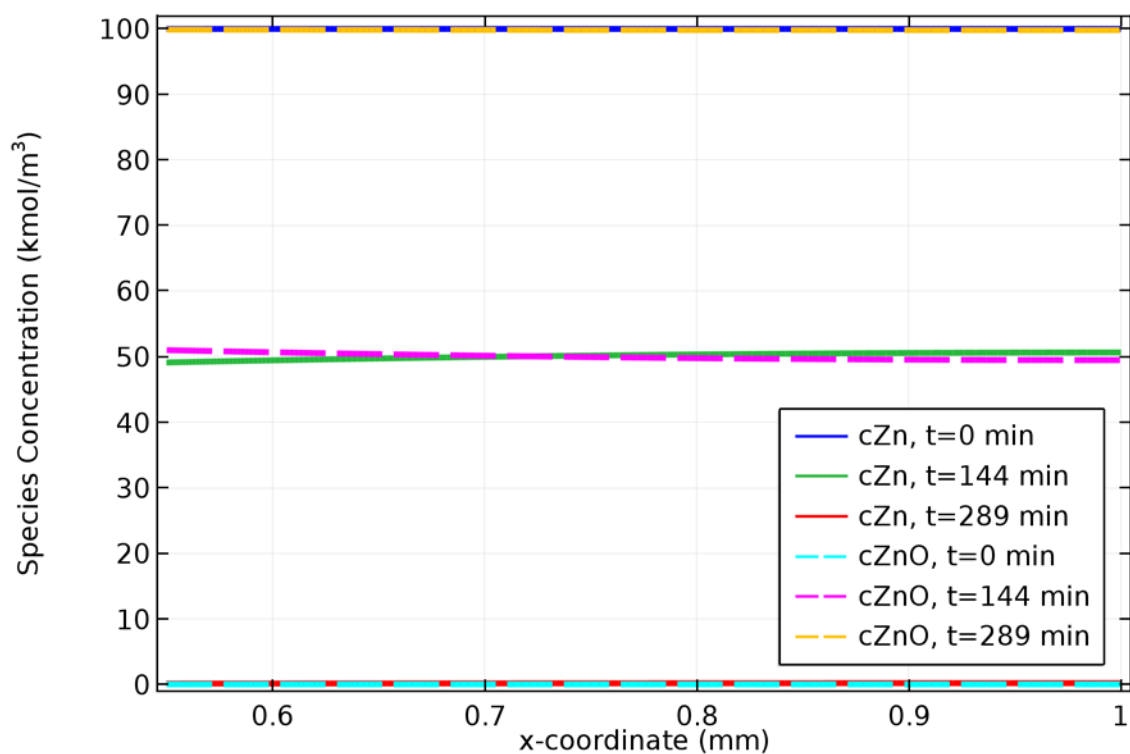


Figure 3.26. Zn and ZnO concentrations inside NiZn cell when the anodic transfer coefficient for zinc electrode reaction is 0.5.

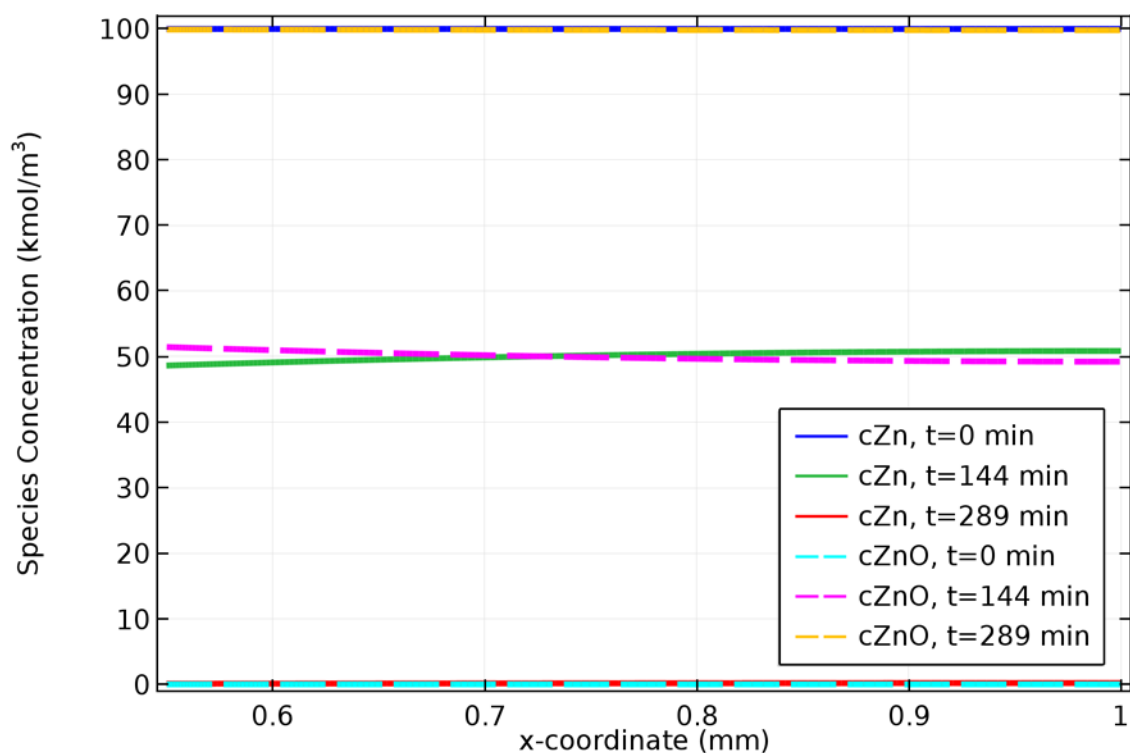


Figure 3.27. Zn and ZnO concentrations inside NiZn cell when the anodic transfer coefficient for zinc electrode reaction is 1.

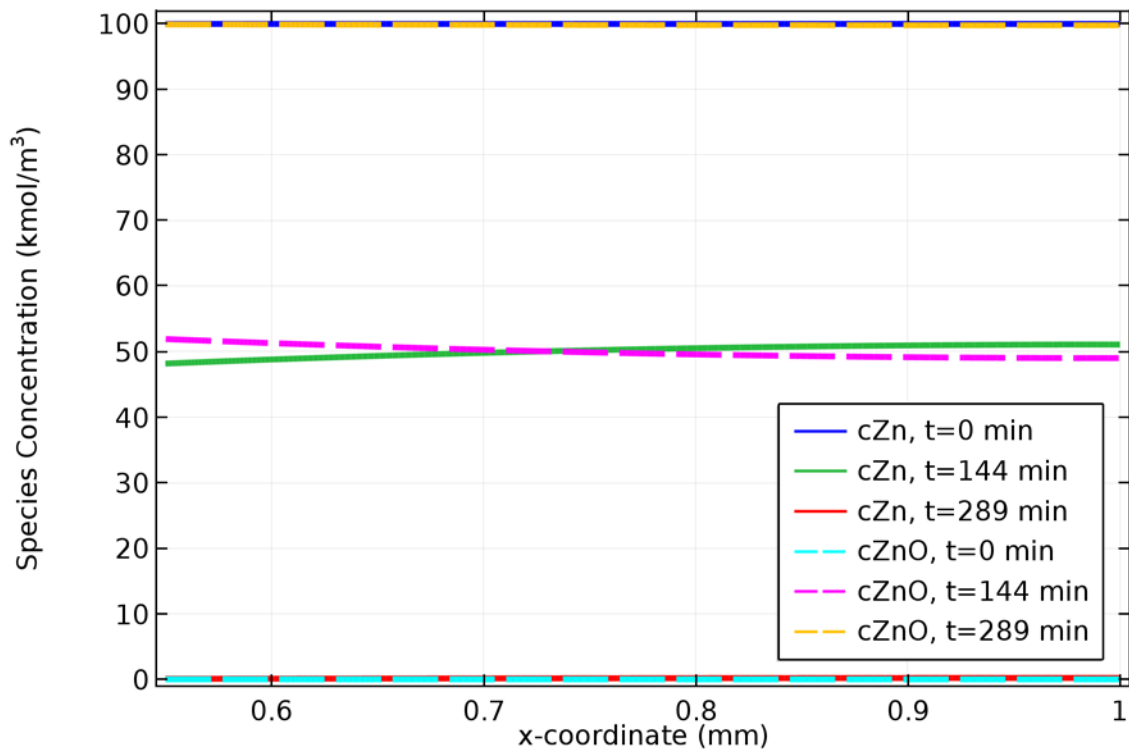


Figure 3.28. Zn and ZnO concentrations inside NiZn cell when the anodic transfer coefficient for zinc electrode reaction is 1.5.

### 3.3.3.3. Nickel Oxyhydroxide and Nickel Hydroxide Species Concentration Changes

Figure 3.29, 3.30, and 3.31 demonstrate that the all nickel oxyhydroxide do not involve in the nickel electrode reaction. Approximately  $50 \text{ kmol/m}^3$  nickel oxyhydroxide do not used.

Another fact that can be seen from these figures is that the zinc electrode reaction transfer coefficients do not have any effect on the species of nickel electrode. The concentration difference between reduced and oxidized species in Ni electrodes does not change as anodic transfer coefficient.

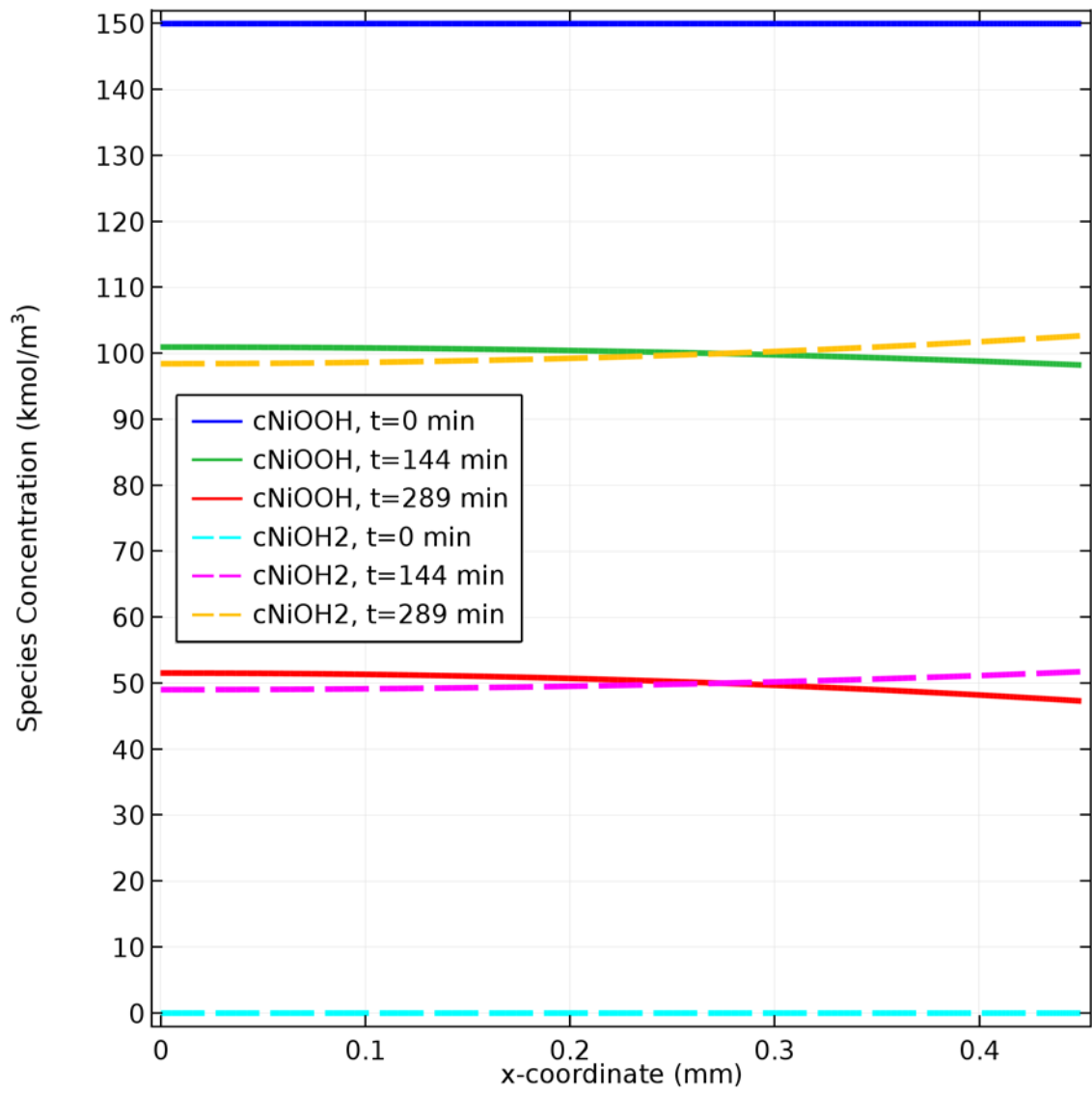


Figure 3.29.  $\text{NiOOH}$  and  $\text{Ni(OH)}_2$  concentrations inside  $\text{NiZn}$  cell when the anodic transfer coefficient for zinc electrode reaction is 0.5.

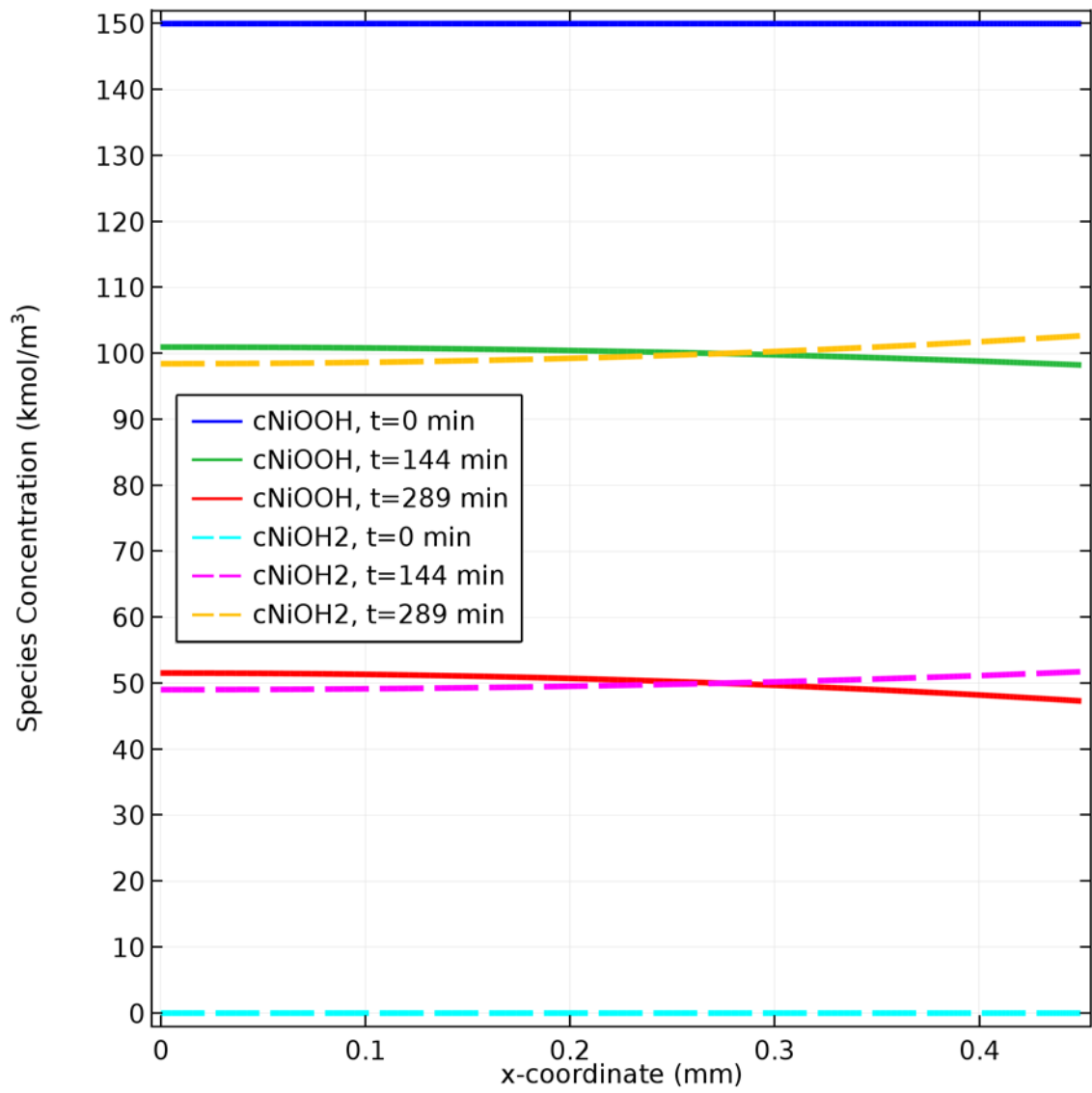


Figure 3.30. NiOOH and Ni(OH)<sub>2</sub> concentrations inside NiZn cell when the anodic transfer coefficient for zinc electrode reaction is 1.

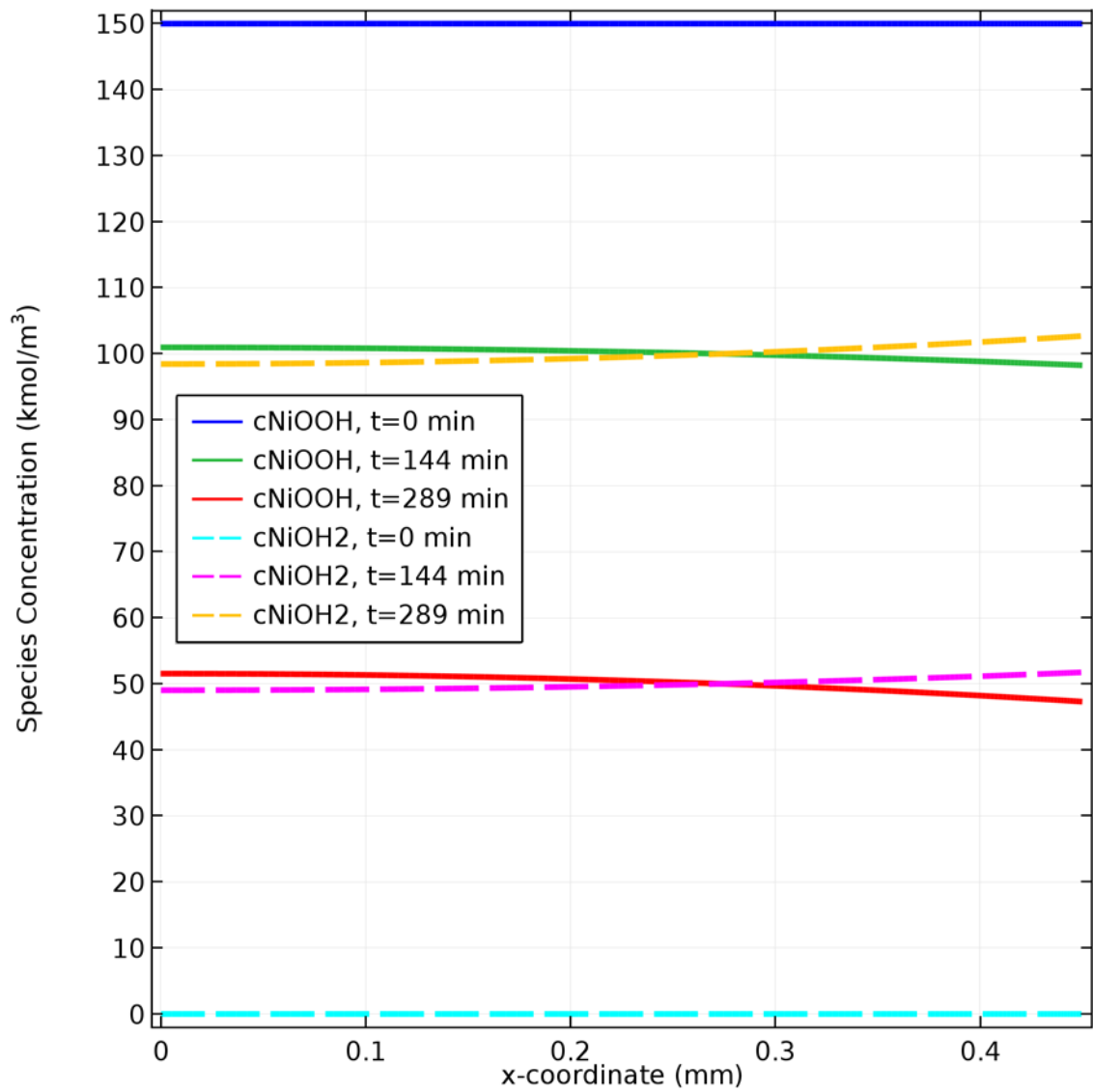


Figure 3.31.  $\text{NiOOH}$  and  $\text{Ni(OH)}_2$  concentrations inside NiZn cell when the anodic transfer coefficient for zinc electrode reaction is 1.5.

### 3.3.3.4. Porosity Changes

Figure 3.32, 3.33, and 3.34 reveal that the transfer coefficients have no effect on porosity changes in either electrode. All figures are identical with each other.

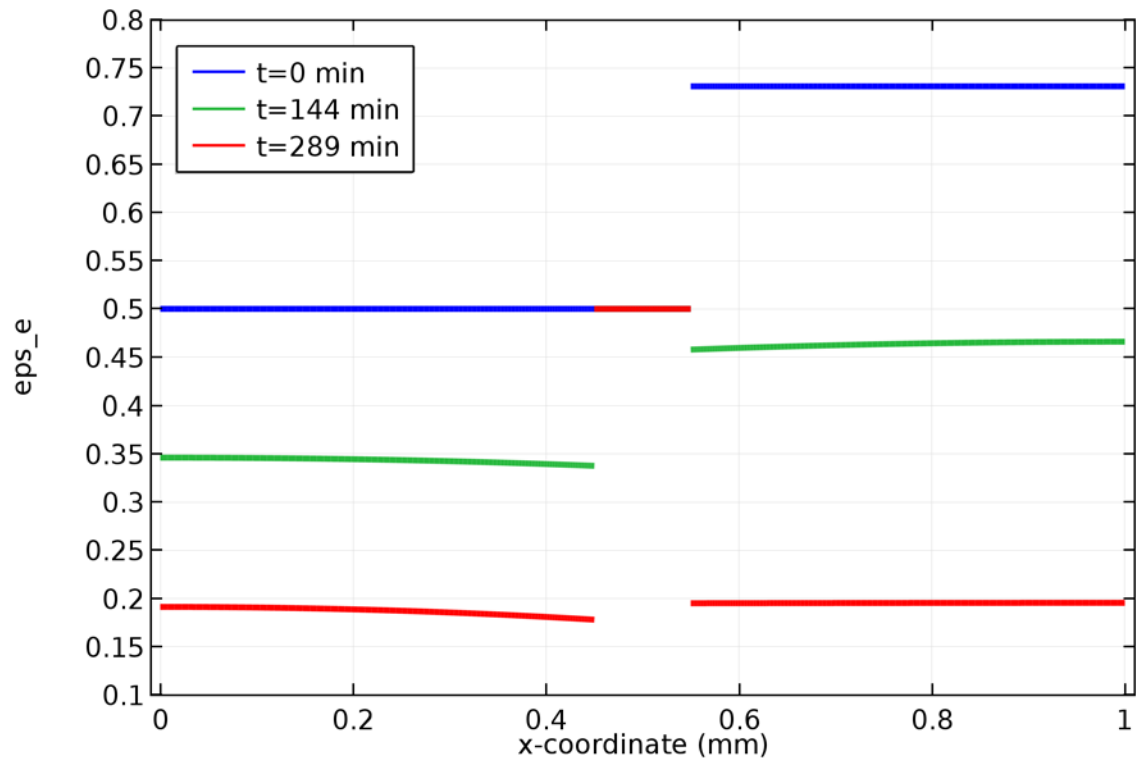


Figure 3.32. Porosity changes when the anodic transfer coefficient for zinc electrode reaction is 0.5.

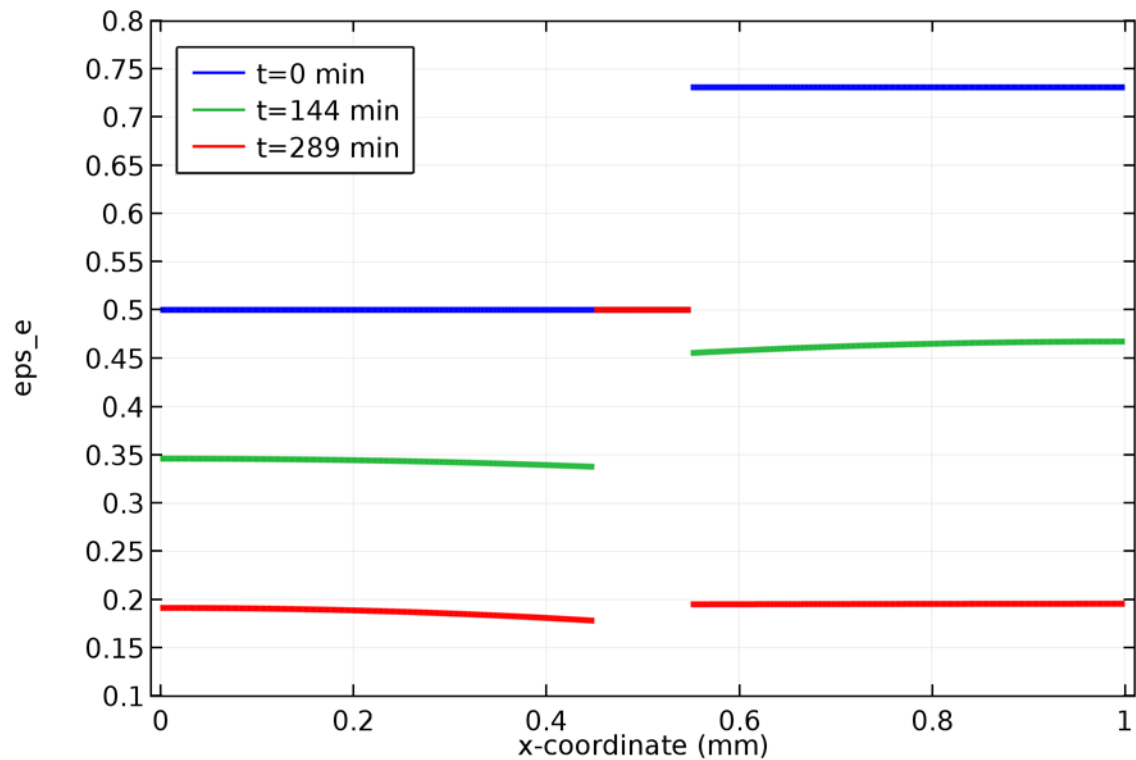


Figure 3.33. Porosity changes when the anodic transfer coefficient for zinc electrode reaction is 1.



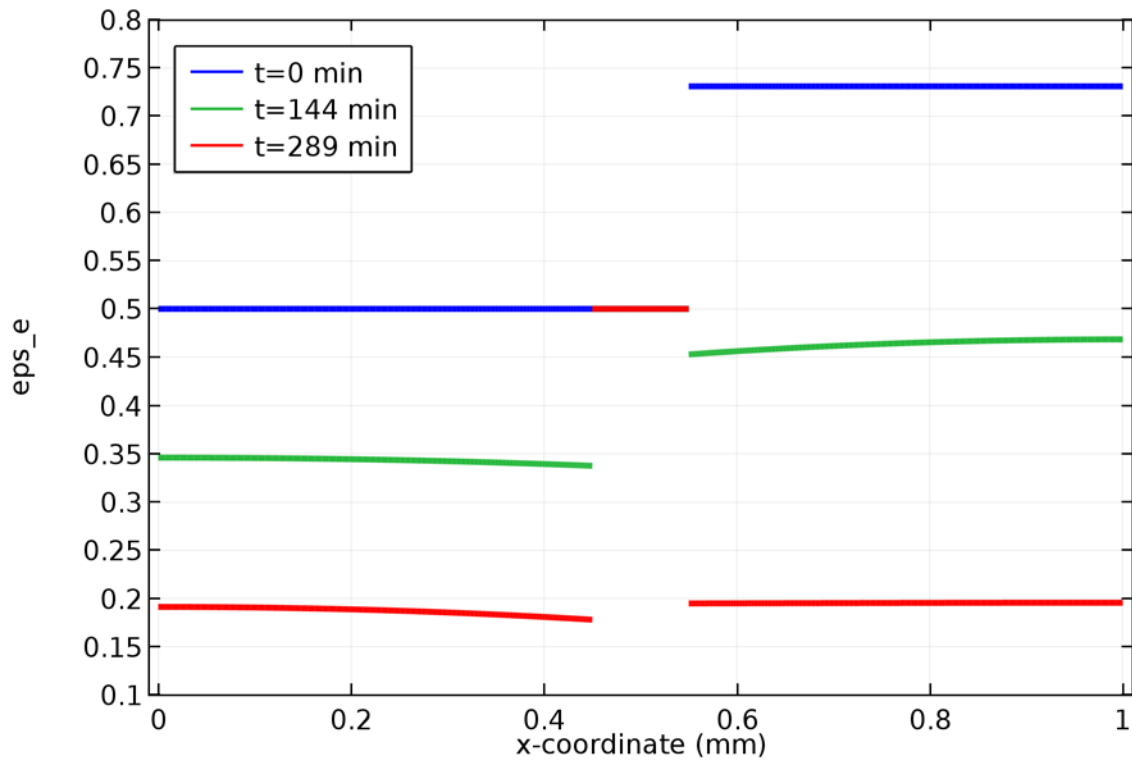


Figure 3.34. Porosity changes when the anodic transfer coefficient for zinc electrode reaction is 1.5.

### 3.3.4. Results for Various Transfer Coefficients for Nickel Electrode Reaction

A similar study to the one with transfer coefficients of zinc electrode reaction have been done with transfer coefficients of nickel electrode reaction. The values for anodic transfer coefficient of nickel electrode reaction have been selected as 0.3, 0.5, and 0.7.

#### 3.3.4.1. Cell Voltage

In Figure 3.35 the transfer coefficients seem to be able to affect the cell voltage at the beginning of discharge process. Beginning magnitude of the cell voltage is 1.81 V if the anodic transfer coefficient is assumed 0.7, 1.73 V for 0.5, and 1.67 V for anodic transfer coefficient of 0.3. Other than the cell voltages at initial time, no significant difference can be observed in this figure, and all three discharge curves are almost identical.

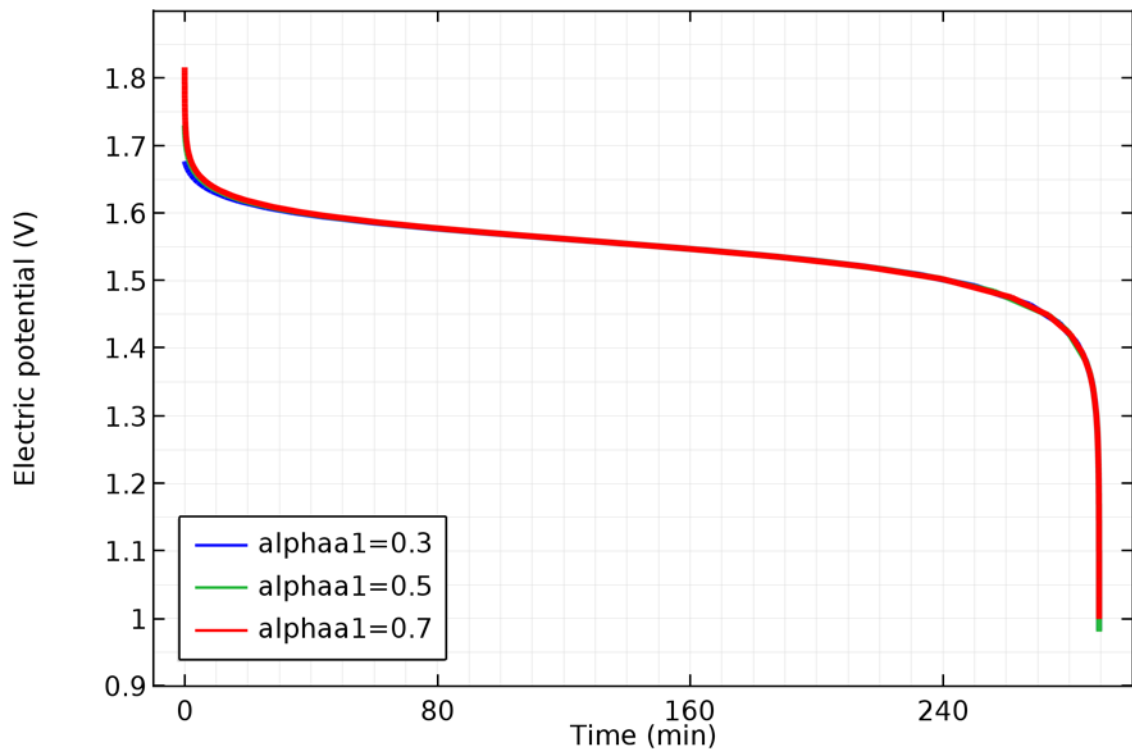


Figure 3.35. Discharge voltage over time for three anodic transfer coefficients for nickel electrode reaction.

#### 3.3.4.2. Zinc and Zinc Oxide Species Concentration Changes

Figure 3.36, 3.37, and 3.38 present zinc and zinc oxide species concentrations in negative electrode according to three anodic transfer coefficients of nickel electrode reaction. Initial zinc concentration is  $100 \text{ kmol/m}^3$  and initial nickel oxyhydroxide concentration is  $150 \text{ kmol/m}^3$ . As the figures indicate that all of the zinc is used in the electrode reaction.

The similarity of concentration profiles in the middle of discharge process reveals that the transfer coefficients of nickel electrode reaction has no significance on the species concentrations in the zinc electrode as suspected and similar to the fact that the zinc transfer coefficients had no effect on the species concentrations of nickel electrode.

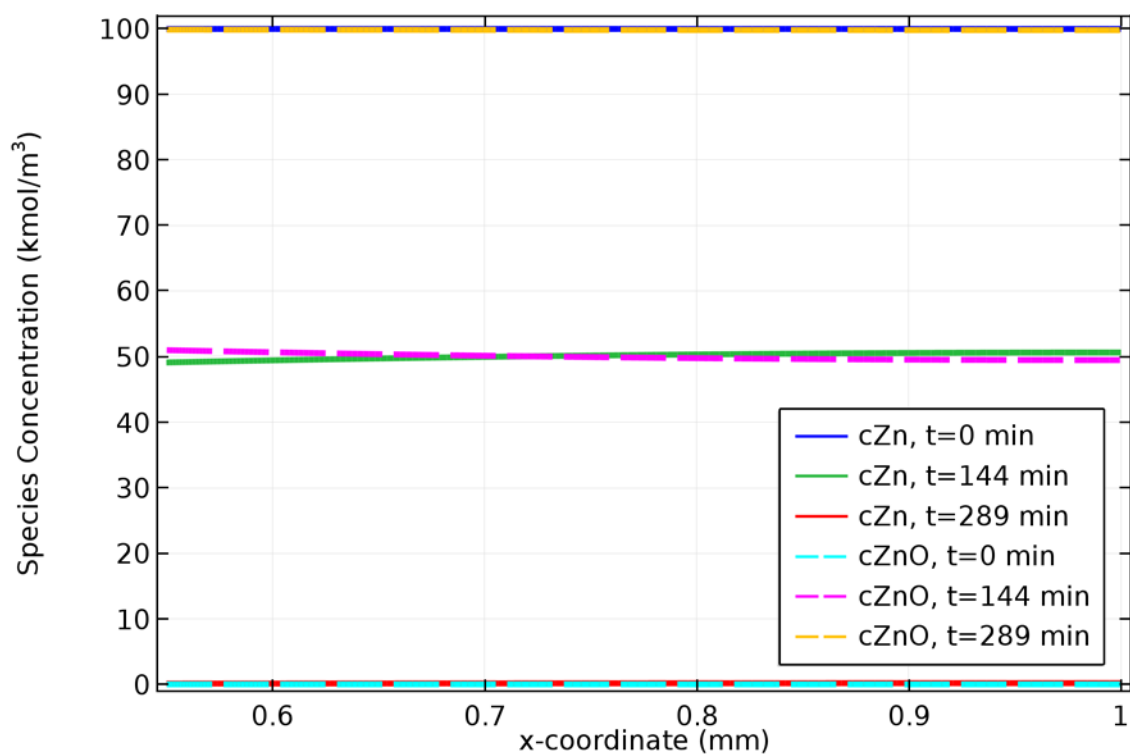


Figure 3.36. Zn and ZnO concentrations inside NiZn cell when the anodic transfer coefficient for nickel electrode reaction is 0.3.

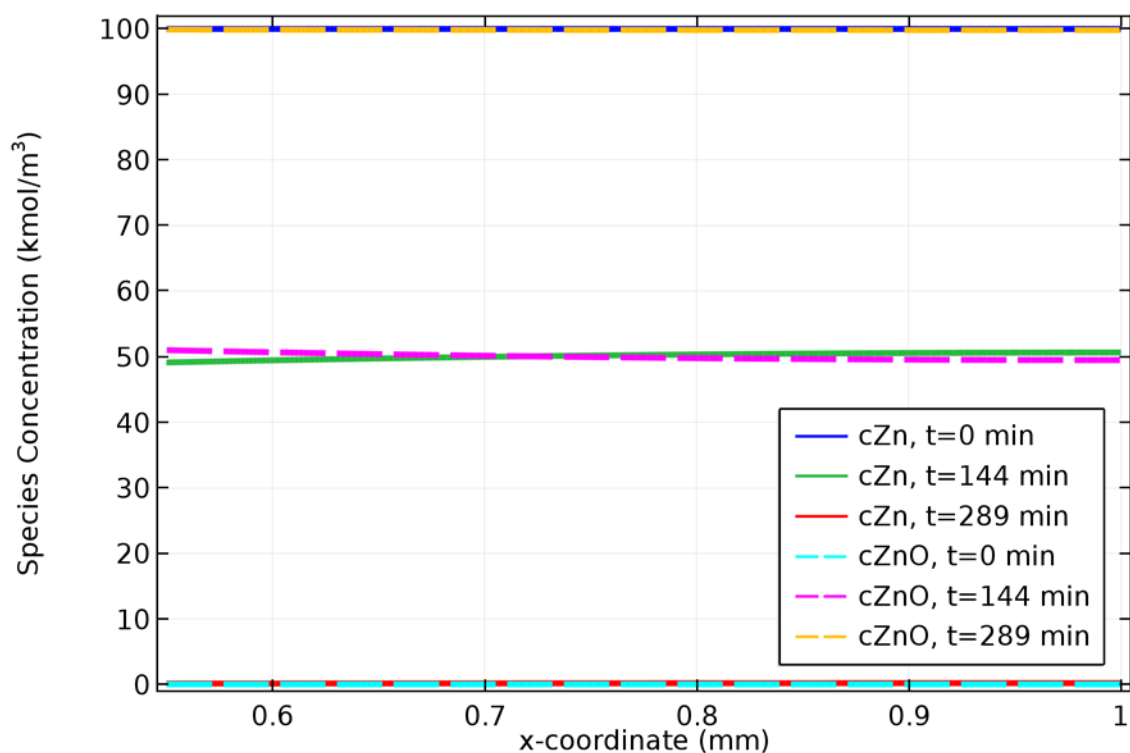


Figure 3.37. Zn and ZnO concentrations inside NiZn cell when the anodic transfer coefficient for nickel electrode reaction is 0.5.

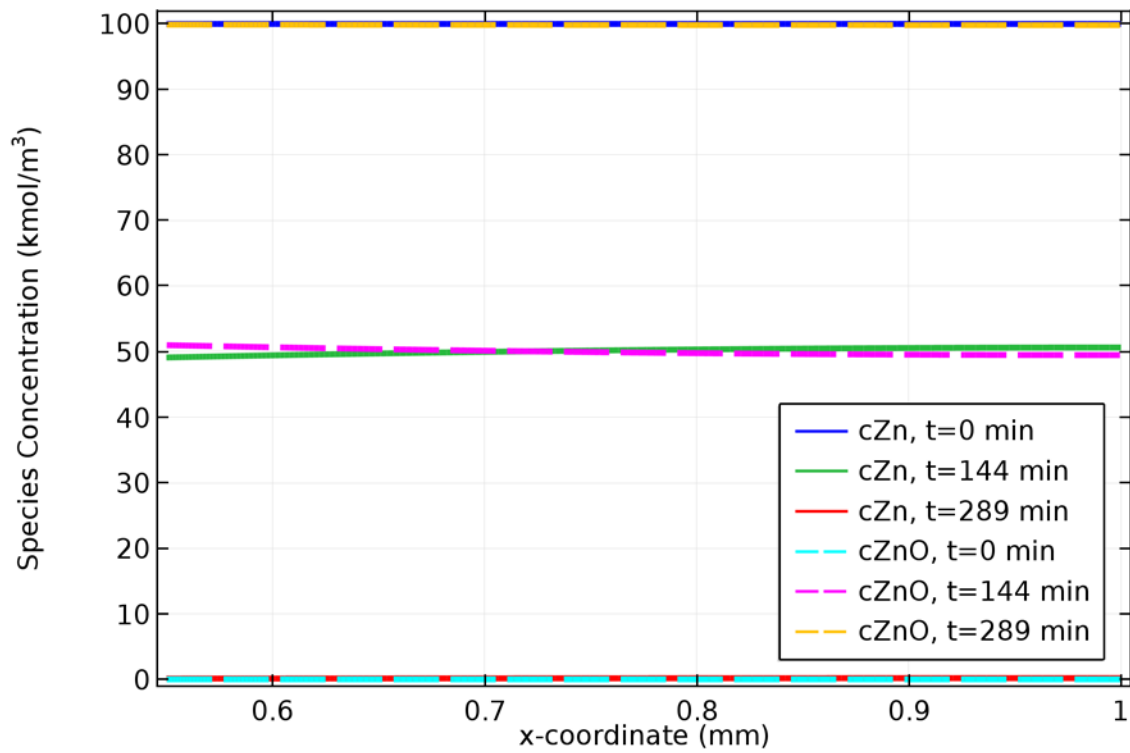


Figure 3.38. Zn and ZnO concentrations inside NiZn cell when the anodic transfer coefficient for nickel electrode reaction is 0.7.

### 3.3.4.3. Nickel Oxyhydroxide and Nickel Hydroxide Species Concentration Changes

Figure 3.39, 3.40, and 3.41 show that the transfer coefficients of the nickel electrode reaction have no influence on species concentration in the nickel electrode. All figures possess the same curves.

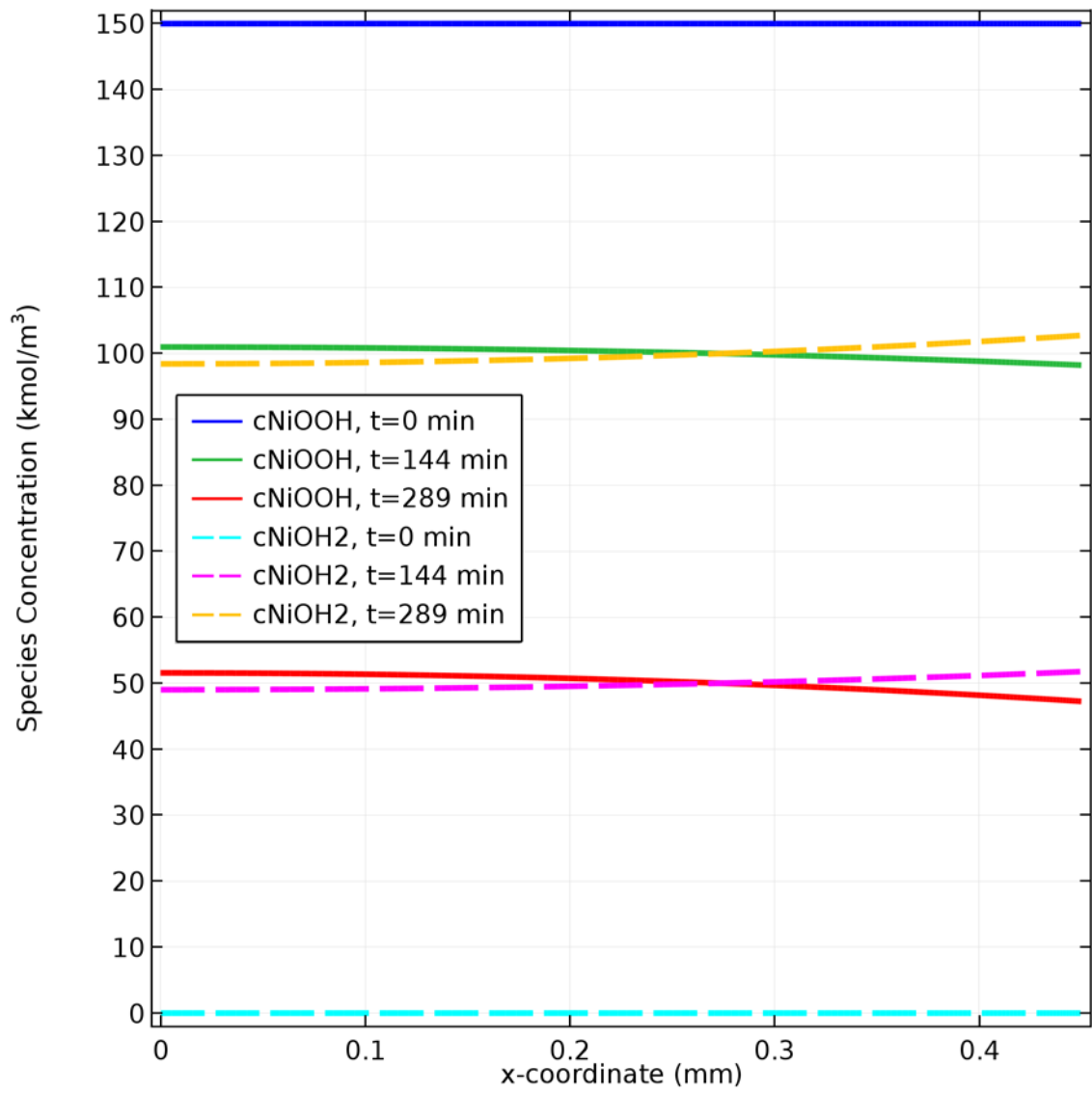


Figure 3.39.  $\text{NiOOH}$  and  $\text{Ni(OH)}_2$  concentrations inside  $\text{NiZn}$  cell when the anodic transfer coefficient for nickel electrode reaction is 0.3.

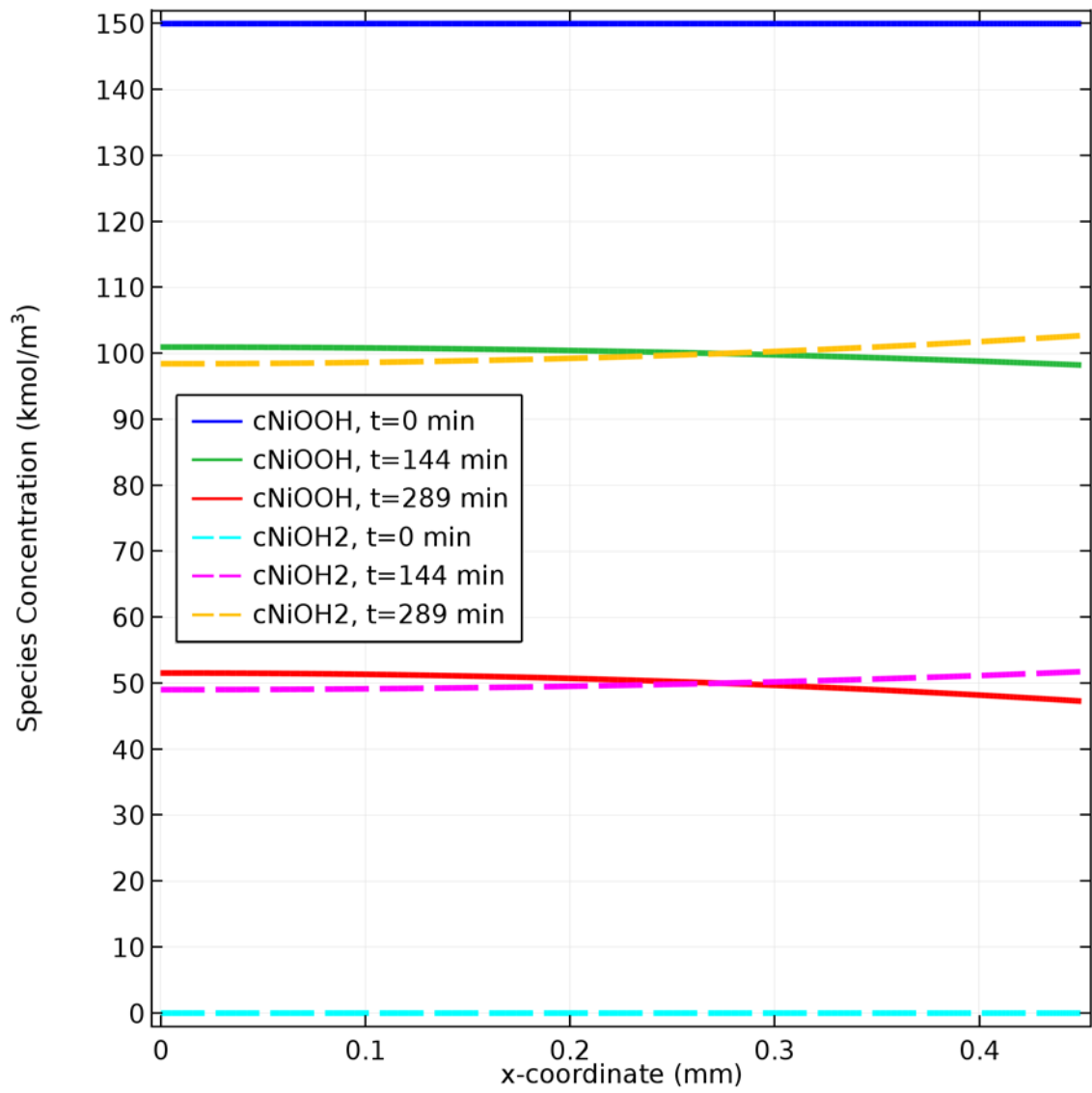


Figure 3.40. NiOOH and Ni(OH)<sub>2</sub> concentrations inside NiZn cell when the anodic transfer coefficient for nickel electrode reaction is 0.5.

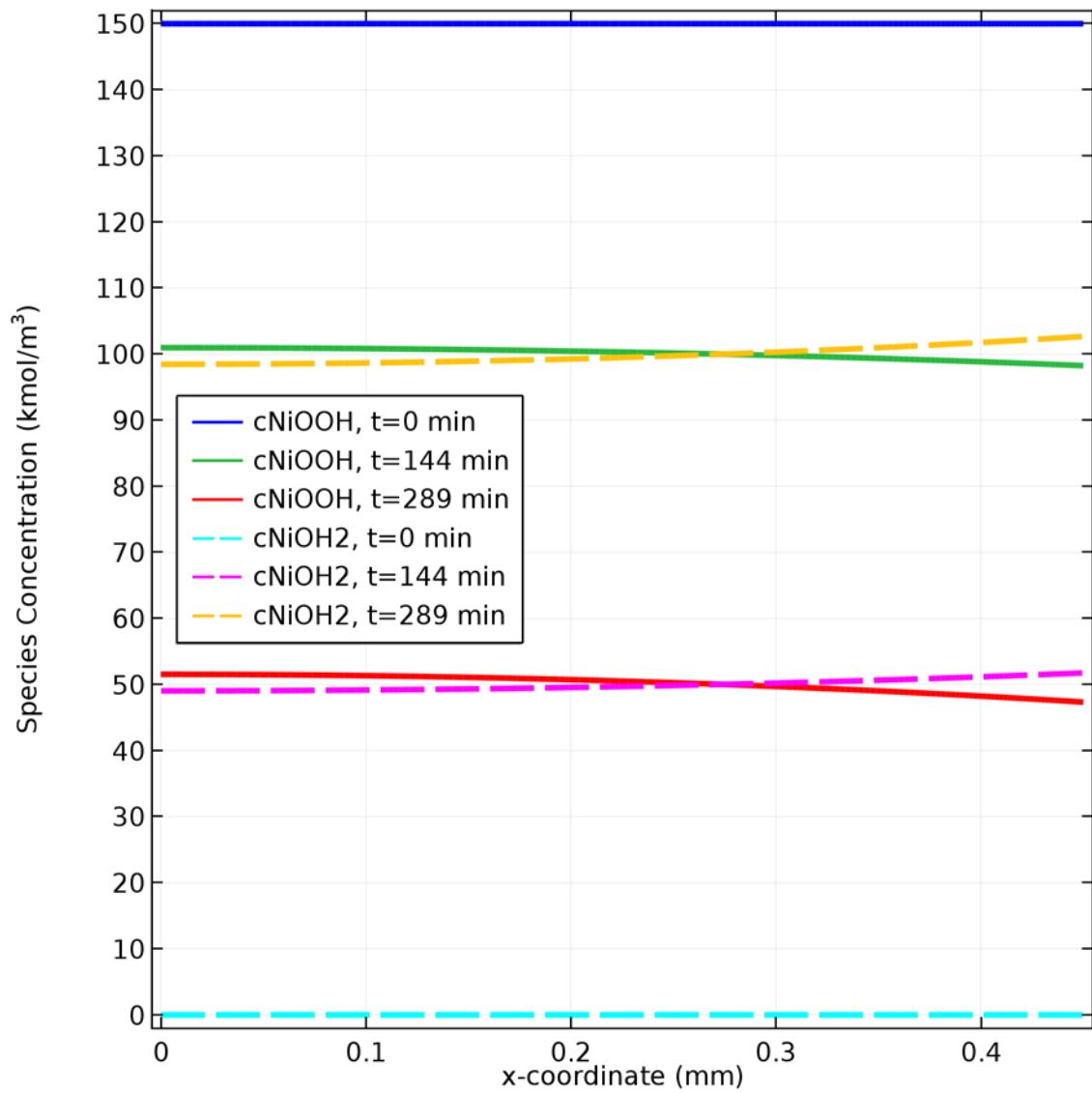


Figure 3.41. NiOOH and Ni(OH)<sub>2</sub> concentrations inside NiZn cell when the anodic transfer coefficient for nickel electrode reaction is 0.7.

#### 3.3.4.4. Porosity Changes

Transfer coefficients of nickel electrode reaction have not any effect on porosity according to Figure 3.42, 3.43, and 3.44. This result is similar to the one obtained from study for zinc electrode reaction transfer coefficients.

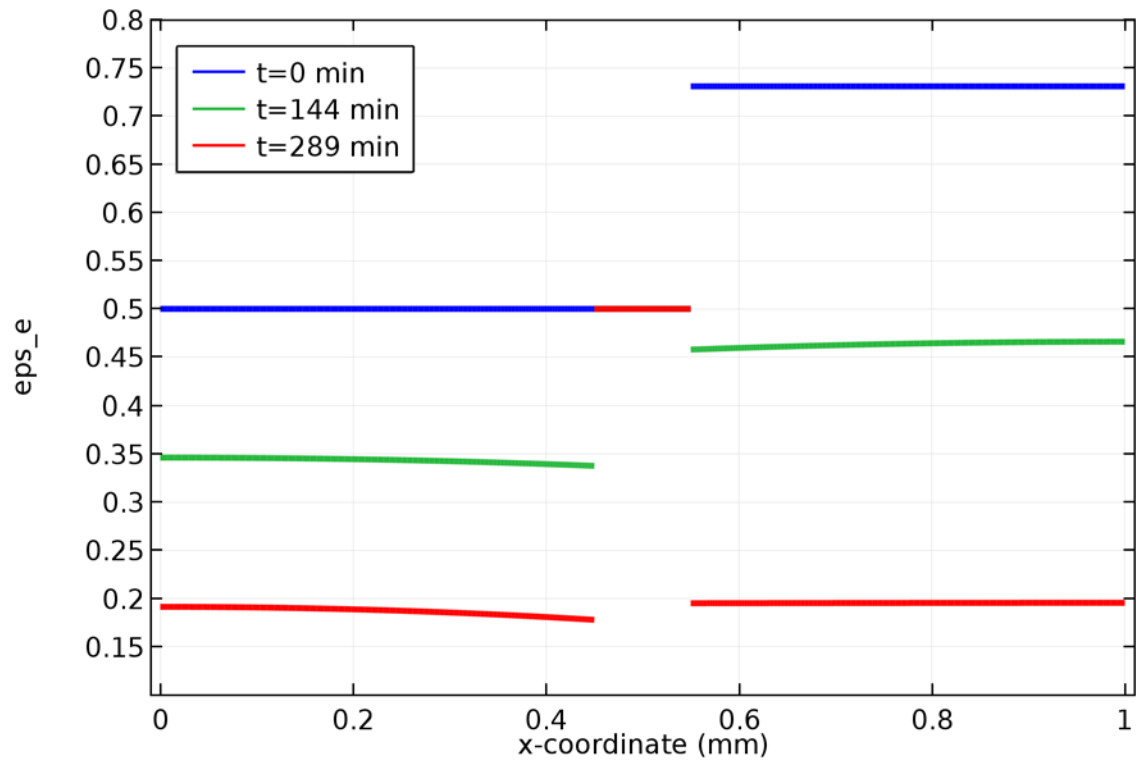


Figure 3.42. Porosity changes when the anodic transfer coefficient for nickel electrode reaction is 0.3.

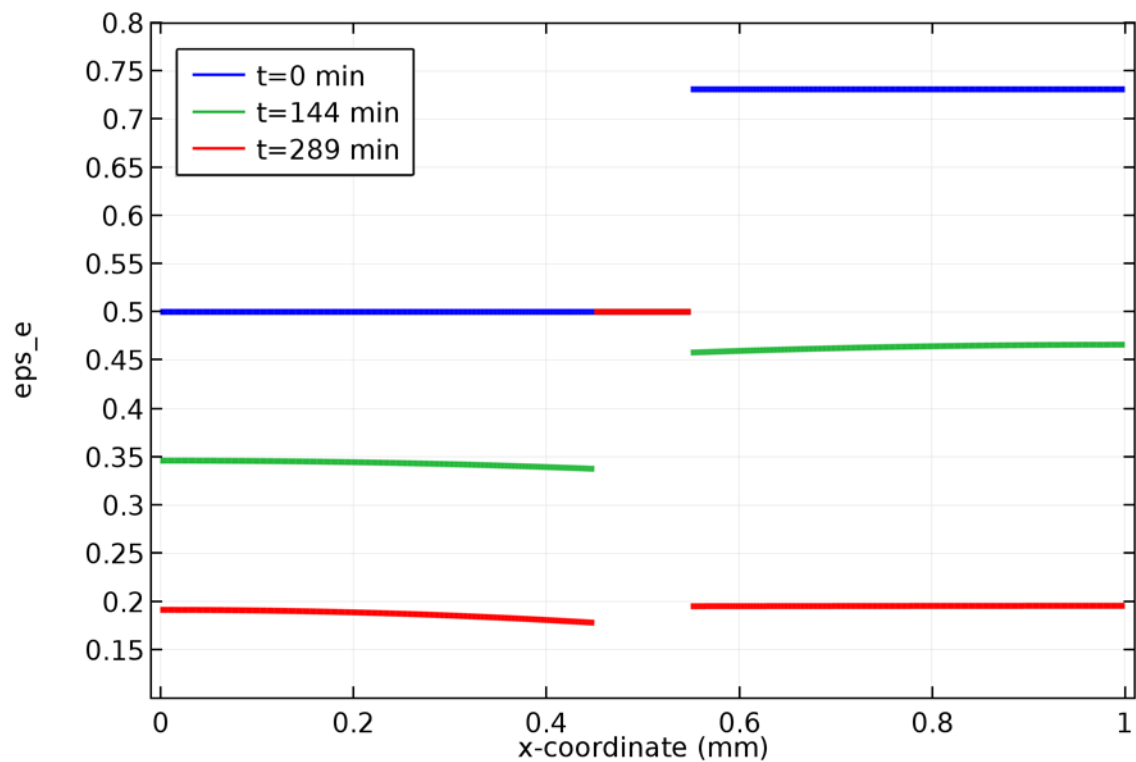


Figure 3.43. Porosity changes when the anodic transfer coefficient for nickel electrode reaction is 0.5.



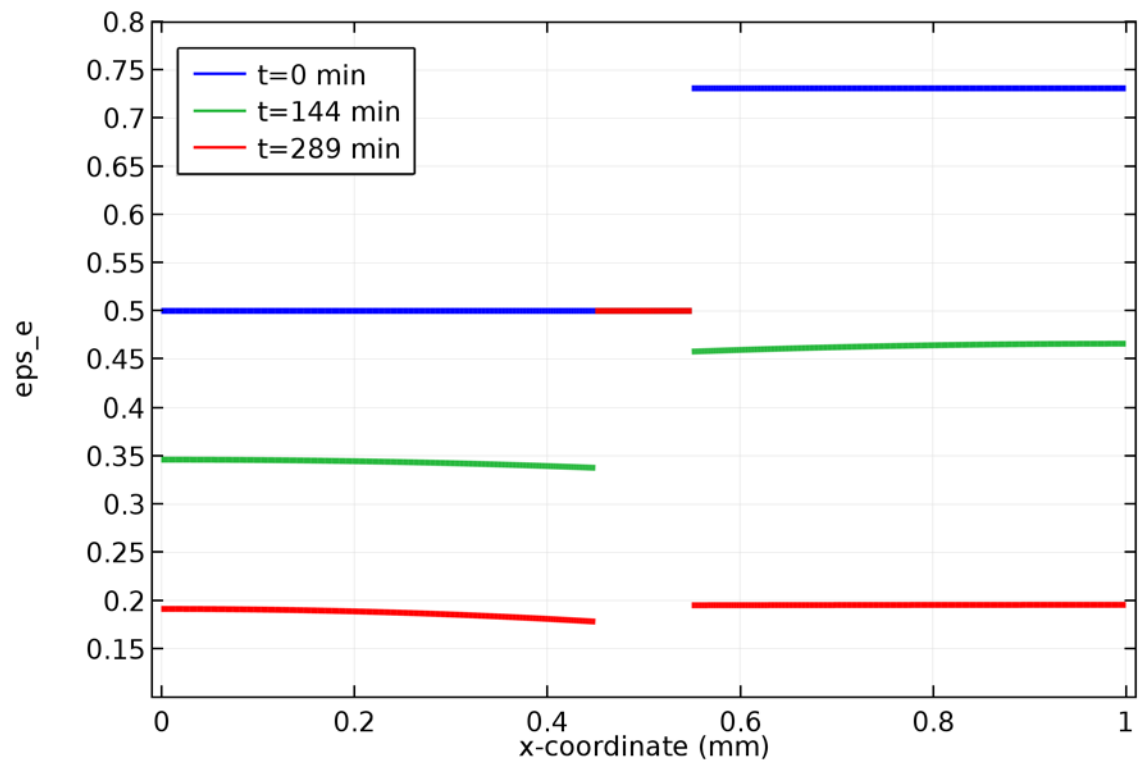


Figure 3.44. Porosity changes when the anodic transfer coefficient for nickel electrode reaction is 0.7.

## CHAPTER 4

### CONCLUSIONS

For the development of nickel-zinc batteries and other zinc based battery systems, a reliable model is the missing piece. The presented model in this dissertation is an attempt to shorten the way leading to zinc based batteries with high energy densities for battery researchers.

While one-dimensional modeling is a low profile study, its influence on battery research can be enormous. Applying the findings of experimental measurements into a mathematical model and numerical analysis afterwards can give valuable information about battery behavior under various conditions. Mathematical modeling can also be used for optimization of cell and battery geometry with better thermal and discharge characteristics.

Numerical analysis and parametric sweep enable one to determine discharge voltages, concentration changes of zinc, zinc oxide, nickel oxyhydroxide, and nickel hydroxide species in both porous electrodes and electrolyte solution, change in electrode porosities during battery discharge for a set of initial parameters that can be controlled such as initial zinc, nickel oxyhydroxide and electrolyte concentrations and cell geometry.

Current density value in the simulation was intentionally selected low as  $0.05 \text{ A/cm}^2$  to prevent passivation of zinc electrode surface with an oxide layer; a problem that is common for commercial zinc based batteries. Results of this study indicate that discharge time at fixed load is determined by the electrode with a lower capacity, as expected. Transfer coefficients of the zinc electrode reaction have an influence over the discharge voltage, the slope of discharge plateau and at the edge of the discharge plateau where voltage begins to drop drastically. Electrode porosity changes becomes significant only one of the species in the electrodes is about to be depleted. Concentrations of reduced and oxidized species inside electrodes at a given time vary slightly indicating that electrochemical reactions are not limited by diffusion of species thanks to high porosities of both anode and cathode. However, when electrode thickness (anode or cathode) is doubled, the effect of diffusion becomes dominant.

The difficulty of modeling a nickel zinc battery comes from the fact that there is no way of validating the simulation results other than current and voltage measurements at fixed or variable load. The number of parameters used in the mathematics expressing zinc battery chemistry is very high. Even zincate ion formation reactions, which might dominate zinc electrode kinetic in certain situations are ignored one must still estimate many parameters that cannot be measured or determined experimentally. Moreover, some of those parameters are either difficult or impossible to measure with an experimental study and they must be estimated. Best way to overcome this problem is to follow a two-channel work in which an experimental process, and a modeling and simulation process are carried out simultaneously. Each process is tuned according to the findings of the other until simulation results mimic real battery behavior.

The model developed in this study is based on many assumptions as explained in previous chapter. In addition, formation of zincate ions which is one of the main reasons for shape change of the electrode with increasing cycle count and dendritic zinc growth during charge leading to poor battery life, are totally ignored. Clearly, a follow up study which is based on this model but with the inclusion of zincate ion formation and related electrochemical reactions is needed.

## REFERENCES

- Bard, Allen J., and Larry R. Faulkner. 2001. *Electrochemical Methods, Fundamentals and Applications*. 2nd Ed. New York: John Wiley & Sons.
- Chang, Wen-Yeau. 2013. "The State of Charge Estimating Methods for Battery: A Review." *ISRN Applied Mathematics* 2013:1-7. doi: 10.1155/2013/953792.
- COMSOL, Inc. 2015. "COMSOL Puts the Power of Simulation in Your Hands." <https://www.comsol.com/comsol-multiphysics>.
- Crow, D. R.. 1974. *Principles and Applications of Electrochemistry*. n.p.: Springer.
- DiPippo, Ronald. 2012. *Geothermal Power Plants: Principles, Applications, Case Studies and Environmental Impact*. 3rd Ed. Waltham: Butterworth-Heinemann.
- Energizer Holdings, Inc.. 2005. *Technical Bulletin: Battery Internal Resistance*. Version 1.1.0 December 2005. <http://data.energizer.com/PDFs/BatteryIR.pdf>.
- Gileadi, Eliezer. 1993. *Electrode Kinetics for Chemists, Chemical Engineers, and Material Scientists*. New York: VCH Publishers.
- Goswami, Yogi D., and Frank Kreith, eds. 2007. *Energy Conversion*. Boca Raton: CRC Press.
- Gu, Hiram, Douglas N. Bennion, and John Newman. 1976. "Analysis of Porous Electrodes with Sparingly Soluble Reactants III. Short Time Transients." *Journal of the Electrochemical Society* 123(9):1364-1370. doi: 10.1149/1.2133076.
- Hua, Chih-Chiang and Meng-Yu Lin. 2000. "A Study Of Charging Control Of Lead-Acid Battery For Electric Vehicles." *Proceedings of the 2000 IEEE International Symposium on Industrial Electronics, 2000.ISIE 2000*. 1:135-140. doi: 10.1109/ISIE.2000.930500.
- IEA (International Energy Agency). 2015. *Key World Energy Statistics*. [https://www.iea.org/publications/freepublications/publication/KeyWorld\\_Statistics\\_2015.pdf](https://www.iea.org/publications/freepublications/publication/KeyWorld_Statistics_2015.pdf).
- IUPAC (International Union of Pure and Applied Chemistry). 2014. "standard conditions for gases" *Compendium of Chemical Technology Gold Book version 2.3.3*. Last modified February 24. <http://goldbook.iupac.org/PDF/goldbook.pdf>.
- Jain, Mukul, and John W. Weidner. 1999. "Material Balance Modification in One-Dimensional Modeling Porous Electrodes." *Journal of The Electrochemical Society* 146(4):1370-1374. doi: 10.1149/1.1391772.
- Lai, Wei, and Francesco Ciucci. 2011. "Mathematical Modeling of Porous Battery Electrodes – Revisit of Newman’s Model." *Electrochimica Acta* 56(2011)4369-4377. doi: 10.1016/j.electacta.2011.01.012.

- Linden, David, and Thomas B. Reddy, eds. 2002. *Handbook of Batteries*. 3rd Ed. New York: McGraw-Hill.
- Maxwell Technologies, Inc. 2015a. *Ultracapacitor Overview*. <http://www.maxwell.com/products/ultracapacitors>.
- Maxwell Technologies, Inc. 2015b. *Ultracapacitor Modules*. <http://www.maxwell.com/products/ultracapacitors/modules>
- Maxwell Technologies, Inc. 2015c. *New 48V Module Datasheet*. [http://www.maxwell.com/images/documents/48V\\_ds\\_DuraBlue\\_3000685\\_2.pdf](http://www.maxwell.com/images/documents/48V_ds_DuraBlue_3000685_2.pdf).
- Maxwell Technologies, Inc. 2015d. *160V Module Datasheet*. [http://www.maxwell.com/images/documents/160vmodule\\_ds\\_3000246-5.pdf](http://www.maxwell.com/images/documents/160vmodule_ds_3000246-5.pdf).
- Maxwell Technologies, Inc. 2015e. *New 16V Small Module Datasheet*. [http://www.maxwell.com/images/documents/datasheet\\_16v\\_small\\_cell\\_module.pdf](http://www.maxwell.com/images/documents/datasheet_16v_small_cell_module.pdf).
- MIT Electric Vehicle Team. 2008. *A Guide to Understanding Battery Specifications*. [http://web.mit.edu/evt/summary\\_battery\\_specifications.pdf](http://web.mit.edu/evt/summary_battery_specifications.pdf).
- Newman, John S., and Charles W. Tobias. 1962. "Theoretical Analysis of Current Distribution in Porous Electrodes." *Journal of The Electrochemical Society* 109(12):1183-1191. doi: 10.1149/1.2425269.
- Newman, John, and Karen E. Thomas-Alyea. 2004. *Electrochemical Systems*. 3rd Ed. New Jersey: John Wiley & Sons.
- Newman, John, and William Tiedemann. 1975. "Porous-Electrode Theory with Battery Applications." *AIChE (American Institute of Chemical Engineers) Journal* 21(1):25-41. doi: 10.1002/aic.690210103.
- Noel, M., and K. I. Vasu. 1990. *Cyclic Voltammetry and the Frontiers of Electrochemistry*. New Delhi: Oxford & IBH Publishing Co. Pvt. Ltd..
- Pang, Shuo, Jay Farnell, Jie Du, and Matthew Barth. 2001. "Battery State-Of-Charge Estimation." *American Control Conference, 2001. Proceedings of the 2001*. 2:1644-1649. doi: 10.1109/ACC.2001.945964.
- Payer, Gizem. 2014. "An Investigation of Electrochemical Stability of Zinc Electrodes For Battery Applications." Master's Thesis, Izmir Institute of Technology.
- Petrucchi, Ralph H., F. Geoffrey Herring, Jeffry D. Madura, and Carey Bissonette. 2011. *General Chemistry, Principles and Modern Applications*. 10th Ed. n.p.: Pearson Canada.
- Pop, Valer, Henk Jan Bergveld, Dmitry Danilov, Paul P. L. Regtien, and Peter H. L. Notten. 2008. *Battery Management Systems. Accurate State-of-Charge Indication for Battery-Powered Applications*. n.p.: Springer.

- Powergenix. 2012a. *8 Ah Prismatic Sealed Nickel Zinc Battery Datasheet*. Updated: 5/3/2012. [http://powergenix.com/wp-content/uploads/2014/04/pgx\\_8ah\\_prismatic\\_data\\_sheet.pdf](http://powergenix.com/wp-content/uploads/2014/04/pgx_8ah_prismatic_data_sheet.pdf).
- Powergenix. 2012b. *40 Ah Prismatic Sealed Nickel Zinc Battery Datasheet*. Updated: 5/3/2012. [http://powergenix.com/wp-content/uploads/2014/04/pgx\\_40ah\\_prismatic\\_data\\_sheet.pdf](http://powergenix.com/wp-content/uploads/2014/04/pgx_40ah_prismatic_data_sheet.pdf).
- Powergenix. 2012c. *80 Ah Prismatic Sealed Nickel Zinc Battery Datasheet*. Updated: 5/3/2012. [http://powergenix.com/wp-content/uploads/2014/04/pgx\\_80ah\\_prismatic\\_data\\_sheet.pdf](http://powergenix.com/wp-content/uploads/2014/04/pgx_80ah_prismatic_data_sheet.pdf).
- Ramadesigan, Venkatasailanathan, Paul W. C. Northrop, Sumitava De, Shriram Santhanagopalan, Richard D. Braatz, and Venkat R. Subramanian. 2012. "Modeling and Simulation of Lithium-Ion Batteries from a Systems Engineering Perspective." *Journal of The Electrochemical Society* 159(3):R31-R45. doi: 10.1149/2.018203jes.
- Rubinstein, Israel, ed. 1995. *Physical Electrochemistry; Principles, Methods, and Applications*. New York: Marcel Decker.
- Snihir, Iryna, William Rey, Evgeny Verbitskiy, Afifa Belfadhel-Ayeb, and Peter H. L. Notten. 2006. "Battery Open-circuit Voltage Estimation by a Method of Statistical Analysis." *Journal of Power Sources* 159(2):1484-1487 doi: 10.1016/j.jpowsour.2005.11.090.
- Sunu, W. G., and D. N. Bennion. 1980. "Transient and Failure Analysis of the Porous Zinc Electrode: I. Theoretical." *Journal of The Electrochemical Society* 127(9):2007-2016. doi: 10.1149/1.2130054.
- Technical Marketing Staff of Gates Energy Products, Inc.. 1992. *Rechargeable Batteries. Applications Handbook*. Boston: Butterworth-Heinemann.
- Ter-Gazarian, A. G. 2011. *Energy Storage For Power Systems*. 2nd Ed. London: The Institution of Engineering and Technology.
- Texas Instruments, Inc.. 2011. *Characteristics of Rechargeable Batteries*. Literature Number SNVA533. <http://www.ti.com/lit/an/snva533/snva533.pdf>.
- Torabi, F., and A. Aliakbar. 2012. "A Single-Domain Formulation for Modeling and Simulation of Zinc-Silver Oxide Batteries." *Journal of The Electrochemical Society* 159(12):A1986-A1992. doi: 10.1149/2.038212jes.
- Vairamohan, Baskar. 2002. "State-of-Charge Estimation for Batteries." Master's Thesis. University of Tennessee, Knoxville.
- Vincent, Colin A., and Bruno Scrosati. 1997. *Modern Batteries, An Introduction to Electro-chemical Power Sources*. 2nd Ed. Eastbourne: Butterworth-Heinemann.
- Walsh, Edward M. 1967. *Energy Conversion. Electromechanical, Direct, Nuclear*. New York: The Ronald Press Company.

- Wang, Haiying, Shuangquan Liu, Shiwei Li, and Gechen Li. 2013. "Study on State of Charge Estimation of Batteries for Electric Vehicle." In *Proceedings, The 2nd International Conference on Advanced Signal Processing, ASP 2013*. ASTL 18:10-14.
- Xiao, Bingjun, Yiyu Shi, and Lei He. 2010. "A Universal State-of-Charge Algorithm for Batteries." *Design Automation Conference (DAC), 2010 47th ACM/IEEE*: 687-692.
- Yu, Aiping, Victor Chabot, and Jiujuun Zhang. 2013. *Electrochemical Supercapacitors for Energy Storage and Delivery, Fundamentals and Applications*. Boca Raton: CRC Press.
- Zhao, Cuimei, and Weitao Zheng. 2015. "A Review For Aqueous Electrochemical Supercapacitors." *Frontiers in Energy Research* 3(23):1-11. doi: 10.3389/fenrg.2015.00023.
- Zumdahl, Steven S., and Susan A. Zumdahl. 2010. *Chemistry*. 8th Ed. Belmont: Brooks Cole.

## APPENDIX A

### TABLES OF PARAMETERS AND VARIABLES

Parameters and variables used in one dimensional nickel-zinc battery model have been given in Table A.1 and Table A.2.

Table A.1. Parameters used in the model.

$L_{Zn}$	0.45[mm]	Length of zinc electrode
$L_{Ni}$	0.45[mm]	Length of nickel electrode
$L_{sep}$	0.1[mm]	Length of separator
$t_+$	0.2	Transport number of the cations
$T$	298[K]	Operating temperature
$\rho$	1500[kg/m <sup>3</sup> ]	Electrolyte solution density
$\rho_{NiOOH}$	3.8[g/cm <sup>3</sup> ]	Density of NiOOH
$\rho_{Ni(OH)_2}$	3.4[g/cm <sup>3</sup> ]	Density of Ni(OH) <sub>2</sub>
$\rho_{Zn}$	7.14[g/cm <sup>3</sup> ]	Density of Zn
$\rho_{ZnO}$	5.606[g/cm <sup>3</sup> ]	Density of ZnO
$M_K$	39.1[g/mol]	Potassium molar mass
$M_{OH}$	17[g/mol]	Anion molar mass
$M_{H_2O}$	18[g/mol]	Solvent molar mass
$M_{NiOOH}$	91.699[g/mol]	Molecular weight of NiOOH
$M_{Ni(OH)_2}$	92.707[g/mol]	Molecular weight of Ni(OH) <sub>2</sub>
$M_{Zn}$	65.38[g/mol]	Molecular weight of Zn
$M_{ZnO}$	81.408[g/mol]	Molecular weight of ZnO
$D_{OH}$	5.26e-9[m <sup>2</sup> /s]	Diffusion coefficient of OH ion
$D_K$	1.96e-9[m <sup>2</sup> /s]	Diffusion coefficient of Zn ion
$\sigma_{NiOOH}$	2500[S/m]	Electronic conductivity of NiOOH

(cont. on next page)



Table A.1. Parameters used in the model. (cont.)

$\sigma_{\text{Ni(OH)}_2}$	10e5[S/m]	Electronic conductivity of $\text{Ni(OH)}_2$
$\sigma_{\text{Zn}}$	1.83e7[S/m]	Electronic conductivity of Zn
$\sigma_{\text{ZnO}}$	1[S/m]	Electronic conductivity of ZnO
$C_{\text{l,init}}$	7[mol/dm <sup>3</sup> ]	Initial electrolyte concentration
$C_{\text{OH,ref}}$	$C_{\text{l,init}}$	Reference electrolyte concentration
$C_{\text{Zn,init}}$	10e4[mol/m <sup>3</sup> ] $\times$ Param( $C_{\text{Zn}}$ )	Initial concentration of Zn in the electrode
$C_{\text{NiOOH,init}}$	15e4[mol/m <sup>3</sup> ] $\times$ Param( $C_{\text{NiOOH}}$ )	Initial concentration of $\text{Ni(OH)}_2$ in the electrode
$E_{\text{eq,Ni}}$	0.49[V]	Equilibrium potential of nickel electrode reaction
$E_{\text{eq,Zn}}$	-1.305[V]	Equilibrium potential of zinc electrode reaction
$i_{0,\text{Ni}}$	1.04e-2[A/cm <sup>2</sup> ]	Exchange current density of nickel electrode reaction
$i_{0,\text{Zn}}$	1.75e-4[A/cm <sup>2</sup> ]	Exchange current density of zinc electrode reaction
$\alpha_{\text{a,Ni}}$	0.6	Anodic transfer coefficient for nickel electrode reaction
$\alpha_{\text{c,Ni}}$	$n_{\text{Ni}} - \alpha_{\text{a,Ni}}$	Cathodic transfer coefficient for nickel electrode reaction
$\alpha_{\text{a,Zn}}$	0.5	Anodic transfer coefficient for zinc electrode reaction
$\alpha_{\text{c,Zn}}$	$n_{\text{Zn}} - \alpha_{\text{a,Zn}}$	Cathodic transfer coefficient for zinc electrode reaction
$n_{\text{Ni}}$	1	Number of transferred electrons at nickel electrode reaction
$n_{\text{Zn}}$	2	Number of transferred electrons at zinc electrode reaction

(cont. on next page)

Table A.1. Parameters used in the model. (cont.)

$a_{Zn}$	50[cm <sup>2</sup> /cm <sup>3</sup> ]	Specific surface area of zinc electrode
$a_{Ni}$	4036[cm <sup>2</sup> /cm <sup>3</sup> ]	Specific surface area of nickel electrode
$\epsilon_{sep}$	0.5	Porosity of separator
$\epsilon_{Ni}$	0.5	Initial porosity of positive electrode
$\epsilon_{Zn}$	0.731	Initial porosity of negative electrode
Param( $C_{Zn}$ )	1	For parametric sweep
Param( $C_{NiOOH}$ )	1	For parametric sweep

Table A.2. Variables used in the model.

$m_{Ni(OH)_2}$	$\max(C_{Ni(OH)_2} \times M_{Ni(OH)_2} / (C_{Ni(OH)_2} \times M_{Ni(OH)_2} + C_{NiOOH} \times M_{NiOOH}), \epsilon)$	Mass fraction of Ni(OH) <sub>2</sub>
$m_{NiOOH}$	$\max(C_{NiOOH} \times M_{NiOOH} / (C_{Ni(OH)_2} \times M_{Ni(OH)_2} + C_{NiOOH} \times M_{NiOOH}), \epsilon)$	Mass fraction of NiOOH
$m_{Zn}$	$\max(C_{Zn} \times M_{Zn} / (C_{Zn} \times M_{Zn} + C_{ZnO} \times M_{ZnO}), \epsilon)$	Mass fraction of Zn
$m_{ZnO}$	$\max(C_{ZnO} \times M_{ZnO} / (C_{Zn} \times M_{Zn} + C_{ZnO} \times M_{ZnO}), \epsilon)$	Mass fraction of ZnO
$\sigma_{l,eff}$	$(\epsilon_l \times F^2 / R / T) \times (D_{K^+} + D_{OH^-}) \times C_l$	Effective electrolyte conductivity
$\sigma_{s,eff,Ni}$	$\sigma_{Ni(OH)_2} \times m_{Ni(OH)_2}^{1.5} + \sigma_{NiOOH} \times m_{NiOOH}^{1.5}$	Effective electrical conductivity Ni electrode
$\sigma_{s,eff,Zn}$	$\sigma_{Zn} \times m_{Zn}^{1.5} + \sigma_{ZnO} \times m_{ZnO}^{1.5}$	Effective electrical conductivity of negative electrode

(cont. on next page)

Table A.2. Variables used in the model. (cont.)

$C_{R,Ni}$	$(C_1 / C_{OH,ref}) \times (C_{Ni(OH)_2} / C_{NiOOH,init})$	Concentration term of reduced species in Ni electrode BV kinetics
$C_{O,Ni}$	$(C_{NiOOH} / C_{NiOOH,init})$	Concentration term of oxidized species in Ni electrode BV kinetics
$C_{R,Zn}$	$(C_1 / C_{OH,ref})^2 \times (C_{Zn} / C_{Zn,init})$	Concentration term of reduced species in Zn electrode BV kinetics
$C_{O,Zn}$	$(C_{ZnO} / C_{Zn,init})$	Concentration term of oxidized species in Zn electrode BV kinetics
$SrcT(\epsilon, Ni)$	$(-1 / 2 / F) \times (M_{NiOOH} / \rho_{NiOOH} - M_{Ni(OH)_2} / \rho_{Ni(OH)_2}) \times a_{Ni} \times i_{loc, Ni}$	Source term for Ni electrode porosity
$SrcT(\epsilon, Zn)$	$((1 / 2 / F) \times (M_{Zn} / \rho_{Zn} - M_{ZnO} / \rho_{ZnO})) \times a_{Zn} \times i_{loc, Zn}$	Source term for Zn electrode porosity
$SrcT(C_{NiOOH})$	$(1 / 2 / F) \times a_{Ni} \times i_{loc, Ni}$	Source term for NiOOH species concentration
$SrcT(C_{Ni(OH)_2})$	$(-1 / 2 / F) \times a_{Ni} \times i_{loc, Ni}$	Source term for Ni(OH) <sub>2</sub> species concentration
$SrcT(C_{Zn})$	$(-1 / 2 / F) \times a_{Zn} \times i_{loc, Zn}$	Source term for Zn species concentration
$SrcT(C_{ZnO})$	$(1 / 2 / F) \times a_{Zn} \times i_{loc, Zn}$	Source term for ZnO species concentration